UNIVERSITY OF CALIFORNIA, SAN DIEGO

The p38 MAP Kinase Pathway in Response and Defense to *Bacillus thuringiensis* Crystal Toxins

A dissertation submitted in partial satisfaction of the

requirements for the degree Doctor of Philosophy

in

Biology

by

Danielle Lee Huffman

Committee in charge:

Professor Raffi V. Aroian, Chair
Professor Bruce Hamilton
Professor William Loomis
Professor Victor Nizet
Professor Kit Pogliano

2006

The dissertation of Danielle Lee Huffman is approved, and it is acceptable in quality and form for publication on microfilm:

_____

_____

_____

_____

_____
Chair

University of California, San Diego

2006

TABLE OF CONTENTS

Signature Page iii

List of Figures vii

List of Tables ix

Acknowledgements x

Vita xi

Abstract xii

Chapter 1 Introduction to Pore-Forming Virulence Factors and the Model Host *Caenorhabditis elegans* 1

1.1 Summary 1

1.2 Bacterial Infection and Virulence Factors 2

1.3 C. elegans as a model for host-pathogen studies 3

1.4 Pore-forming Toxins as Bacterial Virulence Factors 5

1.5 Using Cry5B and C. elegans to understand intoxication by a PFT 7

1.6 Mammalian Intoxication and Responses to Pore-forming Toxins 9

1.7 References 13

Chapter 2 Genomic Analysis of the Host Response to Cry5B 19

2.1 Summary 19

2.2 Introduction 19

2.3 Timecourse of Cry5B Transcriptional Response 23

2.4 Comparing Response to Cry5B with Response to Cadmium 25

2.5 Discussion 28

2.6 Materials and Methods 29

2.7 References 32

Chapter 3 Analysis of Cry5B-Regulated Genes Reveals Toxin Defense Pathways 34

3.1 Summary 34

3.2 Introduction 35

3.3 A MAP Kinase Kinase Transcript, *sek-1*, is Regulated by Cry5B Exposure 40

3.4 JNK-Like MAP Kinase Genes Transcriptionally Regulated by Cry5B 45

3.5 Short Toxin Exposures Require MAP Kinase Mediated Defenses 47

3.6 Site of Action of the PMK-1 Pathway 48

3.7 p38 MAPK Pathway Protects Mammalian Cells Against a PFT 50

3.8 The Relationship Between the p38 and JNK-Like Pathways in *C. elegans* 52

3.9 Identification of Downstream Targets of PMK-1 52

3.10 Identification of Downstream Targets of KGB-1 55

3.11 The *ttm* Genes in Defense Against *S. aureus* α-Toxin 56

3.12 Synergism Between Salt Stress and Cry5B Intoxication 59

3.13 Discussion 61

3.14 Materials and Methods 67

3.15 References 73

Chapter 4 Toxin-Regulated Activation of the PMK-1 MAP Kinase Pathway 77

4.1 Summary 77

4.2 Introduction 78

4.3 Cry5B Acts as a Signal to *C. elegans* to Activate the PMK-1 Protective Pathway 80

4.4 The NSY-1 MAPKKK is Not Required for Cry5B-Induced Activation of PMK-1 84

4.5 Genetic Screen for Loss of Cry5B-Induced PMK-1 Activation 89

4.6 A Ceramide Glucosyltransferase Gene is Required for Activation of PMK-1 92

4.7 Testing for Changes in the Total PMK-1 Protein Levels 98

4.8 Discussion 100

4.9 Materials and Methods 109

4.10 References 115

Chapter 5 Conclusions, Implications and Future Directions 117

5.1 Summary 117

5.2 Pore-Forming Toxins in Immunity 118

5.3 Cry5B Defense in *C. elegans* 120

5.4 Cry Toxins as Bt Virulence Factors 122

5.5 Cell Mediated Immunity 123

5.6 References 123

LIST OF FIGURES

1.1 The effects of Cry5B on *C. elegans* 8

2.1 Quantitative growth-based toxicity assays with N2 and *glp-4*(bn2) 23

2.2 Animals on 1mM cadmium die at a similar rate to animals on Cry5B E. coli 26

2.3 Some of Cry5B transcriptional response is specific 27

2.4 Behavior of 1,670 probe sets induced by one or both of Cry5B and Cd 28

2.5 Using high and low doses of Cry5B to identify mutations affecting intoxication 29

3.1 *nsy-1 – sek-1 – pmk-1* (p38) and *kgb-1* (JNK-like) MAPK pathways protect *C. elegans* from Cry5B 42

3.2 The *kgb-1* MAPK pathway, but not the *sek-1 – pmk-1* pathway, protects *C. elegans* from cadmium intoxication 44

3.3 Quantitative growth-based toxicity assays with N2 and *sek-1*(km4) 45

3.4 Increased toxin sensitivity in sek-1 and kgb-1 mutants is not dependent on the bacterium used as food..... 46

3.5 Short toxin exposures require defense pathways *pmk-1* and *kgb-1* 48

3.6 Intestinal specific expression of *sek-1* rescues hypersensitivity 50

3.7 A p38 MAPK pathway protects mammalian cells against the PFT aerolysin 51

3.8 *ttm-1*, *ttm-2* and *ttm-3* genes are required for defense against Cry5B 55

3.9 Killing curves of animals on *S. aureus* bacteria expressing α-toxin (Hla+) or not expressing α-toxin (Hla-) 58

3.10 Cry5B and salt stress act synergistically in wildtype *C. elegans* 60

3.11 Cry5B and salt stress in *pmk-1* and *sek-1* mutants 60

3.12 A model for ttm gene regulation by the PMK-1 MAP kinase pathway 64

4.1 Cry5B exposure induces phosphorylation of PMK-1 MAP kinase 81

4.2 The PMK-1 MAP kinase is phosphorylated in response to some stress conditions.....82
4.3 The activation of PMK-1 by Cry5B is altered in kgb-1 and bre-4 mutants 83
4.4 *tir-1* is involved in Cry5B defense and loss of *tir-1* or *nsy-1* partially reduces phospho-PMK-1 levels... 84
4.5 A model for PMK-1 activation.....86
4.6 Dose response curves for *C. elegans* mutants with increased sensitivity to Cry5B 88
4.7 Negative control animals and positive control animals from the primary RNAi screen for the Hpo phenotype 90
4.8 The *cgt-3*(tm504) deletion mutant is hypersensitive to Cry5B and fails to activate PMK-1 during toxin exposure.....94
4.9 *cgt-3*(tm504) mutants on cadmium chloride and *Pseudomonas auriginosa* 95
4.10 ClustalW alignment of the *C. elegans* CGT-3 amino acid sequence with the sequence of the UDP-glucose ceramide glucosyltransferase protein from humans.....97
4.11 The *cgt-3*(tm504); *bre-3*(ye28) double mutant is resistant to Cry5B 98
4.12 A western blot using anti-PMK-1 sera 100
4.13 Model 1. The toxin sensor GSL 104
4.14 Model 2. Two toxin-binding GSLs 106
4.15 Model 3. Lipid rafts mediate PMK-1 signaling.....107
5.1 A model summarizing my work in the Aroian Lab.....118

LIST OF TABLES

1.1 Examples of bacteria that are pathogenic towards *C. elegans* 5

1.2 Comparison of pore sizes made by bacterial toxins 12

2.1 Summary of microarray timecourse data 25

3.1 Regulation of Cry5B induced genes *sek-1* and *kgb-1* 40

3.2 The behavior of the *ttm* transcripts in *sek-1*(+) and *sek-1*(-) animals 54

3.3 The behavior of the ttm transcripts in *kgb-1*(+) and *kgb-1*(-) animals 56

3.4 The genes identified from the microarray studies as transcriptioanlly activated by Cry5B in a *sek-1* dependent manner. 65

4.1 The 58 novel hpo genes from RNAi screen of chromosomes II and IV 90

4.2 The 9 *hpo* genes identified in the RNAi screen that were also transcriptionally up-regulated by Cry5B 91

4.3 *kgb-1* dependent *hpo* genes 92

ACKNOWLEDGEMENTS

I wish to thank my advisor, Raffi Aroian, for furthering my professional development as a scientist and my personal development as a critical thinker. I thank my committee for being as honest as they are supportive. I also thank collaborators Roman Sasik for his assistance with the microarray analysis and Laurence Abrami and Gisou van der Goot for demonstrating that our findings with p38 hold true in higher organisms. Finally, I would like to acknowledge the members of the Aroian lab, past and present, for countless scientific discussions and technical assistance.

Chapter 1 was in part adapted from the published work:

Huffman D.L., Bischof L.J., Griffitts J.S., and Aroian R.V. (2004). Pore worms: Using *Caenorhabditis elegans* to study how bacterial toxins interact with their target hosts. *International Journal of Medical Microbiology*, 293: 599-607. Review.

I was the primary author in this publication

Chapters 2 and 3 were in part adapted from the published work:

Huffman D.L., Abrami* L., Sasik* R., Corbeil J., van der Goot F.G., and Aroian R.V. (2004). Mitogen-activated protein kinase pathways defend against bacterial pore-forming toxins. *Proceedings of the National Academy of Sciences*. 101(30): 10995-11000.

I was the primary researcher in this publication

VITA

EDUCATION

B.S. in Biology, with honors (1999)
University of California, Davis

Ph.D. in Biological Sciences (2006)
University of California, San Diego

RESEARCH EXPERIENCE

Graduate Student, University of California, San Diego (2000 – present)
Response and defense to the pore-forming toxin Cry5B in *Caenorhabditis elegans*
Advisor: Raffi V. Aroian

Research Assistant, University of California, Davis (1999 – 2000)
Mutations affecting female meiosis in *Drosophila melanogaster*
Advisor: R. Scott Hawley

PUBLICATIONS

Bischof L.J., Huffman D.L., and Aroian R.V. (In press). Assays for Toxicity Studies in *C. elegans* with Bt Crystal Proteins. C. elegans*: Methods and Applications*. Ed. K. Strange. Humana Press.

Huffman D.L., Abrami* L., Sasik* R., Corbeil J., van der Goot F.G., and Aroian R.V. (2004). Mitogen-activated protein kinase pathways defend against bacterial pore-forming toxins. *Proceedings of the National Academy of Sciences*. 101(30): 10995-11000.

Huffman D.L., Bischof L.J., Griffitts J.S., and Aroian R.V. (2004). Pore worms: Using *Caenorhabditis elegans* to study how bacterial toxins interact with their target hosts. *International Journal of Medical Microbiology*, 293: 599-607. Review.

Griffitts J.S., Huffman D.L., Whitacre J.L., Barrows B.D., Marroquin L.D., Müller R., Brown J.R., Hennet T., Esko J.D., and Aroian R.V. (2003). Resistance to a bacterial toxin is mediated by removal of a conserved glycosylation pathway required for toxin - host interactions. *Journal of Biological Chemistry*, 278(46): 45594-45602.

FELLOWSHIPS

Genetics Training Grant (2001 – 2004)
Ruth L. Kirschstein National Research Service Award
National Institute of Health

Developmental Biology Training Grant (2001 – 2002)
National Research Service Award
Department of Health and Human Services

ABSTRACT OF THE DISSERTATION

The p38 MAP Kinase Pathway in Response and Defense to

Bacillus thuringiensis Crystal Toxins

by

Danielle Lee Huffman

Doctor of Philosophy in Biology

University of California, San Diego, 2006

Professor Raffi V. Aroian, Chair

Most of the bacteria we encounter everyday do us no harm and many are even beneficial. Those that do cause human disease must be able to get past our initial immune defenses, establish an infection site and find proper nutrition to continue to proliferate. These disease-causing bacteria produce gene products, known as virulence factors, to aid in these pathogenic processes.

Pore-forming toxins (PFTs) are among the most common and important virulence factors that bacteria can make. These toxins work by inserting into the membrane of a host cell to form a pore. Pneumolysin from *Streptococcus pneumonia* and streptolysin S made by *Streptococcus pyogenes* are examples of PFTs that are important for virulence. Despite their prevalence, it is often unclear how these toxins affect the host and contribute to virulence.

The agriculturally important bacterium *Bacillus thuringiensis* produces a family of PFTs, called Cry toxins. Using a nematicidal Cry toxin, Cry5B, and the nematode *Caenorhabditis elegans*, I characterized the host response to a PFT at the genomic level. These studies indicated that *C. elegans* responds quickly to Cry5B exposure in a manner that is qualitatively distinct from other forms of stress response. The host response data also lead to the identification of two signal transduction pathways, the p38 MAP kinase cascade and a JNK-1ike MAP kinase, that orchestrate toxin defenses. I then carried out a study to identify the transcriptional targets of both the p38 and JNK pathways in *C. elegans*. The p38 targets were screened genetically for those that play a role in Cry5B defense. This investigation lead to the discovery of the *ttm* gene class, toxin-regulated targets of MAP kinase.

I went on to find that toxin exposure also induces activation of the p38 pathway. To find some of the genes involved in this Cry5B-regulated activation, I performed a genetic screen in the *C. elegans* host. This screen identified a ceramide glucosyltransferase that is important for the toxin-regulated activation of p38 and is also mediates host protection to this toxin. Therefore, with respect to Cry5B response and defense, I identified both upstream and downstream components of the p38 MAP kinase pathway in *C. elegans*.

Chapter 1

Introduction to Pore-Forming Virulence Factors and the Model Host *Caenorhabditis elegans*

1.1 Summary

Pathogenic bacteria produce a wide range of gene products that contribute to their virulence. One particularly common and important type of virulence factor is a group of proteins known as the pore-forming toxins (PFTs). Depending on the particular toxin, the diameter of the pore produced by these proteins may be as small as only 1-2nm, or as large as 30-60 nm, as is observed with the cholesterol-dependent family of PFTs. A widely held misconception is that these toxins promote virulence by causing the targeted host cells to lyse. Recent evidence, however, suggests these toxins are not cytolytic to nucleated cells under physiological concentrations. At these sub-lytic concentrations, there are certain features of how host cells respond to different PFTs that appear to be conserved.

Pore-forming toxins are also seen in bacteria that infect invertebrates. *Bacillus thuringiensis* (Bt), a member of the *Bacillus cereus* group of bacteria, is distinguished by the crystal inclusion that it produces during sporulation. This crystal is composed of pore-forming protein toxins, called Cry toxins, that are toxic strictly to insects and

nematodes. In the Aroian lab, we are using *Caenorhabditis elegans* and one of the nematicidal Bt Cry toxins, Cry5B, as a system for studying host/toxin interactions in a genetically tractable host.

1.2 Bacterial Infection and Virulence Factors

Many notorious human diseases are the result of uncontrolled bacterial infections. Meningitis, gangrene, scarlet fever, cholera, peptic ulcers and many food borne illnesses are caused by pathogenic bacteria proliferating excessively in specific tissues of the body. While the discovery and implementation of antibiotic therapies have greatly aided in controlling infectious diseases, the emergence of antibiotic resistance and an increase in the number of immunocompromised individuals mean that bacterial virulence continues to be of concern to human health in both the developed an developing worlds (for review see (Cohen, 2000)).

In order to cause disease, a potential bacterial pathogen needs to produce the necessary gene products that enable it to reproduce in a susceptible host. These products, known as virulence factors, can include degradative enzymes, such as nucleases and proteases, as well as structural proteins that promote bacterial adhesion and toxins that directly damage host cells and tissues. Virulence factors can be the key proteins that allow the bacterium to gain access to a vulnerable host tissue, evade or disable host defenses or create favorable growth conditions. Any gene product that makes the strain more pathogenic is considered a virulence factor. Theoretically then, any step in the infection process can be aided by these factors and many different sorts of proteins have been identified as virulence factors.

1.3 *C. elegans* as a Model for Host-Pathogen Studies

The nematode *Caenorhabditis elegans* is a soil dwelling, bacterial feeder that has been used as a model system for genetic studies since the 1970's(Brenner, 1974). These animals primarily exist as hermaphrodites, but males are produced spontaneously approximately once in every 1000 fertilizations. Their genomes have five pairs of automosomes and an X chromosome (hermaphrodites are XX, males XO), altogether carrying roughly 20,000 genes. Progeny are laid as eggs that then hatch and go through a series of larval molts (L1 to L4) to finally become fertile adults capable of producing both eggs and sperm. Development takes approximately 50 hours from fertilization to adulthood when grown at 25°C, but adults can live for another three weeks before eventually succumbing to old age. Adult hermaphrodites have about 1000 somatic cells and the lineage of these cells has been carefully described. Additionally, as a fairly transparent organism, they are amenable to microscopic observation of internal structures. Their quick generation time, facile genetics and willingness to readily consume bacteria have recently made them a popular system for studying infectious bacteria in a live host. The pathogencity of specific strains of bacteria can be directly determined by feeding the nematodes the bacteria and looking for effects on the host within hours or a few days (for reviews see (Aballay and Ausubel, 2002; Alegado et al., 2003; Ewbank, 2002)).

Several gram negative and gram positive bacteria have been identified as *C. elegans* pathogens (Table 1.1) and the interactions of several bacterial virulence factors with the *C. elegans* host have been investigated. For example, death of *C. elegans* from initiation of feeding on gram negative *Pseudomonas aeruginosa*

strain PA14 was separated into a fast killing mode (hours) and a slow killing mode (days) that depended on the medium used for the assay (Tan et al., 1999). Subsequent studies on the fast killing mode identified phenazines, pigments that are secreted from *P. aeruginosa*, as toxins, are associated with killing of the worms (Mahajan-Miklos et al., 1999). A different strain of *P. aeruginosa*, PA01, was found to lead to rapid paralysis and death of *C. elegans*, and the toxin responsible for this effect was demonstrated to be hydrogen cyanide (Darby et al., 1999; Gallagher and Manoil, 2001). A transposon based mutagenic screen in *Serratia marcescens* identified a reduced virulence mutant with a transposon inserted in the *shlBA* operon that is required for production of the PFT hemolysin (Kurz et al., 2003). An as yet unidentified toxin or toxins have also been associated with the pathogenicity of *Burkholderia pseudomallei* in *C. elegans* (Gan et al., 2002; O'Quinn et al., 2001) Toxins have also been associated with the killing of *C. elegans* by gram positive bacteria. *Streptococcus pyogenes* grown on Todd-Hewitt broth supplemented with yeast extract killed *C. elegans*, and the toxicity was mediated through hydrogen peroxide (Jansen et al., 2002). The pore-forming toxin α-hemolysin was identified as one of several virulence factors from *Staphylococcus aureus* important for virulence in the nematode (Sifri et al., 2003).

Table 1.1. Examples of Bacteria that are pathogenic towards *C. elegans*

Bacteria	References
Gram Negative	
Aeromonas hydrophila	(Couillault and Ewbank, 2002)
Burkholderia pseudomallei	(Gan et al., 2002; O'Quinn et al., 2001)
Pseudomonas aeruginosa (PA01)	(Darby et al., 1999; Gallagher and Manoil, 2001)
Pseudomonas aeruginosa (PA14)	(Mahajan-Miklos et al., 1999; Tan et al., 1999)
Salmonella typhimurium	(Aballay et al., 2000; Labrousse et al., 2000)
Serratia marcescens	(Kurz et al., 2003; Mallo et al., 2002)
Yersinia pestis	(Darby et al., 2002)
Yersinia pseudotuberculosis	(Darby et al., 2002)
Gram Positive	
Bacillus thuringiensis	(Leyns et al., 1995; Marroquin et al., 2000)
Enterococcus faecalis	(Garsin et al., 2001; Sifri et al., 2002)
Microbacterium nematophilum	(Hodgkin et al., 2000)
Staphylococcus aureus	(Garsin et al., 2001; Sifri et al., 2003)
Streptococcus pneumoniae	(Garsin et al., 2001)
Streptococcus pyogenes	(Jansen et al., 2002)

1.4 Pore-Forming Toxins as Bacterial Virulence Factors

PFTs generally function extracellularly, where they bind to the surface of the host membrane via interaction with a specific receptor and then insert into the bilayer to form an oligomeric pore structure. PFTs can vary widely in sequence, size, structure and host cell receptor. Although some PFTs form pores in the membranes of intracellular organelles of the host cell, most of the known PFTs work by causing damage to host cells at the plasma membrane. Our laboratory is focused on studying the pore-forming Crystal (Cry) toxins made by *Bacillus thuringiensis* (Bt), a gram-positive soil bacterium and potent pathogen of insect larvae and nematodes.

As a member of the *Bacillus cereus* group of bacteria, Bt is distinguished by the crystal inclusion that it produces during sporulation. This crystal is composed of protein toxins, called Cry toxins. There are many different strains of Bt and they each make a different Cry toxin or set of Cry toxins. These different toxins vary in their

host specificities and often have a narrow host range. Many of these Cry toxins fall into a single family of proteins called main family Cry toxins. Several members of this family have been demonstrated to be pore-forming toxins and all main family Cry toxins are presumed to have pore-forming abilities (de Maagd et al., 2001). Because Cry toxins have no demonstrated toxicity towards humans or other mammals, insecticidal Cry toxins have been used extensively in transgenic crops for control of insect pests and as sprays for control of black flies and mosquitoes (de Maagd et al., 2001; Schnepf et al., 1998; Wei et al., 2003). While Cry toxins have traditionally been considered primarily as toxins against insects, specific Cry proteins are clearly toxic towards *C. elegans* as well as other nematodes (Griffitts et al., 2001; Marroquin et al., 2000; Wei et al., 2003). In both insects and nematodes, the pathogenicity of Bt is highly dependent on the pore-forming activity of its Cry toxins. In this way, Bt is similar to many other bacterial pathogens, including some capable of causing disease in humans, in that it makes a PFT to promote its virulence.

Unlike many PFTs, Bt Cry toxins are not secreted, but rather, are released from the bacterium when the mother cell lyses at the conclusion of sporulation. Upon ingestion by a susceptible insect or nematode, the crystal solubilizes within the intestinal lumen of its host, making the Cry protein accessible to intestinal proteases that cleave off the N- and C-termini of the protein. This proteolytic activation step allows the 3-domain toxin to then bind the appropriate receptor(s) on the surface of the intestinal epithelial cells. The toxin oligomerizes, the alpha-helices of domain I insert into the membrane and a pore of ~2nm is formed. The innocuousness of Cry toxins

with respect to vertebrates has been traced to defects in proteolytic activation/stability and lack of toxin binding receptors in vertebrate cells.

1.5 Using Cry5B and *C. elegans* to Understand Intoxication by a PFT

The nematicidal Cry toxins include Cry14A, Cry5B, Cry21A and Cry6A, all of which show toxicity to *C. elegans*. In the Aroian lab, we are using *C. elegans* and the toxin Cry5B to understand the *in vivo* interactions between a PFT and an in-tact host. To focus on the effects of Cry5B alone, we feed *C. elegans* purified Cry5B protein in liquid culture containing attenuated or non-pathogenic bacteria (*E. coli* or *Bacillus subtilis*) as a food source or, alternatively, simply plate the animals on a lawn of attenuated *E. coli* transformed with the Cry5B gene under an inducible promoter. This system enables us to study the intoxication process separately from the infection process.

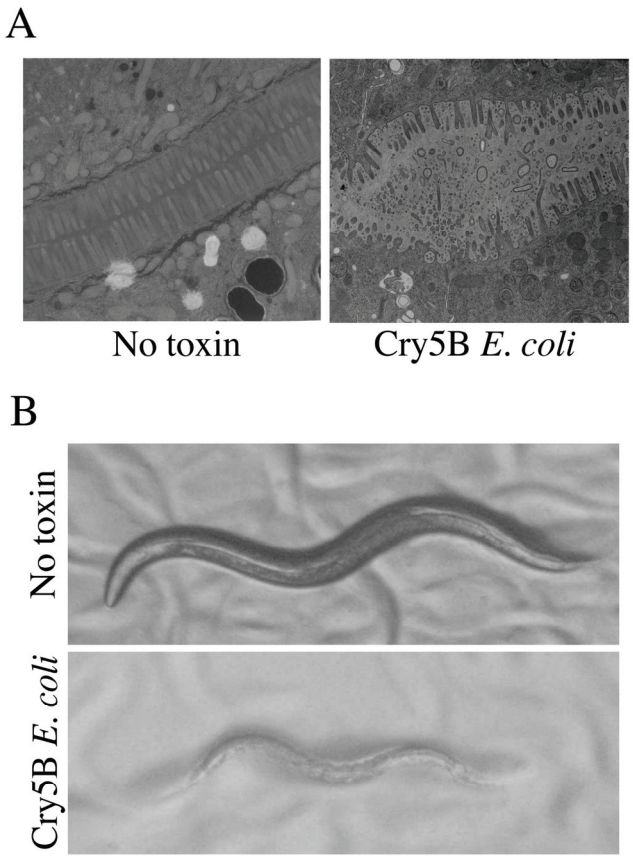

Figure 1.1. The effects of Cry5B on *C. elegans*. A, electron micrographs of animals feeding for 3 hours on either empty vector *E. coli* (No toxin, left hand panel) or *E. coli* expressing Cry5B toxin (Cry5B *E. coli*, right hand panel). B, photographs from a dissecting microscope of animals on empty vector *E. coli* (No toxin, top panel) or *E. coli* expressing Cry5B (Cry5B *E. coli*, bottom panel).

When wild-type *C. elegans* L4 larvae are placed on a lawn of *E. coli* that is expressing the Cry5B protein, damage to the animals becomes increasingly devastating over time. Within the first 30 minutes, the animals will temporarily slow the pumping of the pharynx, an indication that their feeding has slowed down. After three hours of feeding on this toxic *E. coli*, animals examined by electron microscopy show dramatic changes to the intestinal epithelium. Relative to control animals, the toxin fed larvae appear to have distended intestinal lumens and discorganized microvilli that appear to be sloughing off from the cell surface (Figure 1.1A).

Additionally, double-membrane bound organelles are seen in the cytosol of some of the intestinal cells, an indication that these cells are undergoing autophagy. By 24 hours, the effects of intoxication are clearly visible under the dissecting microscope. The animals are smaller and paler than controls (Figure 1.1B). They also behave lethargically and are impaired in egg production. A closer look at these animals shows the intestine is pulling away from the body wall and vacuoles have formed in some of the intestine cells (Marroquin et al., 2000). After five days of continual feeding on these Cry5B *E. coli* plates, the majority of animals are dead.

The fact that the effects of the toxin can be observed within 30 minutes, but death takes several days is, I think, an interesting observation. What determines how long it takes for these animals to finally succumb to this toxin? Is it entirely dependent on the toxin, or does the response of the host play a role in this five day intoxication process? These are the initial, fundamental questions raised by our early observations that I would eventually explore as a graduate student.

1.6 Mammalian Intoxication and Responses to Pore-Forming Toxins

What is known of responses to bacterial pore-forming toxins in mammalian host cells? There are some recurring themes that I will deal with below, specifically, induction of a calcium response, initiation of cell death, and formation of vacuoles.

One commonly reported response of a cell to a PFT is an increase in intracellular calcium levels or the induction of calcium oscillations. By monitoring the first several minutes of toxin exposure, Krause et. al. (Krause et al., 1998) found that purified aerolysin at concentrations of 100ng/ml caused an increase in calcium

levels in human granulocytes that is di-phasic, with the early phase occurring almost immediately upon toxin exposure. This dose dependent response was found to be the result of calcium release from intracellular stores mediated by G-protein activation. Staphylococcal α-toxin and streptolysin O were also found to have effects on calcium levels in this same study. Interestingly, studies examining lower concentrations of aerolysin in T lymphoma cells found that even at subnanomolar concentrations, cytosolic calcium levels increase (Nelson et al., 1999). These increases, however, were attributed to influx from extracellular sources rather than release from stores. *Listeria monocytogenes* is also capable of inducing rapid, multi-phasic calcium elevations in a macrophage-like cell line that are dependent on the pore-forming toxin listeriolysin O (LLO) (Goldfine and Wadsworth, 2002; Wadsworth and Goldfine, 1999). Further work in epithelial cells and kidney cells indicated the source of calcium in these LLO induced influxes is the external medium (Dramsi and Cossart, 2003; Repp et al., 2002). Influx through the cell membrane is also the cause of the calcium oscillations seen in neuroblastomas cells treated with the pneumococcal toxin pneumolysin (Stringaris et al., 2002). Calcium increase in these cells was followed by cell death, with 40% of the cells dieing within three hours of treatment. Here, calcium chelators inhibited this cell death response, suggesting that increased calcium levels caused by pneumolysin may serve to promote cell death. Similar observations have been made in models of aerolysin intoxication where it has been proposed that the toxin-induced calcium increases act as an apoptotic signal (Nelson et al., 1999). Although the association between poisonous levels of calcium and cell death has been well documented, the function of calcium flux as a host response and the downstream

consequences to these fluxes remains unclear. Because calcium plays a role in so many cellular processes, there is potential for these calcium elevations to have wide spread impact.

Induction of cell death, a property that has been reported for many pore-forming toxins, is a good example of how intoxication is the work of both the toxin and the host cell machinery. For the vacuolating cytotoxin from *Helicobacter pylori*, VacA, induction of cell death appears to involve the direct activity of the toxin in the cytosol. When expressed in HeLa cells as a GFP fusion, VacA-GFP localizes to the mitochondria where it activates caspase-3 and causes apoptotic-like cell death (Galmiche et al., 2000). In the case of pneumolysin, recent work suggested that the toxin promotes cell death in neuroblastoma cells by activating the mitogen activated kinase, p38 (Stringaris et al., 2002). p38 MAP kinase is part of a conserved signal transduction cascade that regulates inflammation, immune response and apoptosis and responds to a variety of stress simuli. This result not only demonstrates that pore-forming toxins can act as a signal to the host to trigger immune pathways, but it also shows that the action of pneumolysin at the cell membrane can be translated into activation of the highly regulated, intracellular program of apoptosis. Currently, many questions remain about the role of cell death as a response to PFTs and PFT-producing bacteria. Is cell death largely a protective response that limits the spread of the bacteria, or is it a mechanism used by the toxin to kill off host immune cells? Ultimately, the function of cell death may be found to vary depending on the site and stage of infection.

Table 1.2. Comparison of pore sizes made by bacterial toxins

Pore-forming toxin	Pore diameter	Reference
Vibrio cholera hemolysin	1-2 nm	(Zitzer et al., 1997)
Aerolysin	3.8-4.6 nm	(Tschodrich-Rotter et al., 1996)
Cry toxin	2.0-2.6 nm	(Peyronnet et al., 2002)
Steptolysin O	30 nm	(Bhakdi et al., 1985)

Some bacteria make pore-forming toxins that cause vacuolization of cellular organelles. The VacA protein from *Helicobacter pylori* is a classic example. The vacuoles caused by this toxin are thought to be the result of fusion of late endosomal and lysosomal compartments (Molinari et al., 1997; Papini et al., 1997). The hemolysin produced by *Vibrio Cholera* also causes vacuolization in Vero cells within 30 minutes (Moschioni et al., 2002). These vacuoles contain membranes from the trans-Golgi network as well as from endosomes and lysosomes. The hemolysin from *Serratia marcescens* also causes vacuolization in epithelial cells (Hertle et al., 1999). Abrami et al (1998) found that aerolysin is capable of inducing vacuolization of the endoplasmic reticulum in a variety of cell types. These vacuoles were detectable within an hour of toxin exposure. In this study, vacuoles were not observed in BHK cells treated with steptolysin O, indicating that any permeabilization of the plasma membrane is not sufficient for vacuolization. Furthermore, calcium ionophores failed to induce vacuole formation, ruling out the possibility that vacuoles are the consequence of calcium influx. These findings and others showing vacuolization of mammalian cells by certain PFTs are of particular interest to us because Cry5B has been shown to cause vacuole formation in *C. elegans* intestinal cells *in vivo*. It remains to be seen how these vacuoles contribute to animal intoxication.

What are often missing from these studies using cultured cells as the experimental host, are the *in vivo* consequences of a particular response. Certainly cell death could be a means of promoting virulence, but could it sometimes be protective if it also limits the spread of an infection? Would suppression of vacuolization make the host more susceptible to the pathogen, or does the vacuole protect the cell and the host? Our system using *C. elegans* and Cry5B to study intoxication processes could provide an opportunity to address these sorts of issues.

Part of this chapter was adapted from segments of the following published paper, of which the author of this dissertation was the primary author.

Huffman D.L., Bischof L.J., Griffitts J.S., and Aroian R.V. (2004). Pore worms: Using *Caenorhabditis elegans* to study how bacterial toxins interact with their target hosts. *International Journal of Medical Microbiology*, 293: 599-607. Review.

The images in Figure 1.1A were acquired by J. Griffitts and K. McDonald

1.7 References

References for Table 1.1

Gram negative bacteria

((Aballay et al., 2000; Couillault and Ewbank, 2002; Darby et al., 1999; Darby et al., 2002; Gallagher and Manoil, 2001; Gan et al., 2002; Kurz et al., 2003; Labrousse et al., 2000; Mahajan-Miklos et al., 1999; Mallo et al., 2002; O'Quinn et al., 2001; Tan et al., 1999)

Gram positive bacteria

(Garsin et al., 2001; Hodgkin et al., 2000; Jansen et al., 2002; Marroquin et al., 2000; Sifri et al., 2003; Sifri et al., 2002)

References

Aballay, A., and Ausubel, F. M. (2002). *Caenorhabditis elegans* as a host for the study of host-pathogen interactions. Curr Opin Microbiol *5*, 97-101.

Aballay, A., Yorgey, P., and Ausubel, F. M. (2000). *Salmonella typhimurium* proliferates and establishes a persistent infection in the intestine of *Caenorhabditis elegans*. Curr Biol *10*, 1539-1542.

Alegado, R. A., Campbell, M. C., Chen, W. C., Slutz, S. S., and Tan, M. W. (2003). Characterization of mediators of microbial virulence and innate immunity using the *Caenorhabditis elegans* host-pathogen model. Cell Microbiol *5*, 435-444.

Bhakdi, S., Tranum-Jensen, J., and Sziegoleit, A. (1985). Mechanism of membrane damage by streptolysin-O. Infect Immun *47*, 52-60.

Brenner, S. (1974). The genetics of *Caenorhabditis elegans*. Genetics *77*, 71-94.

Cohen, M. L. (2000). Changing patterns of infectious disease. Nature *406*, 762-767.

Couillault, C., and Ewbank, J. J. (2002). Diverse bacteria are pathogens of *Caenorhabditis elegans*. Infect Immun *70*, 4705-4707.

Darby, C., Cosma, C. L., Thomas, J. H., and Manoil, C. (1999). Lethal paralysis of *Caenorhabditis elegans* by *Pseudomonas aeruginosa*. Proc Natl Acad Sci U S A *96*, 15202-15207.

Darby, C., Hsu, J. W., Ghori, N., and Falkow, S. (2002). *Caenorhabditis elegans*: plague bacteria biofilm blocks food intake. Nature *417*, 243-244.

de Maagd, R. A., Bravo, A., and Crickmore, N. (2001). How *Bacillus thuringiensis* has evolved specific toxins to colonize the insect world. Trends Genet *17*, 193-199.

Dramsi, S., and Cossart, P. (2003). Listeriolysin O-mediated calcium influx potentiates entry of Listeria monocytogenes into the human Hep-2 epithelial cell line. Infect Immun *71*, 3614-3618.

Ewbank, J. J. (2002). Tackling both sides of the host-pathogen equation with *Caenorhabditis elegans*. Microbes Infect *4*, 247-256.

Gallagher, L. A., and Manoil, C. (2001). *Pseudomonas aeruginosa* PAO1 kills *Caenorhabditis elegans* by cyanide poisoning. J Bacteriol *183*, 6207-6214.

Galmiche, A., Rassow, J., Doye, A., Cagnol, S., Chambard, J. C., Contamin, S., de Thillot, V., Just, I., Ricci, V., Solcia, E.*, et al.* (2000). The N-terminal 34 kDa fragment of Helicobacter pylori vacuolating cytotoxin targets mitochondria and induces cytochrome c release. Embo J *19*, 6361-6370.

Gan, Y. H., Chua, K. L., Chua, H. H., Liu, B., Hii, C. S., Chong, H. L., and Tan, P. (2002). Characterization of *Burkholderia pseudomallei* infection and identification of novel virulence factors using a *Caenorhabditis elegans* host system. Mol Microbiol *44*, 1185-1197.

Garsin, D. A., Sifri, C. D., Mylonakis, E., Qin, X., Singh, K. V., Murray, B. E., Calderwood, S. B., and Ausubel, F. M. (2001). A simple model host for identifying Gram-positive virulence factors. Proc Natl Acad Sci U S A *98*, 10892-10897.

Goldfine, H., and Wadsworth, S. J. (2002). Macrophage intracellular signaling induced by Listeria monocytogenes. Microbes Infect *4*, 1335-1343.

Griffitts, J. S., Whitacre, J. L., Stevens, D. E., and Aroian, R. V. (2001). Bt toxin resistance from loss of a putative carbohydrate-modifying enzyme. Science *293*, 860-864.

Hertle, R., Hilger, M., Weingardt-Kocher, S., and Walev, I. (1999). Cytotoxic action of Serratia marcescens hemolysin on human epithelial cells. Infect Immun *67*, 817-825.

Hodgkin, J., Kuwabara, P. E., and Corneliussen, B. (2000). A novel bacterial pathogen, *Microbacterium nematophilum*, induces morphological change in the nematode *C. elegans*. Curr Biol *10*, 1615-1618.

Jansen, W. T., Bolm, M., Balling, R., Chhatwal, G. S., and Schnabel, R. (2002). Hydrogen peroxide-mediated killing of *Caenorhabditis elegans* by *Streptococcus pyogenes*. Infect Immun *70*, 5202-5207.

Krause, K. H., Fivaz, M., Monod, A., and van der Goot, F. G. (1998). Aerolysin induces G-protein activation and Ca2+ release from intracellular stores in human granulocytes. J Biol Chem *273*, 18122-18129.

Kurz, C. L., Chauvet, S., Andres, E., Aurouze, M., Vallet, I., Michel, G. P., Uh, M., Celli, J., Filloux, A., De Bentzmann, S.*, et al.* (2003). Virulence factors of the human opportunistic pathogen *Serratia marcescens* identified by *in vivo* screening. Embo J *22*, 1451-1460.

Labrousse, A., Chauvet, S., Couillault, C., Kurz, C. L., and Ewbank, J. J. (2000). *Caenorhabditis elegans* is a model host for *Salmonella typhimurium*. Curr Biol *10*, 1543-1545.

Leyns, F., Borgonie, G., Arnaut, G., and Dewaele, D. (1995). Nematocidal Activity of Bacillus-Thuringiensis Isolates. Fundamental and Applied Nematology *18*, 211-218.

Mahajan-Miklos, S., Tan, M. W., Rahme, L. G., and Ausubel, F. M. (1999). Molecular mechanisms of bacterial virulence elucidated using a *Pseudomonas aeruginosa-Caenorhabditis elegans* pathogenesis model. Cell *96*, 47-56.

Mallo, G. V., Kurz, C. L., Couillault, C., Pujol, N., Granjeaud, S., Kohara, Y., and Ewbank, J. J. (2002). Inducible antibacterial defense system in *C. elegans*. Curr Biol *12*, 1209-1214.

Marroquin, L. D., Elyassnia, D., Griffitts, J. S., Feitelson, J. S., and Aroian, R. V. (2000). Bacillus thuringiensis (Bt) toxin susceptibility and isolation of resistance mutants in the nematode Caenorhabditis elegans. Genetics *155*, 1693-1699.

Molinari, M., Galli, C., Norais, N., Telford, J. L., Rappuoli, R., Luzio, J. P., and Montecucco, C. (1997). Vacuoles induced by Helicobacter pylori toxin contain both late endosomal and lysosomal markers. J Biol Chem *272*, 25339-25344.

Moschioni, M., Tombola, F., de Bernard, M., Coelho, A., Zitzer, A., Zoratti, M., and Montecucco, C. (2002). The Vibrio cholerae haemolysin anion channel is required for cell vacuolation and death. Cell Microbiol *4*, 397-409.

Nelson, K. L., Brodsky, R. A., and Buckley, J. T. (1999). Channels formed by subnanomolar concentrations of the toxin aerolysin trigger apoptosis of T lymphomas. Cell Microbiol *1*, 69-74.

O'Quinn, A. L., Wiegand, E. M., and Jeddeloh, J. A. (2001). *Burkholderia pseudomallei* kills the nematode *Caenorhabditis elegans* using an endotoxin-mediated paralysis. Cell Microbiol *3*, 381-393.

Papini, E., Satin, B., Bucci, C., de Bernard, M., Telford, J. L., Manetti, R., Rappuoli, R., Zerial, M., and Montecucco, C. (1997). The small GTP binding protein rab7 is essential for cellular vacuolation induced by Helicobacter pylori cytotoxin. Embo J *16*, 15-24.

Peyronnet, O., Nieman, B., Genereux, F., Vachon, V., Laprade, R., and Schwartz, J. L. (2002). Estimation of the radius of the pores formed by the *Bacillus thuringiensis* Cry1C delta-endotoxin in planar lipid bilayers. Biochim Biophys Acta *1567*, 113-122.

Repp, H., Pamukci, Z., Koschinski, A., Domann, E., Darji, A., Birringer, J., Brockmeier, D., Chakraborty, T., and Dreyer, F. (2002). Listeriolysin of Listeria monocytogenes forms Ca2+-permeable pores leading to intracellular Ca2+ oscillations. Cell Microbiol *4*, 483-491.

Schnepf, E., Crickmore, N., Van Rie, J., Lereclus, D., Baum, J., Feitelson, J., Zeigler, D. R., and Dean, D. H. (1998). *Bacillus thuringiensis* and its pesticidal crystal proteins. Microbiol Mol Biol Rev *62*, 775-806.

Sifri, C. D., Begun, J., Ausubel, F. M., and Calderwood, S. B. (2003). *Caenorhabditis elegans* as a model host for *Staphylococcus aureus* pathogenesis. Infect Immun *71*, 2208-2217.

Sifri, C. D., Mylonakis, E., Singh, K. V., Qin, X., Garsin, D. A., Murray, B. E., Ausubel, F. M., and Calderwood, S. B. (2002). Virulence effect of *Enterococcus faecalis* protease genes and the quorum-sensing locus fsr in *Caenorhabditis elegans* and mice. Infect Immun *70*, 5647-5650.

Stringaris, A. K., Geisenhainer, J., Bergmann, F., Balshusemann, C., Lee, U., Zysk, G., Mitchell, T. J., Keller, B. U., Kuhnt, U., Gerber, J.*, et al.* (2002). Neurotoxicity of pneumolysin, a major pneumococcal virulence factor, involves calcium influx and depends on activation of p38 mitogen-activated protein kinase. Neurobiol Dis *11*, 355-368.

Tan, M. W., Mahajan-Miklos, S., and Ausubel, F. M. (1999). Killing of *Caenorhabditis elegans* by *Pseudomonas aeruginosa* used to model mammalian bacterial pathogenesis. Proc Natl Acad Sci U S A *96*, 715-720.

Tschodrich-Rotter, M., Kubitscheck, U., Ugochukwu, G., Buckley, J. T., and Peters, R. (1996). Optical single-channel analysis of the aerolysin pore in erythrocyte membranes. Biophys J *70*, 723-732.

Wadsworth, S. J., and Goldfine, H. (1999). Listeria monocytogenes phospholipase C-dependent calcium signaling modulates bacterial entry into J774 macrophage-like cells. Infect Immun *67*, 1770-1778.

Wei, J. Z., Hale, K., Carta, L., Platzer, E., Wong, C., Fang, S. C., and Aroian, R. V. (2003). *Bacillus thuringiensis* crystal proteins that target nematodes. Proc Natl Acad Sci U S A *100*, 2760-2765.

Zitzer, A., Palmer, M., Weller, U., Wassenaar, T., Biermann, C., Tranum-Jensen, J., and Bhakdi, S. (1997). Mode of primary binding to target membranes and pore formation induced by *Vibrio cholerae* cytolysin (hemolysin). Eur J Biochem *247*, 209-216.

Chapter 2

Genomic Analysis of the Host Response to Cry5B

2.1 Summary

Using microarray technology, a genomic approach was undertaken to characterize the host response in *C. elegans* to the PFT Cry5B. The data uncovered over one thousand genes that showed changes in transcript abundance within the first four hours of toxin exposure. Even as soon as one hour after being placed on Cry5B *E. coli*, over 300 host genes responded to toxin at the transcript level. To better gauge the magnitude and specificity of this response relative to some other kind of stressor, the transcriptional profile of Cry5B-fed nematodes was compared to that of animals exposed to the heavy metal cadmium. This comparison indicated that approximately half of the genes that respond to Cry5B also respond to cadmium, but not necessarily to the same extent. The two different stressors, Cry5B and cadmium, also displayed differences in the kinds of gene classes they preferentially regulate.

2.2 Introduction

The intracellular events that take place during the process of intoxication likely include changes in protein activity, alterations in cytosol composition, morphological

changes to the cell or intracellular organelles and modified gene expression. Presumably, properties of both the toxin and the host shape these events. That is, some of these events are induced by the toxin to promote pathogenesis while other events are the result of the host trying to protect itself or repair the damaged cell. Therefore, an examination of host response could reveal clues on the mechanisms of the toxin as well as uncover some of the protective measures taken by the host. When I started this project, the existing data on the *C. elegans* response to Cry5B had been collected from microscopic observation. My goal was to describe the host response on a more molecular level in order to better understand the intoxication process and host/toxin interactions.

Over the past several years, gene expression analysis has become an increasingly common approach for researchers to get an idea of the genes potentially involved in a particular biological process by determining which genes respond to that process with a change in transcript abundance. By far, the most common technology employed for gene expression analysis is microarrays. Simply put, microarrays are small chips or slides with a grid of spots, where each spot is a sample of oligonucleotide whose sequence is complementary to the mRNA sequence of a single gene in the genome. This tool allows investigators to measure the mRNA abundance of nearly every gene in the genome relative to a control or standard. Microarrays can be particularly useful when the goal is to get an initial global characterization of a particular process in order to generate more specific, testable hypotheses about that process. For all the above reasons, I chose to begin my project on the host response to Cry5B with a microarray experiment to find genes that respond to Cry5B exposure.

Several commercially available microarray platforms exist. To date, Affymetrix gene chips continue to be an industry standard for microarray expression studies. The oligonucleotide probes are synthesized directly on the chip, eliminating much of the chip-to-chip variability that comes from spotting the samples onto the matrix robotically. Each probe is a 25mer of complementary sequence and each gene in the genome is represented by 11 unique, non-overlapping probes. The collection of probes for a particular gene/transcript is known as a probe set.

A handful of studies have been reported in the literature examining the transcriptional response to specific bacterial toxins. One such study examined the response of mouse macrophages exposed to cytotoxic enterotoxin from *Aeromonas hydrophila* (Act) (Galindo et al., 2003). These investigators used a sublethal dose of Act (6ng/ml) and checked two exposure times, 2 hours and 12 hours. At two hours, they identified 157 up-regulated genes and another 35 that were down-regulated with respect to untreated control cells. Among the list of up-regulated genes were 13 with roles in apoptosis. Because of this trend, they tested if Act induces apoptosis in their macrophage cell line and found that it did. The ability of Act to induce apoptosis had not previously been reported.

Another group used microarray analysis to look for gene expression changes in a human cell line exposed to a toxin from *Helicobacter pylori* called CagA (Yokoyama et al., 2005). As a virulence factor, CagA is injected into the host cell by the bacterium via the type IV secretion system. Once inside the host cell, CagA is phosphorylated by members of the Src family of kinases. This phosphorylation event then allows CagA to bind a number of different signal transduction proteins in the cell,

including certain oncoproteins, and de-regulate their activity. In their microarray study, the authors ectopically expressed CagA in gastric epithelial cells and monitored for changes in transcript levels at several time-points within the first 24 hours of transgene injection. They identified 71 genes that are transcriptionally activated by CagA expression shortly after transgene expression is detected. They then examined the promoter regions of these 71 genes and found that binding sites for the NFAT family of transcription factors were over-represented in these promoters. As a result of this finding, they went on to show that NFAT transcription factors are activated by CagA and this activation is dependent on CagA phosphorylation.

Yet another study explored gene expression changes in response to an infectious bacterium that produces a pore-forming toxin (Rogers et al., 2003). In this case, the investigators made use of two isogenic strains of *Streptococcus pneumoniae*, one that makes the pore-forming toxin pneumolysin and one that does not. They used microarrays to find genes that are regulated by *S. pneumoniae* exposure in a human monocyte cell line and, more specifically, to determine how much of this gene regulation is dependent on pneumolysin expression. From these studies, this group of researchers found 116 genes that are up-regulated in a pneumolysin-dependent manner and only one gene this is up-regulated by *S. pneumoniae* independent of pneumolysin. This result suggests a potentially pivotal role for this virulence factor in eliciting a host response at the transcript level.

Taken together, these studies indicate that new insights into bacterial toxin action can be made through the study of host response using microarray analysis.

2.3 Timecourse of Cry5B Transcriptional Response

I used Affymetrix *C. elegans* genome chips to determine how gene expression profiles change in *C. elegans* whole animals upon exposure to Cry5B crystal toxin. Instead of the standard wild-type *C. elegans* strain, N2, I used a temperature sensitive mutant strain, *glp-4*(bn2). The *glp-4* mutants have somatic gonad cells, but the germ cells fail to proliferate, reducing transcriptional noise from this non-intestinal tissue (Beanan and Strome, 1992). Quantitative dose response curves show that the *glp-4*(bn2) strain has a wild-type susceptibility to Cry5B (Figure 2.1).

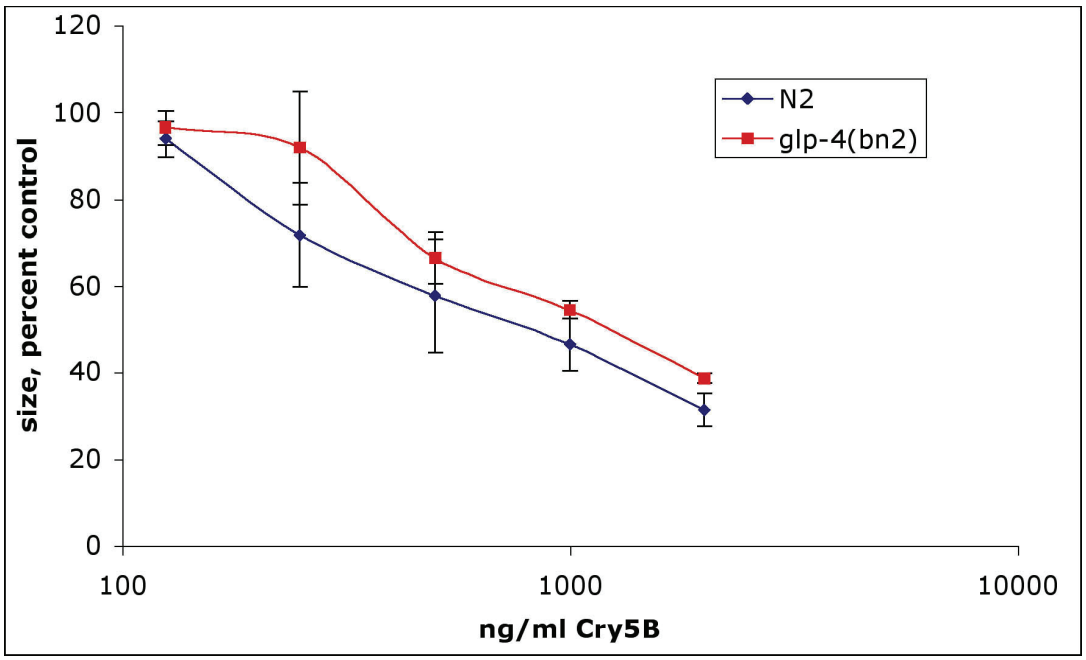

Figure 2.1: Quantitative growth-based toxicity assays with N2 and *glp-4*(bn2). Various doses of Cry5B are plotted on a logarithmic scale. The ordinate axis shows the size of nematodes relative to no-toxin controls run in parallel. Each point represents ~60 animals from three independent experiments. Standard error bars are indicated.

I started with a synchronous population of ~160,000 L4-staged hermaphrodites. From this population, approximately 20,000 animals were pipetted onto each of eight agar plates. Four of the agar plates had *E. coli* lawns expressing

Cry5B toxin while the other four were control plates of *E. coli* expressing the Bt toxin Cry5A. Cry5A and Cry5B are related crystal proteins, but Cry5A shows no toxicity towards *C. elegans* and so it served as the negative control in these experiments. Because my goal was to identify genes that respond to intoxication and not just ingestion of a crystal protein, *per se*, Cry5A was chosen as a control rather than *E. coli* producing no Crystal toxin at all. After one hour of feeding, the worms from one Cry5A plate and one Cry5B plate were separately harvested for RNA isolation. This was repeated again at two hours and four hours, so that at each time-point there was an RNA sample from Cry5B-treated animals and an RNA sample from Cry5A-treated animals. Each RNA sample was then given to the UCSD Genomics Core for processing, chip hybridization, scanning and analysis. The entire time-course was repeated twice more, for a total of three independent samples at each time-point.

Analysis was carried out by Dr. Roman Sasik at the UCSD Genomics Core using the Corgan program to calculate a signal intensity for each probe set under each condition in each of the three replicates (Sasik et al., 2002). Then, the statistical package FOCUS was used to determine which genes showed significant differences in transcript abundance between the Cry5B and Cry5A conditions at the identical time-point (Cole et al., 2003). A brief summary of the results of this analysis is presented in Table 2.1. Overall, this study identified a total of 546 genes that get transcriptionally up-regulated by Cry5B toxin within the first four hours of treatment and another 380 genes that are down-regulated within that same time.

Table 2.1: Summary of microarry timecourse data. Numbers of genes found to be regulated by Cry5B exposure after 1, 2, or 4 hours. A 2x or 10x change refers to the ratio of the average signal intensity in one RNA sample relative to the other RNA sample (Cry5B/Cry5A for up-regulated and Cry5A/Cry5B for down-regulated).

	Up-regulated genes			Down-regulated genes		
	Total # genes	2x and above	10x and above	Total # genes	2x and above	10x and above
1 hour	263	175	26	95	32	0
2 hours	216	171	30	209	151	4
4 hours	345	270	44	177	144	8
Overall	546			380		

2.4 Comparing Response to Cry5B with Response to Cadmium

To help gauge the specificity of this response, I wanted to better understand: 1) what level of transcriptional change is typical for animals exposed to a toxic agent, 2) which of the Cry5B responsive genes represent a general stress response and, 3) which genes appear to be regulated specifically by Cry5B. I again used microarray analysis to compare the Cry5B response to the response to another kind of stress agent, the heavy metal cadmium. Cadmium is capable of damaging lipids, proteins and DNA. It was chosen because, like Cry5B, cadmium kills worm in a dose dependent manner and has observable effects on worm health. However, unlike Cry5B, cadmium is a small molecule with little specificity and, importantly, it is not a pore-forming protein toxin. For this set of arrays, I exposed L4-staged *glp-4*(bn2) animals to Cry5B or cadmium for three hours. For Cry5B, the treated animals were placed on *E. coli* expressing Cry5B and the control animals were fed *E. coli* carrying the empty vector. For cadmium, the treated animals were placed on lawns of OP50 *E. coli* with 1mM cadmium chloride in the agar. The control animals for the cadmium group were put on OP50 *E. coli* plates without the cadmium chloride. A 1mM

concentration of cadmium chloride was chosen because worms die on this dose at the same rate as they die on Cry5B *E. coli* (Figure 2.2). RNA from Cry5B treated animals was compared to RNA from empty vector treated animals. RNA from cadmium treated animals was compared to RNA from animals put on non-cadmium plates. Then, the list of genes regulated by Cry5B was compared to the list of genes regulated by cadmium. One caveat of these comparisons is that the nonpathogenic *E. coli* strains used for the Cry5B experiments was JM103 and the *E. coli* strain used for the cadmium experiments was OP50. However, in each case, the non-toxic control is appropriately matched.

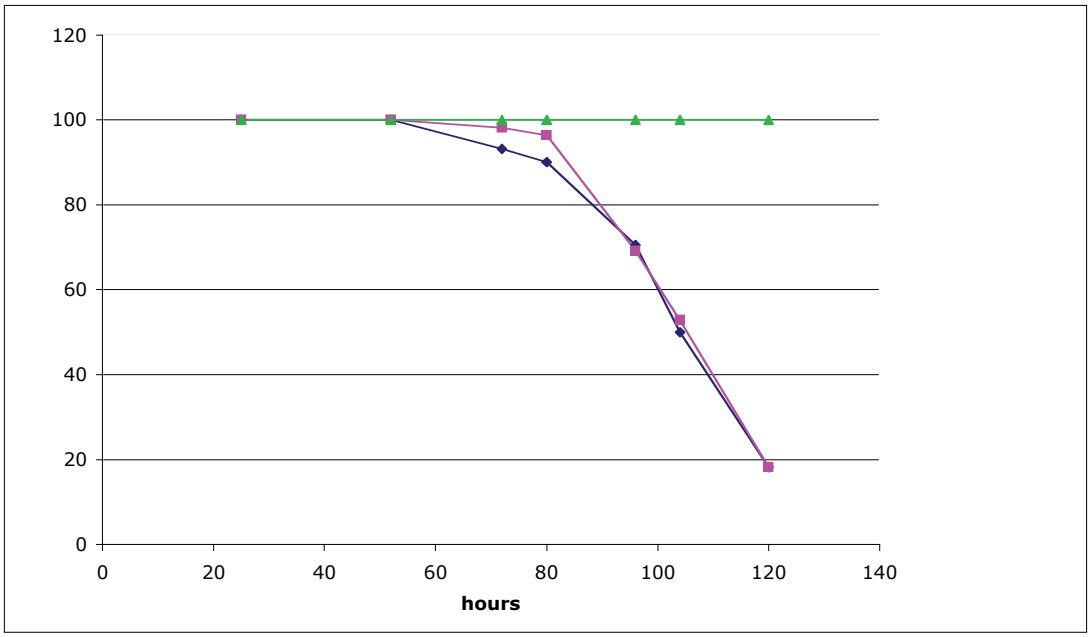

Figure 2.2: Animals on 1mM cadmium die at a similar rate to animals on Cry5B *E. coli*. On the Y axis is the percent of animals alive over time on three different conditions: Cry5B *E. coli*, agar plates containing 1mM cadmium, or no toxin. *glp-4*(bn2) animals were placed on assay conditions at L4 stage.

The results of this comparison indicated that both stressors regulate a similar number of genes at the three hour time-point: 1092 genes for Cry5B and 1083 genes for cadmium. However, just under 50% of the genes regulated by one stressor were

regulated by the other stressor as well (Figure 2.3). Moreover, even genes that showed transcriptional changes with both toxins were sometimes regulated to very different degrees under the two different conditions. Figure 2.4 illustrates this point by plotting the behavior of individual genes with the two treatments. This figure also points out reoccurring gene classes that show preference for one stress or the other. From this analysis, several transcription factors and cytoskeletal genes appear to be specifically regulated by Cry5B while cadmium is inducing more heat shock and detoxification genes.

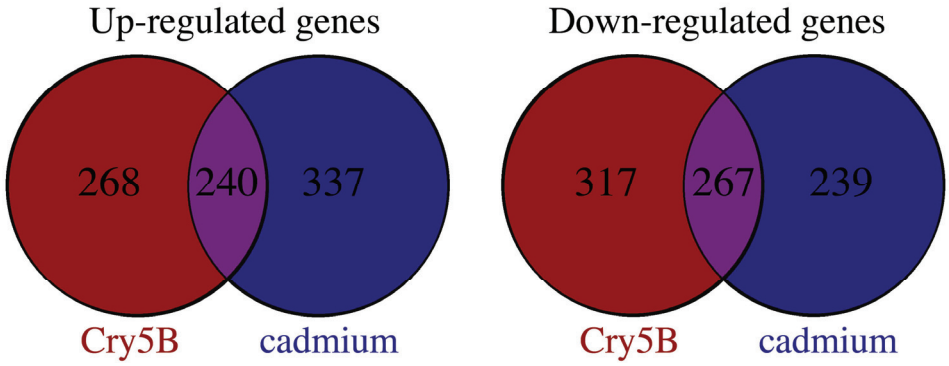

Figure 2.3: Some of Cry5B transcriptional response is specific. Venn diagram illustrating the overlap between genes regulated by Cry5B exposure to genes regulated by cadmium exposure after 3 hours

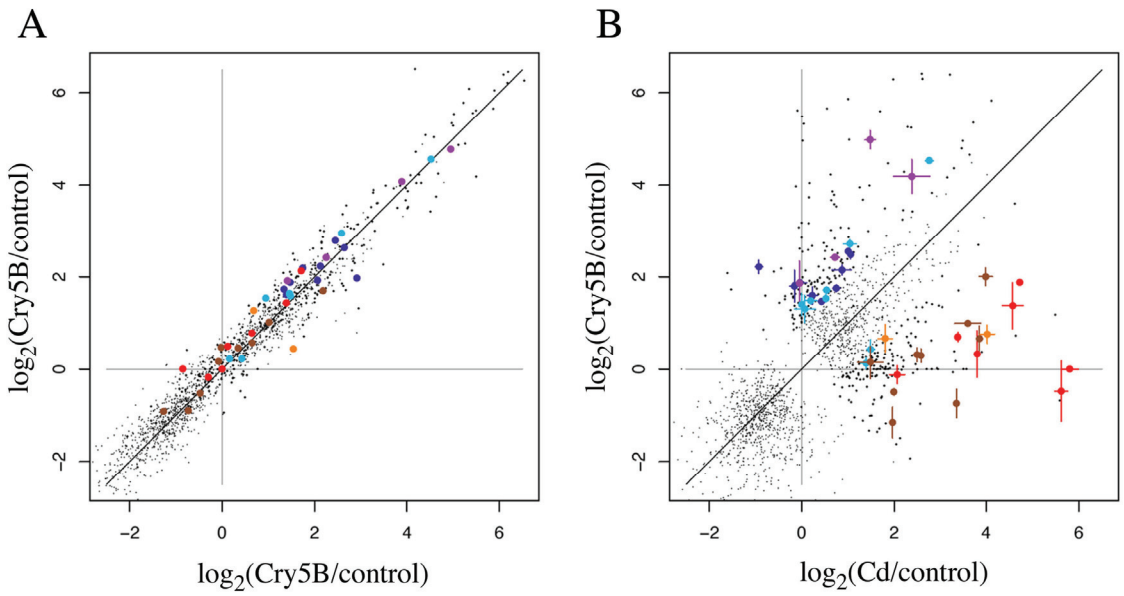

Figure 2.4: Behavior of 1,670 probe sets induced by one or both of Cry5B and Cd treatment. A few strongly down-regulated genes were omitted to improve plot resolution for up-regulated genes. (*A*) The fold induction of the probe sets for two of the independent Cry5B trials plotted against each other. The plot demonstrates excellent correlation between the two trials. (*B*) The fold induction of the probe sets for Cd trials (average of three trials) and for Cry5B (averaged over three trials) plotted against each other. Although the fold induction of some probe sets is similar, other probe sets (located off the diagonal) show significant differences, indicative of different responses to Cry5B and Cd. Some genes that show 2-fold difference between the two conditions were grouped based on their ontology and are shown in color. A few genes preferentially induced by Cd are glutathione *S*-transferase genes (brown), heat-shock genes(red), and known stress-induced genes (orange). A few genes preferentially induced by Cry5B include pathogen or pathogen-associated induced genes (purple) and cytoskeletal and cell adhesion genes (dark blue). Shown in light blue are transcription factor genes; two are preferentially induced by Cd, and six others are preferentially induced by Cry5B.

2.5 Discussion

Our results demonstrate that the PFT Cry5B elicits a robust transcriptional response from target cells. The transcriptional response of *C. elegans* to Cry5B can be qualitatively discriminated from the response seen to the heavy metal cadmium, which elicits a more generalized stress response as indicated by the preferential induction of heat-shock proteins and glutathione *S*-transferase genes. Conversely, four genes induced by pathogens or pathogen-associated factors in other systems are preferentially up-regulated by Cry5B, consistent with the idea that *C. elegans*

identifies Cry5B as part of a pathogenic attack.

The function of these Cry5B-responsive genes in host/toxin relations can be explored using *C. elegans* genetics. If a particular gene plays a role that favors intoxication, reducing the function of that gene should make the animals more resistant to the toxin (Figure 2.5, A). Conversely, if the gene product serves to protect the animal, reducing the function of the gene should make the animals more susceptible to the toxin (Figure 2.5, B).

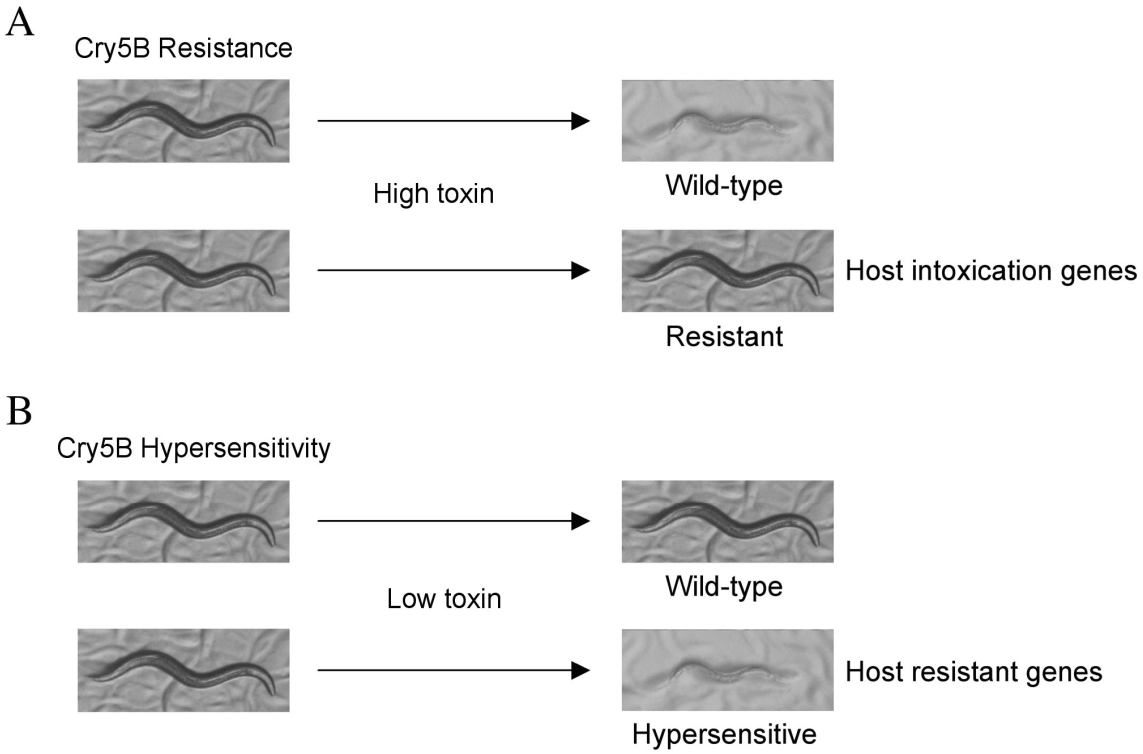

Figure 2.5. Using high (A) and low (B) doses of Cry5B to identify mutations affecting intoxication

2.6 Materials and Methods

Microarrays. Sample prepartion and Gene Chip hybridization. *C. elegans* mutant *glp-4*(bn2) was used in place of N2 for studying wild-type responses to Cry5B.

Synchronous populations of this strain were prepared using standard techniques. Animals were grown to L4 stage on high growth plates seeded with OP50. At L4-stage, the worms were washed off these OP50 plates with water, pelleted, washed with 5mL water and pelleted again. For Cry5B assays, half the population was pipetted onto plates seeded with JM103 *E. coli* expressing Cry5B while the other half was plated on JM103 expressing Cry5A (1, 2 and 4 hour time-points) or JM103 with empty vector (3 hour time-point). For cadmium assays, half the population was plated on 1mM cadmium plates and the other half was plated on identical plates lacking the cadmium chloride. At the end of the exposure time, the animals were washed off the assay plates with water, pelleted, washed with 5mL water and pellet again. Total RNA was extracted and isolated as described at http://cmgm.stanford.edu/~kimlab/germline, and further purified using Qiagen RNeasy columns. 10 μg of RNA were used to generate double stranded cDNA according to Affymetrix protocols (see http://genomics.ucsd.edu/). Biotinylated cRNA was *in vitro* transcribed from the double-stranded cDNA template using the Ambion MessageAmp aRNA kit (manufacturer's protocol). 15 μg of biotinylated cRNA "target" were hybridized to each *C. elegans* genome GeneChip array overnight at 45° C. After several washes, the arrays were doubly stained with streptavidin-phycoerythrin to enhance signal sensitivity (Affymetrix published protocols).

Data analysis. All microarray hybridization data was analyzed using the Corgon program (Sasik et al., 2002) (available for download at http://corgon.ucsd.edu/~sasik/) to calculate a normalized signal intensity for each probe set on each gene chip. The statistical package Focus (Cole et al., 2003) was

used to find genes differentially expressed by either Cry5B or cadmium, relative to appropriate controls, based on the three trials. The Focus criteria used were 1) interest score > 7.0, 2) mean expression level in treatment or control > 100, and 3) log-value contrast p-value < 0.01. This analysis identified 1083 probe sets significantly modulated by Cry5B treatment and 1092 probe sets significantly modulated by cadmium treatment. There are 174 up-regulated probe sets whose fold change by Cry5B is at least twice that elicited by cadmium and 163 up-regulated probe sets whose fold change by cadmium is at least twice that of Cry5B. Together, this group of 337 probe sets was analyzed for gene ontology classification (see below).

Gene Ontology in Figure 2.4. Gene ontology assignments were made based on prominent motifs in the predicted protein sequence and Gene Ontology terms listed in WormBase.

Cry5B induced:

Transcription factors: C06C6.4, F22A3.1, M02H5.6, T27F2.4, Y17D7B.1, ZK1037.5; *Cell adhesion/cytoskeleton related*: C10G11.7, F25E2.4, F25H9.5, F43G9.9, F54D1.6, R31.1, W03D8.6, Y18D10A.20; *Pathogenesis related*: B0348.2, F28D1.3, T12A7.1, Y22D7AL.15

cadmium induced:

Heat shock genes: C12C8.1, F44E5.4, T27E4.8, T27E4.9, Y46H3A.2, Y46H3A.3, F52E1.7; *Glutathione-S-transferases*: F11G11.2, F35E8.11, F35E8.8, F37B1.5, K01D12.11, K08F4.7, R03D7.6, R07B1.4, R107.7; Stress induced genes: F40F8.7, F58E10.4; *Transcription factors*: C48D5.1, T01G6.6.

Error bars represent standard deviations of $\log_2$-ratios, calculated from 3 replicates each of treatment and control. When the error bars are invisible, they are smaller than the symbol size. The error bars are given only for the colored spots.

Part of this chapter was adapted from segments of the following published paper, of which I was the primary researcher.

Huffman D.L., Abrami* L., Sasik* R., Corbeil J., van der Goot F.G., and Aroian R.V. (2004). Mitogen-activated protein kinase pathways defend against bacterial pore-forming toxins. *Proceedings of the National Academy of Sciences*. 101(30): 10995-11000.

Sasik and Corbeil performed the statistical analysis of the microarray data

Firgure 2.5 was adapted from the following published paper, of which I was the primary author.

Huffman D.L., Bischof L.J., Griffitts J.S., and Aroian R.V. (2004). Pore worms: Using *Caenorhabditis elegans* to study how bacterial toxins interact with their target hosts. *International Journal of Medical Microbiology*, 293: 599-607. Review.

2.7 References

Beanan, M. J., and Strome, S. (1992). Characterization of a germ-line proliferation mutation in C. elegans. Development *116*, 755-766.

Cole, S. W., Galic, Z., and Zack, J. A. (2003). Controlling false-negative errors in microarray differential expression analysis: a PRIM approach. Bioinformatics *19*, 1808-1816.

Galindo, C. L., Sha, J., Ribardo, D. A., Fadl, A. A., Pillai, L., and Chopra, A. K. (2003). Identification of Aeromonas hydrophila cytotoxic enterotoxin-induced genes in macrophages using microarrays. J Biol Chem *278*, 40198-40212.

Rogers, P. D., Thornton, J., Barker, K. S., McDaniel, D. O., Sacks, G. S., Swiatlo, E., and McDaniel, L. S. (2003). Pneumolysin-dependent and -independent gene expression identified by cDNA microarray analysis of THP-1 human mononuclear cells stimulated by Streptococcus pneumoniae. Infect Immun *71*, 2087-2094.

Sasik, R., Calvo, E., and Corbeil, J. (2002). Statistical analysis of high-density oligonucleotide arrays: a multiplicative noise model. Bioinformatics *18*, 1633-1640.

Yokoyama, K., Higashi, H., Ishikawa, S., Fujii, Y., Kondo, S., Kato, H., Azuma, T., Wada, A., Hirayama, T., Aburatani, H., and Hatakeyama, M. (2005). Functional antagonism between Helicobacter pylori CagA and vacuolating toxin VacA in control of the NFAT signaling pathway in gastric epithelial cells. Proc Natl Acad Sci U S A *102*, 9661-9666.

Chapter 3

Analysis of Cry5B-Regulated Genes Reveals Toxin Defense Pathways

3.1 Summary

The robust transcriptional response we observed in the *C. elegans* host when exposed to Cry5B lead us to speculate that the animals could be mounting a defense against the toxin. With this hypothesis in mind, I scanned the list of Cry5B-induced genes for ones with demonstrated or predicted roles in innate immunity. Among the genes fitting this description were members of the p38 and JNK MAP kinase pathways in *C. elegans*. One of these up-regulated genes was *sek-1*, a MAP kinase kinase that is upstream of the *C. elegans* p38 ortholog *pmk-1*. In addition to *sek-1*, a gene encoding a JNK-like MAP kinase, *kgb-1*, was also up-regulated by toxin in the microarray study. Genetic deletion of *sek-1*, *pmk-1* or the upstream MAPKK kinase, *nsy-1*, resulted in increased Cry5B sensitivity, indicating that this pathway mediates toxin defenses in *C. elegans*. Mutation of the *kgb-1* gene also resulted in toxin hypersensitivity as well as increased sensitivity to the heavy metal cadmium, suggesting this particular MAP kinase pathway controls defenses to a broader range of

stress-inducing agents. These data demonstrated for the first time that animal's have innate defenses to pore-forming toxins.

The transcriptional targets of the PMK-1 MAP kinase pathway and the KGB-1 MAP kinase pathway were identified through microarray analysis of the *sek-1*(km4) and *kgb-1*(um3) mutants, respectively. Overall, the KGB-1 pathway appears to regulate more genes than the PMK-1 pathway, although the two pathways share many transcriptional targets. The PMK-1 targets were screened by reverse genetics to determine if any are involved in Cry5B defense. Three genes, named *ttm-1, 2* and *3*, were identified in this screen. The *ttm* transcripts were induced by Cry5B exposure in a *sek-1* dependent manner and reduction of these gene products by RNAi resulted in hypersensitivity to Cry5B. These genes were the first targets of the *C. elegans* p38 MAP kinase pathway to be discovered and published.

3.2 Introduction

When a susceptible host organism encounters a potential bacterial pathogen, the host's immune system is responsible for tackling the invader. In humans and other vertebrates, we often categorize the mechanisms of the immune system as either specific or nonspecific. Specific defenses, also called acquired immunity, are those that provide the host immunity to any pathogen against which an immune response has been previously mounted. This branch of the immune system is called specific immunity because the mediators of these defenses, such as antibodies and cytotoxic T cells, recognize unique properties of each pathogen to target those microorganisms specifically. Although it can take the specific immune system days, or even weeks, to

successfully overcome a newly encountered pathogenic bacterium or virus, the immunity acquired against that pathogen can last for decades.

The nonspecific defenses refer to those elements of immunity that are effective against many different kinds of bacteria and viruses. Because the efficiency of these responses does not rely on recognition of the pathogen from a previous exposure, nonspecific defenses are often referred to as the innate immunity of an animal. In the interaction between host and pathogen, the innate immune system is responsible for the first-line defenses. In fact, at its most fundamental, the innate immune system includes the physical barriers, such as a layer of epithelial cells, that keep bacteria out of infection prone tissues. Other mechanisms of innate immunity include complement activation, phagocytosis of bacterial cells, the production of anti-bacterial peptides and the secretion of cytokines to signal the presence of a potential invader to other host cells, including specialized immune cells. In invertebrates, many of the genes and cell types required for specific immunity are absent, making innate defenses the only option for protection from pathogenic microorganisms.

Cooperatively, the various components of our innate immune systems can prevent bacteria from gaining access to potential infection sites, directly kill bacterial cells, make conditions unfavorable for bacterial growth and kill off host cells infected with an intracellular pathogen. On the bacterial side, there are often numerous virulence factors produced by the pathogen that promote the establishment and spread of infection. Thus, host-pathogen interactions are a two way street. Interestingly, there is considerable evidence for particular virulence factors that work by disabling immune cells or immune effectors. By the same token, there are many examples of

the host immune system being triggered by the presence of particular virulence factors. The induction of the inflammatory response following exposure of cells to lipopolysaccharide (LPS) is a classic example. However, there is little evidence that the immune system ever targets a single virulence factor or class of virulence factor as a means of limiting its harm or attenuating the virulence of the pathogen. There are some examples of antibodies and T cells that bind a particular purified virulence protein and the immune response can include the production of proteases that could nonspecifically degrade whatever bacterial proteins are accessible. Still, given the importance of virulence factors in the infection process and the multitude of mechanisms employed by the immune system, it seems a reasonable approach for hindering an invading microorganism would be the neutralization of the gene products that make it a pathogen. Using our model system for studying host-toxin interactions, I explored the possibility that the *C. elegans* host possesses defenses against the PFT Cry5B that are triggered by the toxin itself.

The use of *C. elegans* as a model host for the study of innate immunity is a relatively new field. Early investigators took advantage of the fact that *C. elegans* is a bacterial feeder and fed the nematodes a pathogenic strain of *Pseudomonas auriginosa*. The result was an accumulation of the bacteria in the *C. elegans* intestine and premature death of the nematode host. In 2002, a report came out describing a forward genetic screen in *C. elegans* to identify mutants that are killed more rapidly by *P. auriginosa* than the wild-type N2 strain. This investigation identified the *C. elegans* orthologs of the p38 MAP kinase pathway as important mediators of

immunity to *P. auriginosa*. The MAP kinase of this pathway, PMK-1, is 60% identical and 75% similar to the p38β human protein (Berman et al., 2001).

The p38 type mitogen-activated protein (MAP) kinase cascade is a well-studied signal transduction pathway. This pathway is activated in response to certain extracellular stimuli that trigger activation of the kinase cascade, amplifying the signal and translating it into changes in cellular activity. Like other MAP kinases, p38 needs to be phosphorylated in order to activate its enzymatic activity as a kinase. This phosphorylation is carried out by a MAP kinase kinase (MAPKK), a so-called dual-specificity kinase for its unique property of phosphorylating serine and threonine residues contained within the MAP kinase primary sequence. This unusual specificity ensures that MAPK's can only be activated by a MAPKK. The MAPKK itself also needs to be phosphorylated in order to become an active enzyme. The kinase responsible for phosphorylating and activating the MAPKK is the MAPKK kinase (MAPKKK). The MAPKKK also requires proper activation, but the exact post-translational modifications essential for MAPKKK activation are often less well understood and may be significantly more complicated. Ultimately, however, activation of the MAPK leads to phosphorylation of a variety of protein targets, both cytosolic and often nuclear.

The first member of the p38 family of MAP kinases to be cloned was that from *Saccharomyces cerevisiae*. This gene, called HOG1 in yeast, was identified along with PBS2, the MAPKK in this pathway, in a genetic screen for mutants with increased sensitivity to osmotic stress (Brewster et al., 1993). Since then, many of the players in this pathway have been identified including an upstream osmosensor

protein important for PBS2 activation and a downstream glycerol synthesis enzyme that appears to be one of the key genes transcriptionally up-regulated by this pathway (Albertyn et al., 1994; Maeda et al., 1995).

In wild-type yeast cells, osmotic stress causes increased phosphorylation (i.e. activation) of HOG1. In mammalian organisms and cells, the p38 MAP kinases have been reported to be activated in response to a variety of stimuli, including osmotic stress, the endotoxin LPS, inflammatory cytokines, heat shock, the unmethylated CpG motifs found in bacterial DNA and many others. Often, however, these studies are performed *in vitro* with cultured cells and the *in vivo* consequences of p38 activation in response to a particular stimulus are left unexplored. Even still, studies with cell culture have revealed many valuable insights into p38 signaling including its involvement in apoptosis regulation and inflammation (for review see (Zarubin and Han, 2005)).

In the previous chapter, I reported our findings on the *C. elegans* transcriptional response to a PFT from *Bacillus thuringiensis*, Cry5B. Because the response appeared somewhat specific, we hypothesized that the animals could be activating genes that counteract the toxin or the toxin's effects on the cell, in effect, providing a kind of immune protection against this virulence protein. The products of such defense genes would then be capable of promoting resistance to Cry5B and therefore, these genes would be expected to mutate to a toxin-hypersensitive phenotype. We suspected that identifying such a Cry5B defense gene would shed some light on host/toxin interactions. When we saw that the *sek-1* gene showed

transcriptional induction by Cry5B on the microarrays, it seemed like an excellent candidate for further testing.

3.3 A MAP Kinase Kinase Transcript, *sek-1*, is Regulated by Cry5B Exposure

SEK-1 is a MAPKK that is immediately upstream of the *C. elegans* p38 MAPK, PMK-1, and immediately downstream of the MAPKKK, NSY-1 (Kim et al., 2002; Tanaka-Hino et al., 2002). Because of the role for this pathway in *C. elegans* innate immunity, the *sek-1* gene was of immediate interest. In the Cry5B/Cry5A microarray time-course described in the previous chapter, induction of *sek-1* was seen at the 1 hour exposure (2.61-fold, on average) and the two hour exposure (4.76-fold on average). Real-time PCR analysis confirmed that *sek-1* RNA was induced by Cry5B at the three hour time-point where empty vector *E. coli*, rather than *E. coli* expressing Cry5A, served as the control condition (Table 3.1).

Table 3.1: Regulation of Cry5B induced genes *sek-1* and *kgb-1*. Data are from the microarrays (Affy) and real time PCR (RT PCR) after a 3 hour Cry5B exposure.

transcript	fold toxin-induced (Affy)[1]	fold toxin-induced (RT PCR)
sek-1	3.7	4.8
kgb-1	2.6	3.6

[1] average induction seen on Affymetrix array experiments at 3 hour time-point.

To test whether this induced MAPKK gene, *sek-1*, functions in Cry5B intoxication, we fed animals lacking the *sek-1* gene [deletion allele *sek-1*(*km4*)] high and low doses of Cry5B toxin expressed in *E. coli*. In the absence of toxin, *sek-1*(*km4*) animals developed normally and generally were as healthy as wild-type animals, as previously reported (Kim et al., 2002). When fed Cry5B *E. coli*, both

wild-type and *sek-1*(*km4*) animals became intoxicated; they rapidly became lethargic, turned pale, and degenerated over the course of 1–2 days (Figure 3.1, column 2), although *sek-1*(*km4*) animals appeared to become more intoxicated. The mutant was also tested on a dose of toxin that is just barely toxic to wild-type. These low-dose toxin assay plates were made by mixing a culture of Cry5B *E. coli* with a culture of *E. coli* carrying the empty expression vector to make a culture in which only 10% of the cells express Cry5B. The resulting lawn produced a dose of toxin that had very marginal effects on the wild-type N2 strain. These animals were large, had good coloration, moved well, and did not degenerate. In contrast, *sek-1*(km4) animals were still severely intoxicated even by this low dose of toxin (Figure 3.1, column 3). This result extended to the other genes in the same MAPK pathway. Animals lacking the p38 MAPK in this pathway (*pmk-1*) were also hypersensitive to Cry5B as were animals lacking the upstream MAPKKK *nsy-1* (Figure 3.1). The protection conferred by this pathway against Cry5B is specific in at least two ways. First, animals lacking another p38 MAPK, *pmk-3,* were not hypersensitive to Cry5B (data not shown). Second, animals mutant for *sek-1* or *pmk-1* were not overly hypersensitive to the heavy metal cadmium (Figure 3.2). Because animals lacking *sek-1* were more readily intoxicated by Cry5B, we concluded that one wild-type function of *sek-1* is to protect *C. elegans* against this toxin.

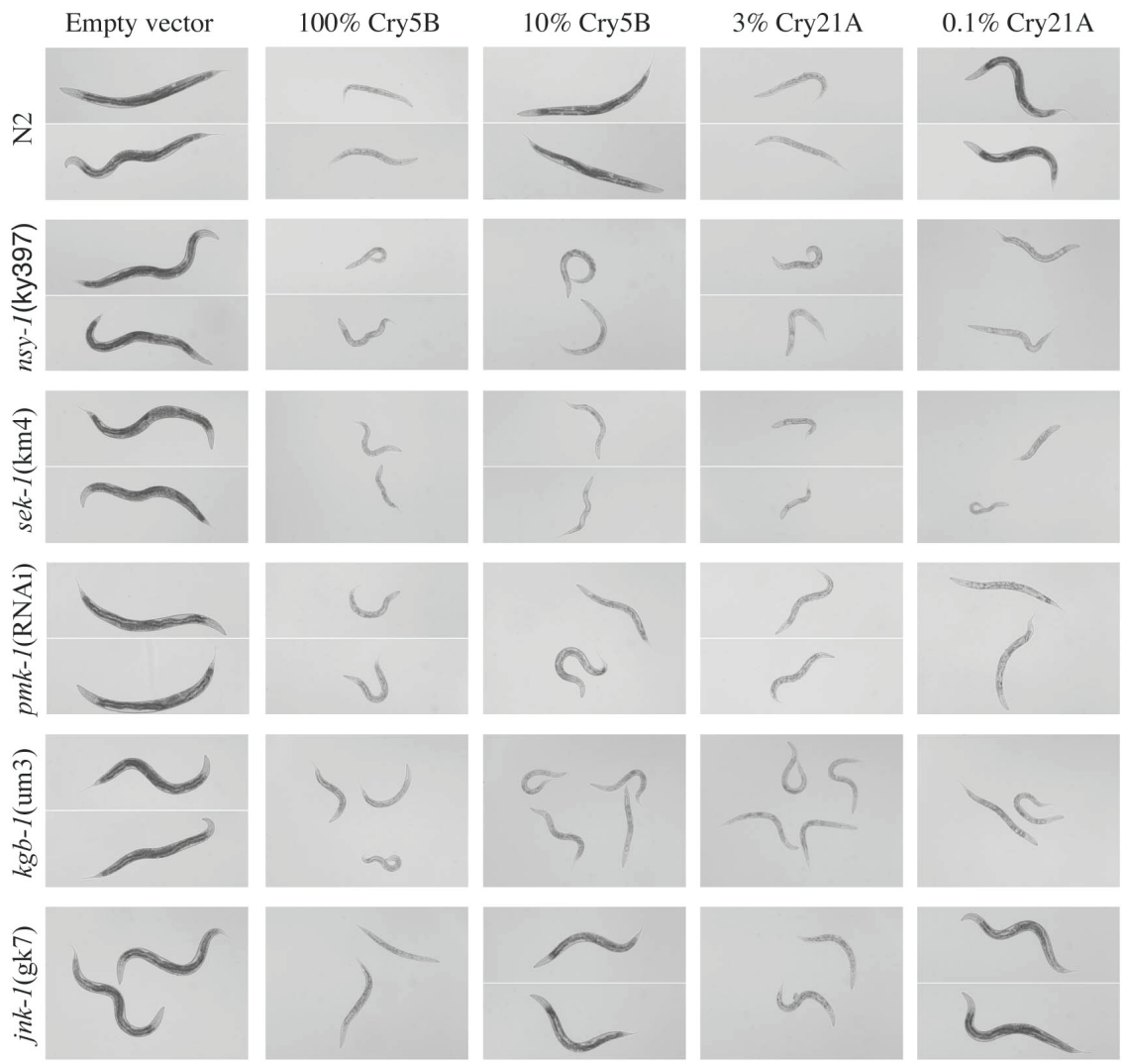

Figure 3.1: *nsy-1-sek-1–pmk-1* (p38) and *kgb-1* (JNK-like) MAPK pathways protect *C. elegans* from Cry5B. As indicated above each column, L4 animals were plated on the lawns of *E. coli* containing empty vector, high levels of Cry5B toxin (100% Cry5B), low levels of Cry5B toxin (10% Cry5B), high levels of Cry21A toxin (3% Cry21A), low levels of Cry21A toxin (0.1% Cry21A). Representative animals are shown after 40 h of feeding at each condition. Each row corresponds to a different genotype, as indicated on the left hand side of the column. All nematodes are shown at the same magnification.

In order to quantify how much more sensitive to Cry5B the animals become when this MAPK pathway is disrupted, I made use of a growth-based assays designed to measure the degree of growth inhibition in the presence of Cry5B. This assay was performed in liquid culture with populations of L1 larvae exposed to a range of

concentrations of purified Cry5B protein in the presence of an *E. coli* food source (strain OP50) and bacteriostatic antibiotics. After 60 hours of development, the animals were photographed to measure differences in the average size of the animals on the increasing toxin concentrations. With this assay, the *sek-1*(*km4*) animals were an order of magnitude more sensitive to Cry5B than wild-type animals (Figure 3.3). In contrast, *sek-1*(*km4*) animals displayed only slightly increased sensitivity to cadmium in this assay (2-fold; Figure 3.3). Additionally, hypersensitivity of p38 pathway mutants is not restricted to one Cry toxin. Animals lacking the *nsy-1* MAPKKK, the *sek-1* MAPKK or the p38 MAPK *pmk-1* were also hypersensitive to nematicidal Cry21A toxin (Figure 3.1, columns 4 & 5). Furthermore, animals lacking *sek-1* were hypersensitive to Cry5B when the Gram-positive bacterium *Bacillus subtilis* was used as the food source instead of *E.coli*, demonstrating that hypersensitivity is associated with the toxin and not the bacterium used as a food source (Figure 3.4).

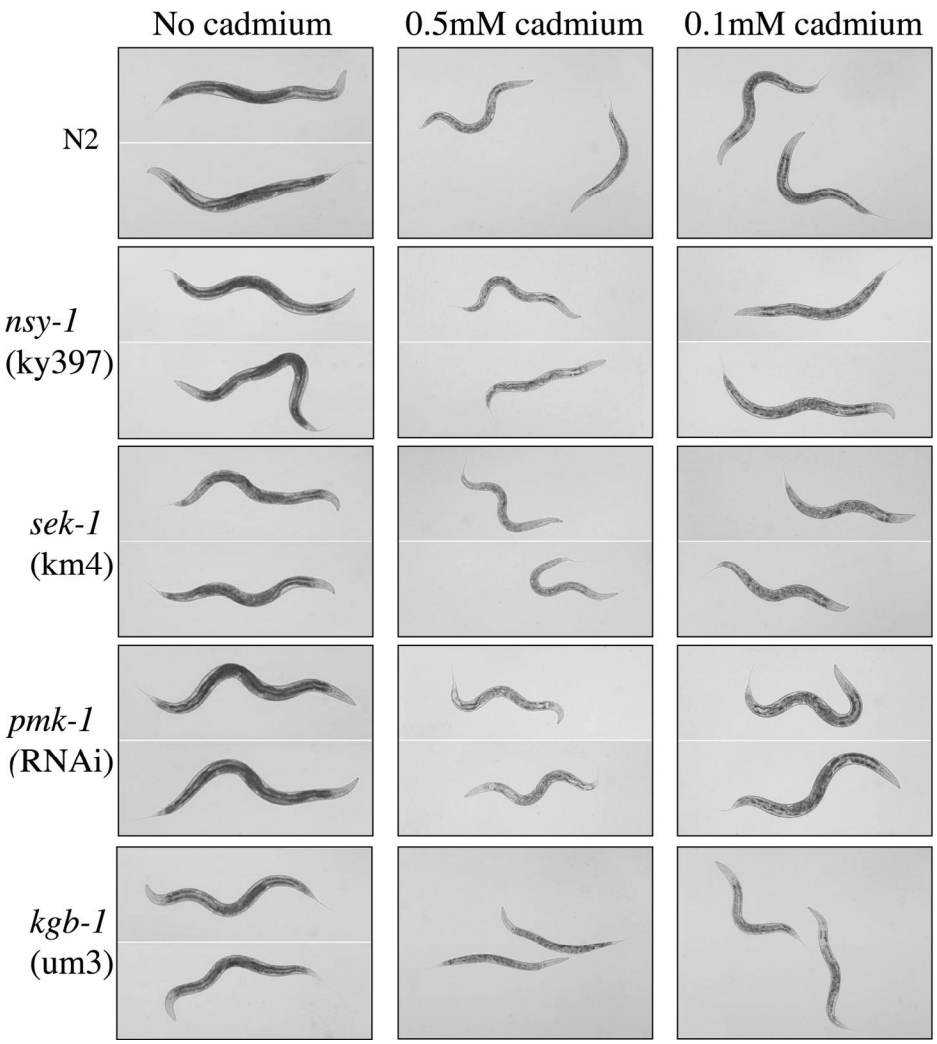

Figure 3.2: The *kgb-1* (JNK-like) MAPK pathway, but not the *sek-1–pmk-1* (p38) pathway, protects *C. elegans* from cadmium intoxication. As indicated above each column, L4 animals were plated on agar plates of *E. coli* containing no CdCl2 (No cadmium), moderate levels of CdCl2 (0.5mM cadmium), and low levels of CdCl2 (0.1mM cadmium). Representative animals are shown after 48 h of feeding at each condition. Each row corresponds to a different genotype, as indicated on the left hand side of the column. All nematodes are shown at the same magnification.

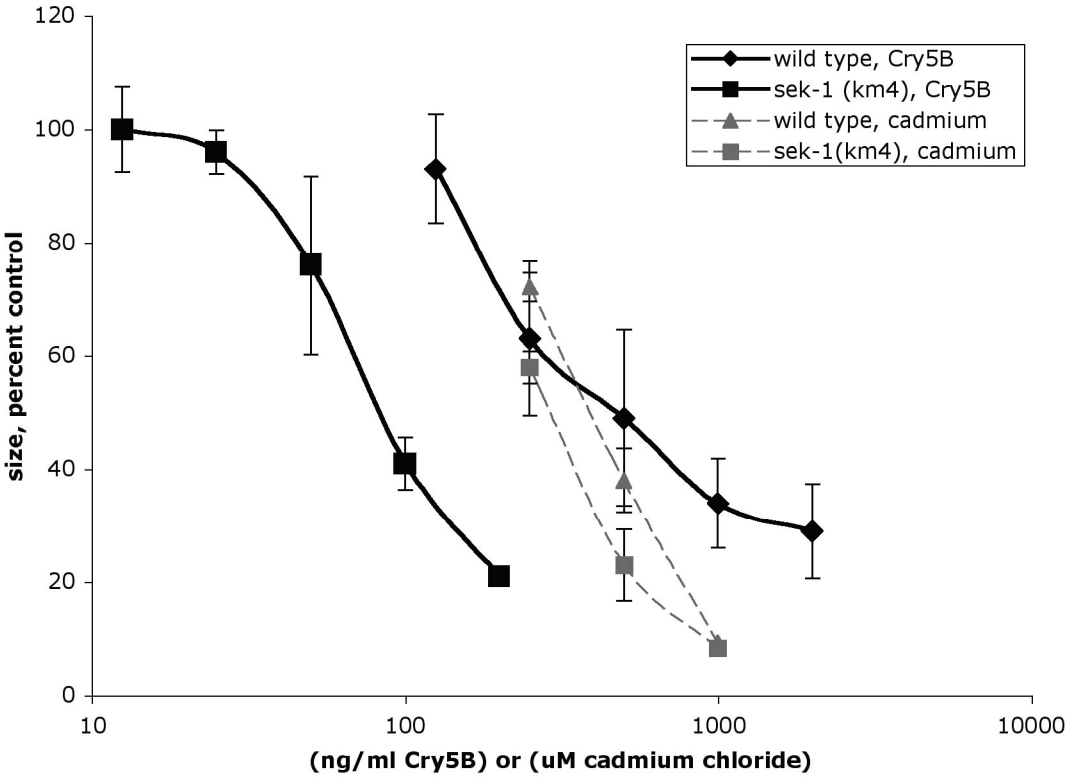

Figure 3.3: Quantitative growth-based toxicity assays with N2 and *sek-1*(*km4*). Various doses of Cry5B and Cd are plotted on a logarithmic scale. L1-staged animals were exposed to indicated doses of stressors in microtiter wells, and after 60 h, their cross-sectional areas were measured. The ordinate axis shows the size of nematodes relative to no-toxin controls run in parallel. Each point represents 60 animals from three independent experiments. SE bars are indicated.

3.4 JNK-Like MAP Kinase Genes Transcriptionally Regulated by Cry5B

Two JNK-family MAPK genes, *kgb-1* and *kgb-2,* were also induced by Cry5B on the microarrays. The *kgb-1* transcript was up-regulated an average of 2.53-fold after two hours of Cry5B exposure (relative to Cry5A exposure) and 2.6-fold after three hours (relative to empty vector control). The *kgb-2* transcript was only found to be up-regulated in the three hour experiment that used empty vector *E. coli* as the control treatment (4.08-fold, on average). Animals with a mutation in the *kgb-1* gene [deletion allele *kgb-1*(*um3*)] appeared healthy in the absence of toxin at the

temperature assayed (20°C; Figure 3.1, column 1). However, like *sek-1*mutant animals, we found that *kgb-1*(*um3*) animals were hypersensitive to low doses of Cry5B and Cry21A (Figure 3.1). Again, as with *sek*-1 mutants, *kgb-1*(*um3*) animals were still hypersensitive to Cry5B when *B. subtilis* was used as the food source (Figure 3.4). The *kgb-1* mutant animals also appeared hypersensitive to low doses of cadmium (Figure 3.2), as has been reported (Mizuno et al., 2004), suggesting that this pathway has broader functions than the p38 pathway in controlling stress responses. Interestingly, the *kgb-1* transcript, but not the *sek-1* transcript, was identified as a cadmium-responsive gene on the microarrays (up-regulated 2.03 fold). No mutant allele for *kgb-2* was available, and RNAi of *kgb-2* did not give rise to animals hypersensitive to Cry5B. We have confirmed that not all JNK-like MAPKs are required for protection because animals that lack a different JNK-like MAPK, *jnk-1,* were not hypersensitive to Cry5B (Figure 3.1, bottom row).

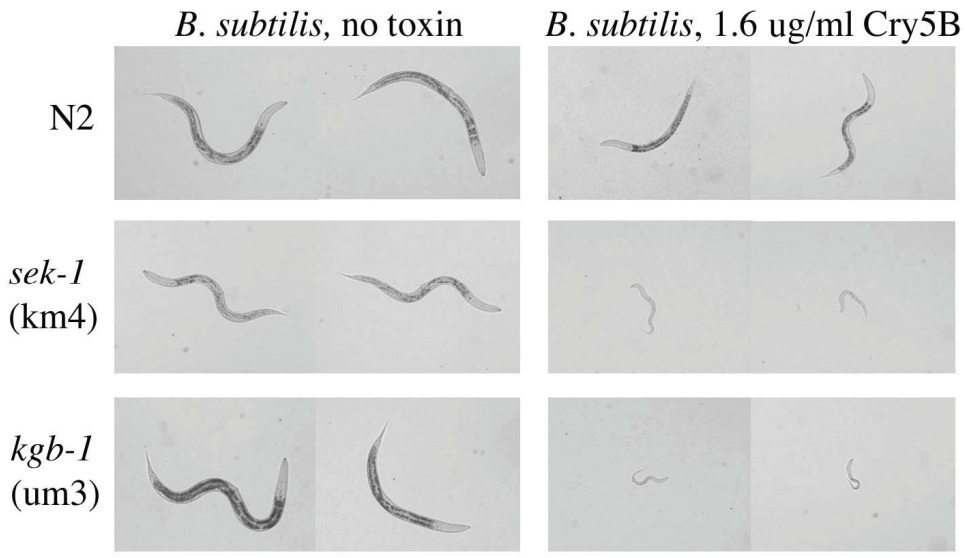

Figure 3.4: Increased toxin sensitivity in *sek-1* and *kgb-1* mutants is not dependent on the bacterium used as a food source. L1 animals were placed in wells with *Bacillus subtilis* and either no Cry5B or 1.6ug/ml of purified Cry5B protein.

3.5 Short Toxin Exposures Require MAP Kinase Mediated Defenses

Both Bt and many free-living nematodes coexist in the soil. These nematodes ingest bacteria as a food source and Bt has evolved Cry toxins that kill diverse nematodes (Wei et al., 2003). It therefore seems probable that these two organisms encounter each other in the wild, where the nematode might transiently come across Bt and its associated crystals, ingest some, and then move away. Potentially, an important form of defense for soil nematodes is to be able to recover from a short exposure to a relatively concentrated dose of Bt Crystal toxin.

With this theory in mind, I put wild-type animals and two of the MAP kinase pathway mutants on 100% Cry5B *E. coli* plates for only 30 minutes, then transferred them to non-toxic plates of OP50 *E. coli* and scored them the next day (30 hours later) for intoxication phenotypes. Wild-type animals tolerate this pulse of toxin well and, one day later, were fairly healthy (Figure 3.5, top row). In contrast, *sek-1* or *kgb-1* mutant animals could not tolerate this short exposure to toxin (Figure 3.5). These animals degenerated even in the absence of toxin. After 30 hours of recovery on OP50 *E. coli* plates, the mutants appeared nearly as intoxicated as their un-recovered counterparts that remained on the 100% Cry5B *E. coli* plates for the 30-hour period (Figure 3.5). Similar results were obtained for *pmk-1* RNAi and *nsy-1* mutants (Figure 3.5 and data not shown). Additionally, N2 and the *sek-1*(km4) mutant were tested in this assay with a range of toxin exposure times from 5 minutes to 8 hours, all with the same general outcome.

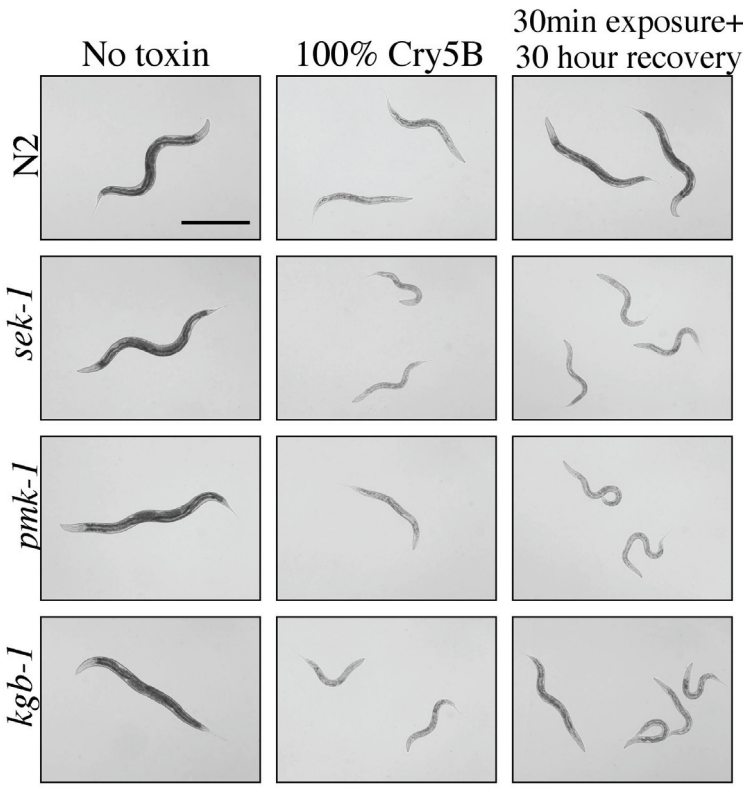

Figure 3.5: Short toxin exposures require defense pathways *pmk-1* and *kgb-1*. Column 1 shows no toxin controls. Column 2 shows L4 animals that were placed on 100% Cry5B-expressing *E. coli* lawns and imaged 30 h later. Column 3 shows L4 animals that were placed on 100% Cry5B-expressing *E. coli* lawns for 30 min, removed to nontoxin-expressing *E. coli* lawns, and imaged 30 h later. Each row shows representative animals for each genotype at the same magnification.

3.6 Site of Action of the PMK-1 Pathway

As with other Bt crystal toxins, the tissue targeted by Cry5B in *C. elegans* is the intestine. By compound and electron microscopy, the effects on the intestine include sloughing off of the intestinal microvilli, autophagy within intestinal cells, contraction of the intestine away from the body wall of the animal and formation of vacuoles within the cytoplasm of the intestinal cells (see Chapter 1). For these reasons, we speculated that the intestine could be the site of action of the PMK-1 MAP kinase pathway. However, work from other labs has shown these genes to be

expressed in multiple tissues, including but not limited to the intestine (Tanaka-Hino et al., 2002).

To address the issue of site of action, I generated animals that only express the *sek-1* gene in the intestine and asked if these animals appeared to have a wild-type susceptibility to Cry5B when the PMK-1 pathway is only functional in this tissue. To generate these animals, the *sek-1* genomic coding region, including 3' UTR, was amplified and fused downstream of the *cpr-1* promoter (P*cpr-1*) using PCR (for technique see(Hobert, 2002)). The *cpr-1* promoter drives expression specifically in the intestine (Griffitts et al., 2003). The amplified product consisting of the promoter and *sek-1* gene was injected with the *rol-6* dominant marker into *sek-1*(km4) animals. The resulting transgenic strains were tested on 10% Cry5B *E. coli* plates to determine if the toxin hypersensitivity phenotype had been rescued with intestinal expression of the *sek-1* gene. Unlike the *sek-1*(km4) mutants, the transgenic P*cpr-1*::*sek-1* animals did not look highly intoxicated on the low toxin dose. Instead, they appeared healthy, with good coloration and size (Figure 3.6). This result that expression of *sek-1* exclusively in the intestinal cells is sufficient for the pathway to provide toxin protection indicates that the protection is mediated within the tissue that the toxin targets. A similar experiment was performed in which *pmk-1*(km25) mutants were injected with the *pmk-1* cDNA under control of the *cpr-1* promoter. These animals also showed normal sensitivity to toxin (data not shown), corroborating the result that the intestine is the site of action for the genes of this pathway.

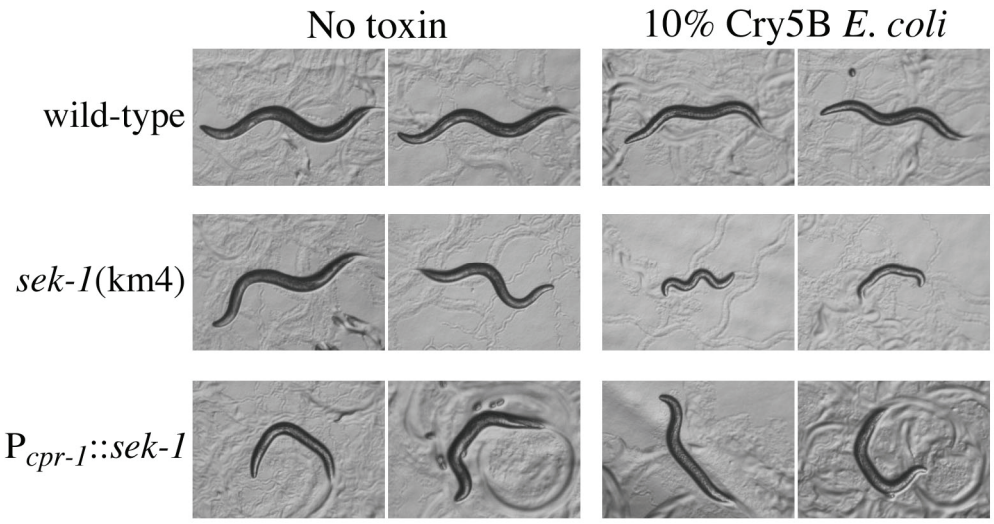

Figure 3.6. Intestinal specific expression of *sek-1* rescues hypersensitivity. On the left, transgenic *sek-1* mutants expressing the *sek-1* transgene under control of the intestinal specific promoter, P*cpr-1*. On the right, non-transgenic *sek-1*(km4) siblings.

3.7 p38 MAPK Pathway Protects Mammalian Cells Against a PFT

Because MAPK pathways are well conserved between *C. elegans* and mammals, we hypothesized that MAPK pathways might protect mammalian cells against PFTs as well. To test this hypothesis, baby hamster kidney (BHK) cells were pretreated with the p38-specific inhibitor SB203580 for 30 minutes and then exposed briefly (either 45 seconds or three minutes) to the PFT proaerolysin made by the human pathogen *Aeromonas hydrophila*. In agreement with our results in *C. elegans*, inhibition of p38 in BHK cells resulted in hypersensitivity to proaerolysin (Fig. 3.7). At all concentrations of proaerolysin, a 2- to 5-fold increase in the number of cells undergoing cell death was evident when p38 was inhibited.

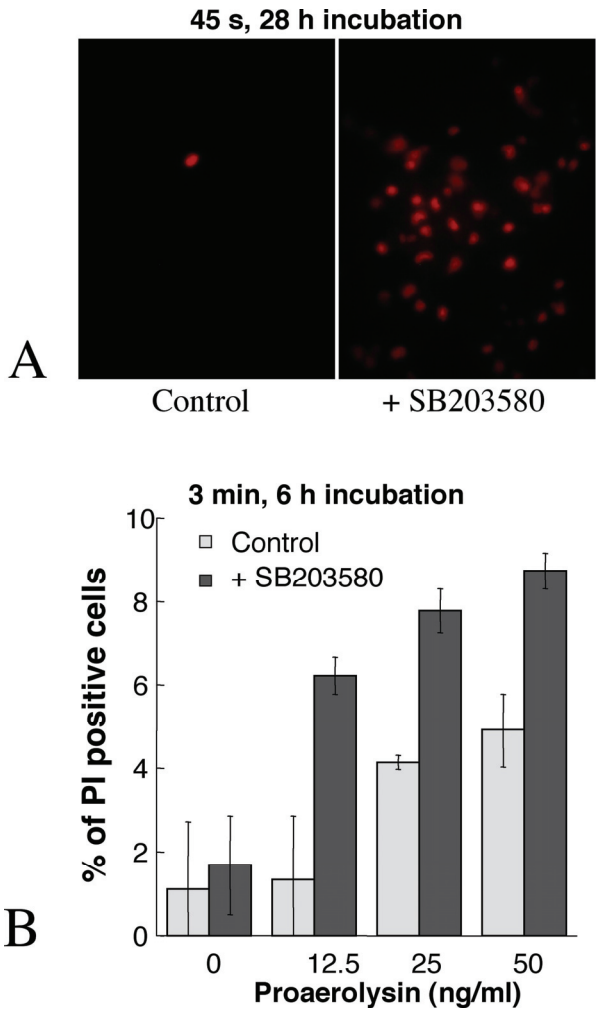

Figure 3.7. A p38 MAPK pathway protects mammalian cells against the PFT aerolysin. (*A*) Baby hamster kidney cells were incubated in either media (*Left*) or media plus p38 inhibitor SB203580 (*Right*) for 30 min and then incubated for 45 sec with 20 ng ml proaerolysin. After being washed, cells were cultured for 28 h and stained with propidium iodine (PI, a marker for cell death). An increased number of dying cells is evident in the presence of the p38 inhibitor (both panels contain similar numbers of cells in a confluent lawn not shown). (*B*) Quantitation of cell death. Baby hamster kidney cells were prepared as above without or with SB203580, treated with proaerolysin for 3 min, cultured for 6 h, and stained with propidium iodine (PI). The percentage of PI-positive cells is shown. Shown is the average number of PI-positive cells for three independent trials with SE bars.

3.8 The Relationship Between the p38 and JNK-Like Pathways in *C. elegans*

The finding that two MAP kinase pathways operate in toxin defense opened up questions about a possible relationship between these two pathways. Do the two pathways act in parallel to separately activate different defense mechanisms? Do they

share some transcriptional targets and differ in others? Does one pathway activate the other? Is there crosstalk between the pathways; for example, could SEK-1 phosphorylate KGB-1 under toxic conditions? A genetic approach was taken in an effort to address these questions.

If the two pathways act in parallel to control different modes of defense, then genetically knocking out both pathways in the same animal should cause a hypersensitivity phenotype that is more severe than knocking out just one pathway. Alternatively, if they control the same mode of defense because one pathway acts upstream of the other, then a double mutant lacking both pathways would not be any more sensitive to Cry5B than the single mutant. To distinguish between these possibilities, I generated a *C. elegans* double mutant strain with deletions in the *pmk-1* and *kgb-1* genes. I also generated a double mutant with deletions in *sek-1* and *kgb-1*. These mutants were then tested in toxin sensitivity assays. Unfortunately, the results of this investigation were not clear. When animals were exposed to toxin at the L4 stage, neither the *pmk-1; kgb-1* mutants nor the *sek-1*; *kgb-1* mutants looked detectably more sensitive to Cry5B than any of the single mutant lines. Interestingly, however, when the animals were fed toxin from the L1 stage, the *pmk-1; kgb-1* double mutant did appear to be at a disadvantage relative to a *pmk-1* or *kgb-1* single mutant. This unusual outcome was not further explored.

3.9 Identification of Downstream Targets of PMK-1/p38

An important effect of MAPK pathways is transcriptional activation of downstream target genes. The robust genomic response seen in nematodes to Cry5B

suggested that we might be able to identify functional downstream targets of the MAPK pathway by using microarrays. We therefore compared the genomic responses of *C. elegans* to Cry5B with and without the p38 MAPK pathway intact to identify genes whose up-regulation depends on the pathway. Animals from two strains, *glp-4*(*bn2*);*sek-1*(+) and *glp-4*(*bn2*);*sek-1*(*km4*), were fed Cry5B *E. coli* and, for comparison, empty vector *E. coli.* RNA from these animals was harvested after three hours and then processed and hybridized to Affymetrix arrays. In collaboration with Dr. Roman Sasik of the UCSD Genomics Core, this microarray data was analyzed to identify transcripts that were up-regulated by Cry5B exposure in *sek-1*(+) animals, but significantly less up-regulated in *sek-1*(-) animals. This analysis identified 90 potential target genes whose up-regulation by Cry5B on the microarrays showed statistical dependence on the presence of a functional p38 pathway (Table 3.4).

For these 90 genes identified as candidate targets, I was interested in determining if any are involved in Cry5B defense. To address this question, I made use of an RNAi feeding library for *C. elegans* that was recently made available for sale to the public by the Ahringer lab (Kamath et al., 2003). In *C. elegans*, knock-down of a gene by RNA-mediated interference can be accomplished by feeding the animals *E. coli* that is producing double-stranded RNA complementary to the gene of interest. The Ahringer library has RNAi vectors for ~85% of the genes in the *C. elegans* genome already in the proper *E. coli* strain. Using this library, I tested if knock-down of any of these 90 target gens caused animals to become hypersensitive to Cry5B. The screen was performed by placing the RNAi-fed animals on 10% Cry5B *E. coli* lawns and visually scoring for animals that looked significantly more

intoxicated than control animals that were fed an empty RNAi vector. With this method, I screened through 86 of the 90 candidate target genes and identified three that play roles in Cry5B defense: Y39E4A.2, F26G1.4 and H06H21.10. As confirmed by real-time PCR, all three genes are induced by toxin and require the MAPKK SEK-1 for full induction (Table 3.2). These genes were thus named *ttm-1* (Y39E4A.2), *ttm-2* (F26G1.4) and *ttm-3* (H06H21.10) for Toxin-Regulated Target of MAP Kinase to recognize that their response to toxin depends on an intact MAPK pathway.

Table 3.2. The behavior of the *ttm* transcripts in *sek-1*(+) and *sek-1*(-) animals

transcript	*sek-1* genotype[1]	fold toxin-induced (Affy)[2]	fold toxin-induced (RT PCR)
Y39E4A.2 *ttm-1*	+	4.7	5.3
Y39E4A.2 *ttm-1*	-	1.1	1.3
F25G1.4 *ttm-2*	+	3.5	3.5
F26G1.4 *ttm-2*	-	1.4	1.8
H06H21.10 *ttm-3*	+	12.0	22.5
H06H21.10 *ttm-3*	-	6.3	12.5

[1] + = *glp-4(bn2)*; - = *glp-4(bn2); sek-1(km4).*
[2] average induction seen on Affymetrix array experiments.

Reducing the products of any of the *ttm* genes by RNAi gave rise to animals that were healthy in the absence of toxin but hypersensitive to low, chronic doses of Cry5B (Figure 3.8). Hypersensitivity to Cry5B seen by reduction of the *ttm* gene products was robust but not as severe as with loss of *sek-1*. Interestingly, RNAi of *ttm-1* also led to hypersensitivity to cadmium (Figure 3.8, last column) and the *ttm-1* transcript was regulated by cadmium on the microarrays described in Chapter 2 (data

not shown). Potential roles for the *ttm* gene products in toxin defense will be presented in the Discussion.

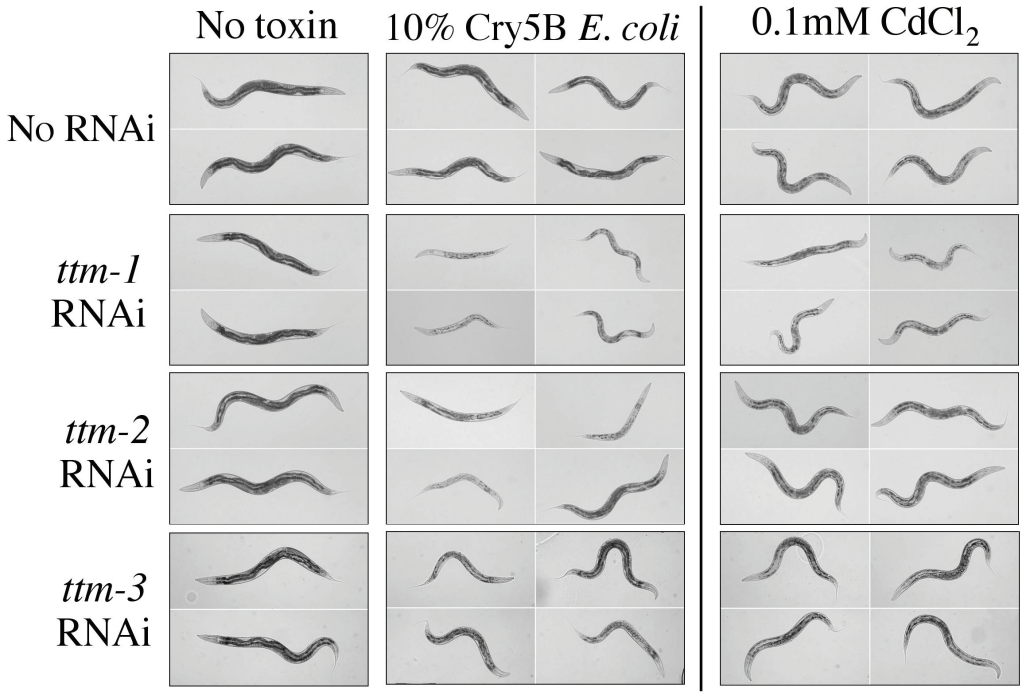

Figure 3.8. *ttm-1, ttm-2* and *ttm-3* genes are required for defense against Cry5B. *rrf-3*(*pk1426*) L4 animals were fed double-stranded RNA-producing bacteria containing empty vector (no RNAi control), a Y39E4A.2 insert (*ttm-1*), a F26G1.4 insert (*ttm-2*), or a H06H21.10 insert (*ttm-3*). Nematodes were then transferred to *E. coli* plates expressing no toxin, 10% Cry5B, or 0.1 mM CdCl2. Representative nematodes are shown after 40 h (control, Cry5B) or 48 h (Cd).

3.10 Identification of Downstream Targets of KGB-1

In a similar approach, I also sought to identify the transcriptional targets of the KGB-1 MAPK defense pathway using microarray analysis. For these experiments, two strains, *glp-4*(*bn2*);*kgb-1*(+) and *glp-4*(*bn2*);*kgb-1*(*um3*), were fed Cry5B *E. coli* and, for comparison, empty vector *E. coli*. After three hours, RNA from these animals was harvested, processed, and hybridized to Affymetrix arrays. As was done for the identification of the p38/PMK-1 targets above, this set of microarray data was

analyzed to identify transcripts that are up-regulated by Cry5B exposure in *kgb-1*(+) animals, but significantly less up-regulated in *kgb-1*(-) animals. This time, the results of the analysis revealed 274 genes whose up-regulation by Cry5B on the microarrays showed statistical dependence on the presence of a functional KGB-1 pathway. These 274 genes were considered potential transcriptional targets, direct or indirect, of the KGB-1 MAPK pathway. Of these 274 candidate targets of KGB-1, 69 of these genes were also among those identified as possible targets of the PMK-1 pathway, including all three *ttm* genes (Table 3.3)

Table 3.3. The behavior of the *ttm* transcripts in *kgb-1*(+) and *kgb-1*(-) animals

transcript	*kgb-1* genotype[1]	fold toxin-induced (Affy)[2]
Y39E4A.2 *ttm-1*	+	4.5
Y39E4A.2 *ttm-1*	-	0.9
F25G1.4 *ttm-2*	+	4.5
F26G1.4 *ttm-2*	-	1.0
H06H21.10 *ttm-3*	+	9.8
H06H21.10 *ttm-3*	-	1.3

[1] *+ = glp-4(bn2)*; *- = glp-4(bn2); kgb-1(um3).*
[2] average induction seen on Affymetrix array experiments.

3.11 The *ttm* Genes in Defense Against *S. aureus* α-toxin

Staphylococcus aereus is a Gram positive bacterium that has been implicated in infections of the eye and skin, particularly in hospital settings where this bacterium is ubiquitous (for review see (Bamberger and Boyd, 2005)). *S. aureus* produces a pore-forming toxin, **α**-toxin (also called **α**-hemolysin) that is important for virulence in

both mammals and a *C. elegans* infection model ((Jonsson et al., 1985; Sifri et al., 2003). Using isogenic strains of *S. aureus*, one that produces **α**-toxin and one that does not, I examined the role of the *ttm* genes in defense against this PFT. I knocked-down each of the *ttm* genes with RNAi and placed the animals on plates spread with one of the two different strains of *S. aureus*. I then counted the number of dead and alive animals at various time-points. The results of a representative trial are shown in Figure 3.9.

From these data, in animals not treated with RNAi, the *S. aureus* strain that produced **α** -toxin (Hla+) was more virulent that the strain that did not produce **α**-toxin (Hla-). Also, it appeared that knock-down of *ttm-2* had no affect on the animals' ability to defend against S. *aureus*, regardless of whether or not the **α**-toxin virulence factor was being produced (Figure 3.9). RNAi of *ttm-3* did make the animals more susceptible to killing by *S. aureus*, but the production of **α**-toxin was not a major influence on this increased susceptibility (Figure 3.9C). This result could indicate that TTM-3 does not protect the host against **α**-toxin, but plays a role in defense in some other manner, perhaps towards another *S. aureus* virulence factor. For *ttm-3*, again, the RNAi animals were more susceptible to both *S. aureus* strains than the control animals (Figure 3.9A). However, it strongly appeared that eliminating toxin production ameliorated the degree of hypersensitivity of the *ttm-3* RNAi animals. This result is difficult to interpret, however, because the toxin deficient strain was still virulent to the *ttm-3* knock-downs, making it difficult to conclude if *ttm-3* mediated defenses to *S. aureus* are directed towards **α**-toxin or some other aspect of *S. aureus* virulence.

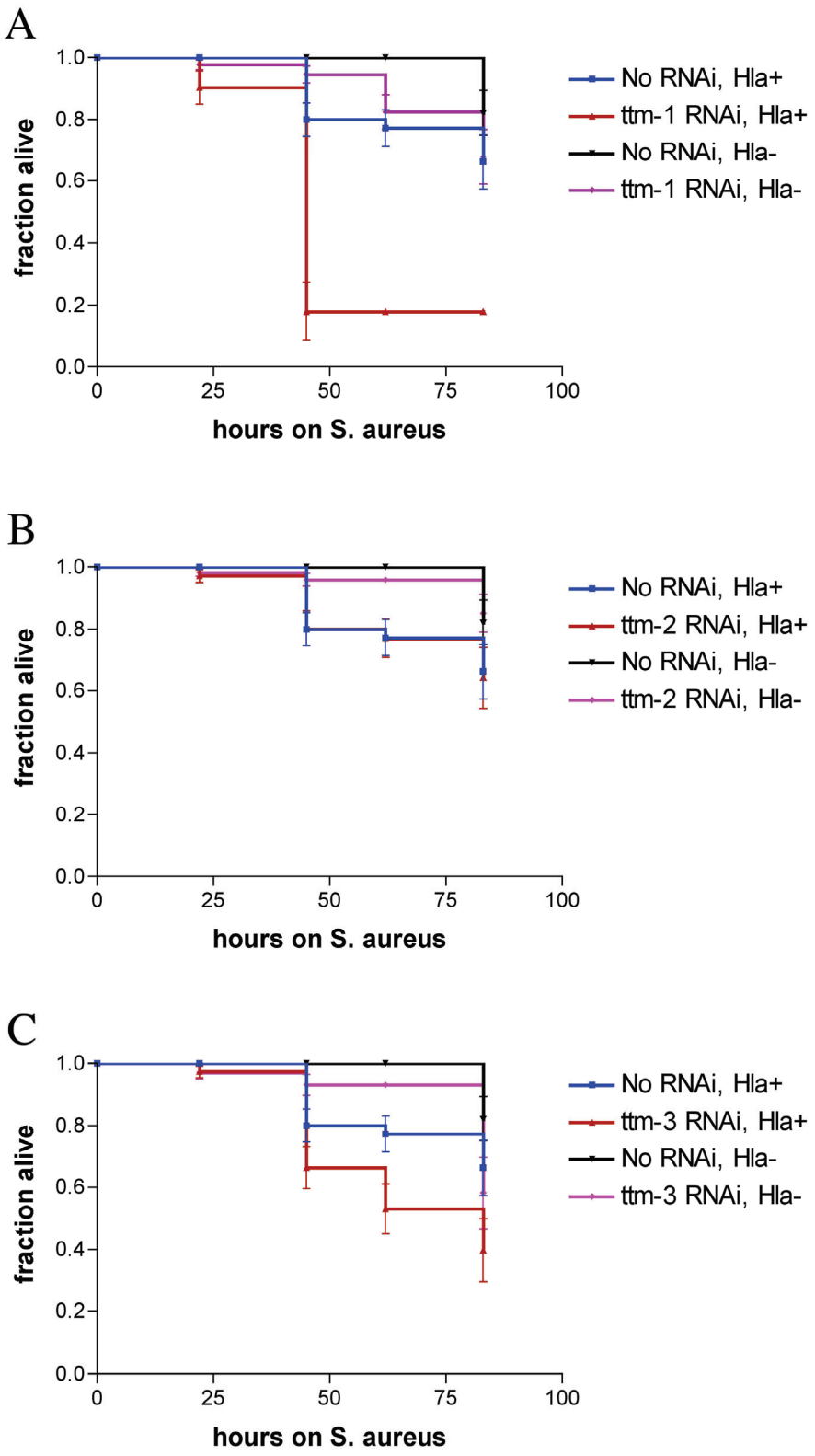

Figure 3.9. Killing curves of animals on *S. aureus* bacteria expressing α-toxin (Hla+) or not expressing α-toxin (Hla-). A, *ttm-1* vs control. B, *ttm-2* vs. control. C, *ttm-3* vs. control

3.12 Synergism Between Salt Stress and Cry5B Intoxication

The finding that a cation efflux transporter homolog, *ttm-1*, was involved in Cry5B defense raised questions about the involvement of cytosolic cations in promotion of intoxication. Could the pore result in an osmotic or ionic imbalance inside the cell that is countered by the action of TTM-1? As a means of addressing this possibility, I performed killing assay with *C. elegans* exposed to Cry5B in media containing increasing amounts of sodium chloride above that which is normally present in the buffer used for liquid culture of *C. elegans*. These data revealed a synergistic effect between Cry5B and salt stress. For example, at either 1ug/ml of Cry5B or 150mM excess NaCl, more than 80% of the animals were alive after a five-day exposure (Figure 3.10). However, when given both 1ug/ml Cry5B and 150mM excess NaCl, approximately 20% of the animals were still alive. Statistically, combining the two stressors caused a response that was beyond additive. I also visually examined wild-type *C. elegans* and *sek-1* and *pmk-1* mutants on a low dose of Cry5B (1ug/ml), a mild salt stress (100mM excess NaCl), and a low dose of Cry5B combined with mild salt stress (1ug/ml Cry5B + 100mM excess NaCl). The kinase mutants were visibly more affected than wild-type on the low dose of Cry5B (Figure 3.11). On the mild salt stress or the Cry5B combined with salt stress, the mutants appeared very similar in health to the wild-type N2 strain (Figure 3.11, bottom row). While these results were intriguing, it was not clear from these observations how toxin and salt stress are related.

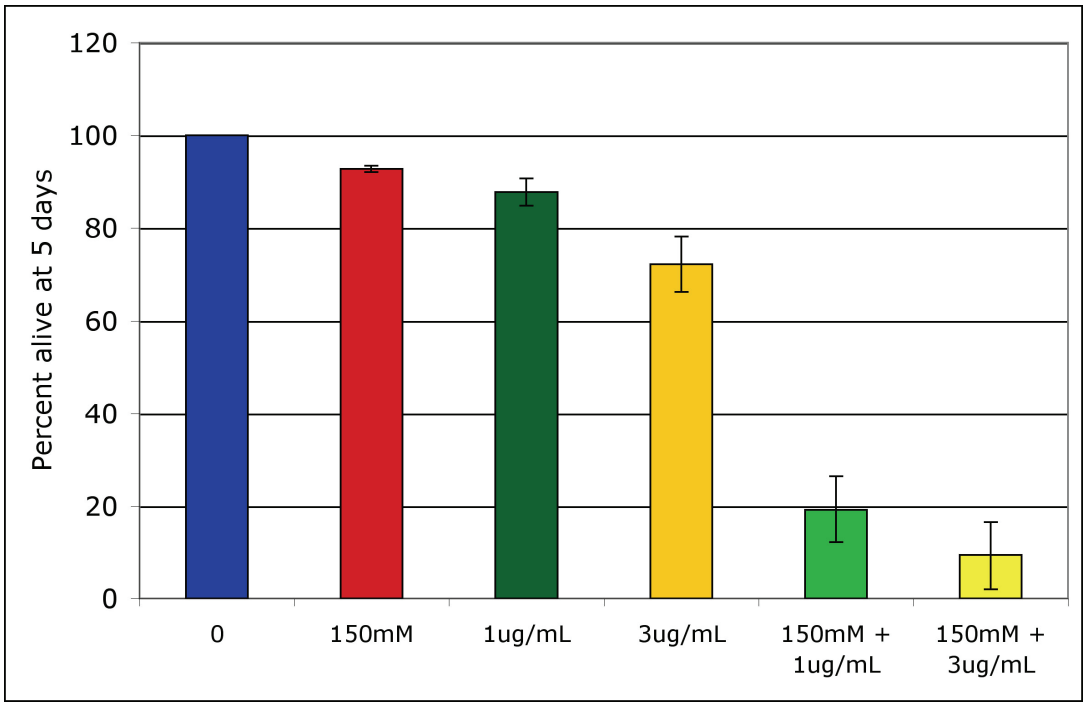

Figure 3.10. Cry5B and salt stress act synergistically in wild-type *C. elegans*. L4 N2 larvae were placed in multi-well plates with the indicative amount of purified Cry5B protein and the indicated level of excess NaCl present in the buffer. After 5 days at 25 degrees C, dead and alive animals were counted.

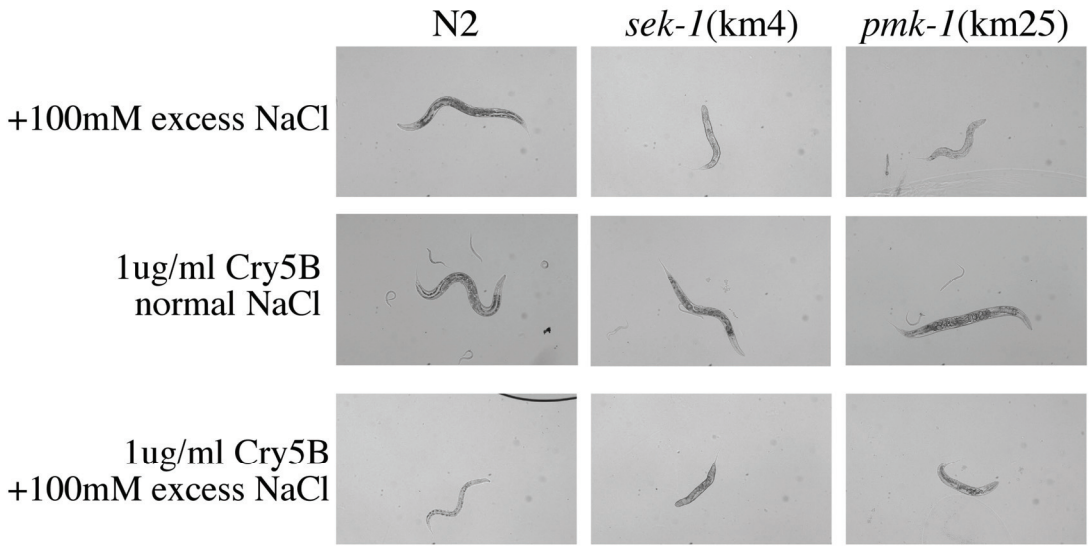

Figure 3.11. Cry5B and salt stress in *pmk-1* and *sek-1* mutants. Wild-type N2 strain and *sek-1*(km4) and *pmk-1*(km25) mutants on low salt (top row), low toxin (middle row) and both (bottom row). Animals were placed on these conditions as L4 larvae and photographed the next day.

3.13 Discussion

Loss of any of the three genes (*nsy-1, sek-1* and *pmk-1*) that make up the p38 MAPK cascade results in *C. elegans* that are hypersensitive to low, chronic doses of Cry5B or to high doses of Cry5B given for short periods. Dramatically, we were able to extend these results to mammalian cells by demonstrating that inhibition of the p38 pathway in hamster cells results in hypersensitivity to a pulse of aerolysin, a PFT associated with the human pathogen *A. hydrophila*. These results demonstrated for the first time that (*i*) animal cells have a defense against PFTs, and (*ii*) the defense depends on the conserved p38 pathway. The p38 pathway plays an important role in mammalian innate immunity. In *C. elegans*, this pathway provides an innate immune defense against *Pseudomonas aeruginosa*, *Salmonella enterica*, and *Staphylococcus aureus* because *C. elegans* mutants lacking an intact p38 pathway are killed more readily by these pathogens. My work has differed from these studies by focusing on one bacterial toxin rather than an entire bacterium. By showing that inhibition of this pathway leads to hypersensitivity of *C. elegans* to Bt Cry toxins and hypersensitivity of mammalian cells to aerolysin, we demonstrated that p38-mediated defensive mechanisms exist in these organisms to help counter the effects of a single virulence factor, a PFT. Hence, we discovered a role for the p38 pathway in the protection against PFTs. Equally significant, the fact that we were able to extend our results with Cry5B and *C. elegans* to aerolysin interactions with mammalian cells suggests that studying Cry toxins and *C. elegans* can yield insight into some of the conserved features of how PFTs interact with their targets and how target cells protect themselves against the toxins.

I also found that a second MAPK pathway is also required for protection against Cry toxins because loss of the JNK-like MAPK *kgb-1* lead to hypersensitivity to Cry5B and Cry21A toxins. Like p38 MAPKs, JNK MAPKs are important for innate immune responses in mammals and, more recently, were shown to be important for innate immune defense of *C. elegans* against *P. aeruginosa* infection (Constant et al., 2000; Dong et al., 1998; Mizuno et al., 2004).

Why two MAPK pathways, p38 and JNK, are both required for protection against Cry toxins is not clear. The results of the microarray studies indicated that these two pathways share many transcriptional targets. Indeed, for the PMK-1 pathway, of the 90 genes identified as potential targets, 69 of these were also on the list of potential targets of the KGB-1 pathway. Also, it is interesting that the KGB-1 pathway was found to be responsible for the toxin-regulated induction of so many more genes than were identified for the PMK-1 pathway (274 for KGB-1 compared to 90 for PMK-1). Considering that a total of 508 genes were up-regulated by Cry5B on the microarrays at the three-hour time-point, finding that over half of those were statistically dependent on *kgb-1* for this regulation was surprising. Perhaps this result is an indication that the KGB-1 pathway controls a broader range of defenses than the PMK-1 pathway. Consistent with this model was the cadmium result that showed *kgb-1*(um3) animals had impaired defenses to cadmium stress, whereas the mutants of the p38 pathway were not significantly deficient in these defenses.

Our data suggested that protection provided by the two MAPK pathways has real consequences for survival of the nematode in the wild. Wild-type *C. elegans* exposed briefly to Bt toxin in the soil are likely to crawl away, recuperate, and give

rise to progeny, whereas animals lacking *sek-1* or *kgb-1* exposed briefly to Bt toxin might never recover. Thus, these pathways may have evolved to allow the species to propagate under the adverse conditions in the natural environment.

A key and often challenging step in further understanding MAPK pathways is the identification of downstream targets that are activated by the MAPK. Analysis of microarrays with RNA from a *sek-1* mutant followed by RNAi of the candidate targets lead to the identification of three transcsriptional targets of the MAPK pathway, *ttm-1, ttm-2* and *ttm-3*. All three targets were transcriptionally induced by Cry5B toxin, required the *sek-1* MAPK pathway for their full induction, and were required for protection of the animal against the toxin. These data suggested that activation of MAPK pathway leads directly or indirectly to increased production of these proteins that in turn leads to protection and defense against the toxin (Figure 3.12). That RNAi of *ttm-1, ttm-2* or *ttm-3* lead to a less dramatic hypersensitivity phenotype than that caused by loss of *sek-1* could mean (*i*) that elimination of the *ttm* gene products by RNAi was incomplete and or (*ii*) that the MAPK pathway activates many toxin-defense genes in response to Cry5B, each of which provides incremental protection against the toxin

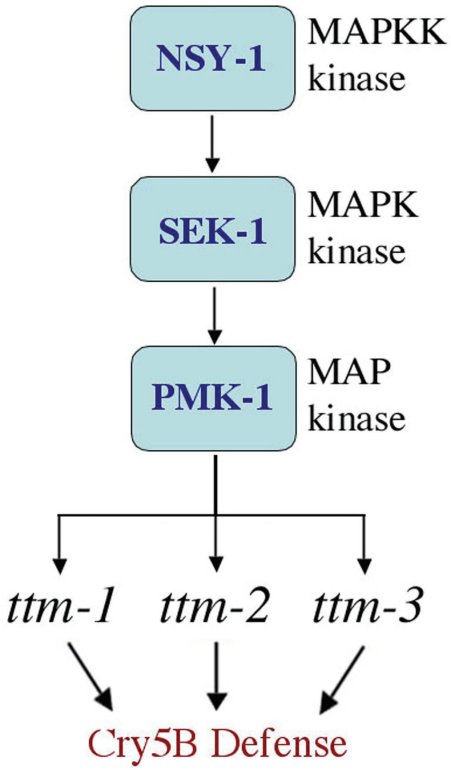

Figure 3.12. A model for *ttm* gene regulation by the PMK-1 MAP kinase pathway

The identity the *ttm-1* gene was particularly intriguing. The TTM-1 protein shows significant amino acid identity to cation efflux channels and is conserved in mammals (e.g., 34% amino acid identity to the human zinc transporter, ZnT-3). Based on this result, we speculated that one consequence of pore formation might be an increase in intracellular levels of cytotoxic cations that could be alleviated by up-regulation of an efflux transporter. Consistent with this model, examination of our microarray data indicated that *ttm-1* was induced upon exposure to the cytotoxic cation cadmium and RNAi of *ttm-1* lead to cadmium hypersensitivity. These data could suggest *ttm-1* plays a role in removing cytotoxic cations from the cytosol, either when coming from high levels in the diet or when coming into the cell by means of the action of PFTs.

As mentioned in the introduction, in mammals, the innate immune system includes the complement pathway, phagocytic cells and signaling cytokines. Homologs of complement and cytokine genes are absent from the *C. elegans* genome and *C. elegans* do not have specialized immune cells like macrophages or other bacterial phagocytes. Our model for *C. elegans* immunity is that the very cells under attack by the pathogen or virulence protein will mount a defense on their own behalf. We call this model cell mediated immunity.

Table 3.4. The genes identified from the microarray studies as transcriptionally activated by Cry5B in a *sek-1* dependent manner. The average fold change (avg FC) for each other the two *C. elegans* strains are indicated in the 2nd and 3rd columns. The last column denotes whether or not this gene was tested by RNAi or with a genetic mutant for hypersensitivity to Cry5B.

Probe ID	**avg FC *sek-1*(km4)**	**avg FC *sek-1*(+)**	**Gene**	**Tested on Cry5B?**
178830_at	6.98	10.35	B0001.1	n
183142_at	13.23	33.30	B0348.2	y
177894_at	6.91	7.95	C01A2.4	y
182323_at	1.28	3.92	C02H6.2	y
172035_x_at	1.77	3.38	C06C6.5	y
174150_at	1.23	2.67	C15B12.7	y
177487_at	1.00	2.32	C29F3.7	y
183555_at	1.07	3.06	C34H4.3	y
185253_at	17.89	107.79	C37C3.10	y
190156_s_at	2.27	4.79	C48B4.1	y
179430_s_at	11.65	14.42	C49C3.9	y
184711_at	4.73	14.77	C49G7.10	y
183639_at	7.82	17.02	F13A7.11	y
192874_at	1.78	3.19	F20D6.4	n
190899_at	3.98	4.81	F21H7.1	y
180364_s_at	5.22	6.12	F23C8.6	y
181052_at	1.44	3.45	F26G1.4	y
189171_at	2.11	2.74	F32A5.1	y
185153_s_at	7.99	7.48	F35E12.10	y
179914_at	2.89	10.36	F35E12.8	y
180204_at	6.77	8.42	F35E12.9	y
175705_s_at	3.27	4.62	F38A5.3	y
175918_at	1.45	2.52	F41B4.3	y
192010_s_at	1.54	4.64	F43E2.8	y

Table 3.4 continued

187668_at	3.14	3.81	F47D12.6	Y
178067_at	1.99	12.89	F48F7.7	y
181459_at	1.12	26.75	F49H6.13	y
177816_at	1.31	51.75	F49H6.3	y
180642_at	51.31	70.35	F53A9.2	y
182388_at	1.75	6.41	F53C11.1	y
187523_s_at	6.29	12.75	H06H21.10	y
186413_at	2.65	5.26	H20E11.1	y
185588_at	1.69	5.81	K02G10.1	y
184107_at	4.31	26.71	K09D9.1	y
183324_at	4.75	10.45	K10D11.5	y
184313_s_at	2.81	24.15	K11H12.4	y
188979_at	2.25	3.35	M04F3.4	y
192392_at	1.09	3.70	R03G5.2	y
190298_s_at	3.49	3.98	R05D8.8	y
177771_at	4.73	10.22	R08H2.8	y
180810_at	1.52	5.78	R10D12.9	y
187403_at	2.39	3.43	R10E12.1	y
177808_at	3.44	5.56	R11H6.4	y
191965_at	1.32	1.80	T05E11.3	y
172069_x_at	20.16	34.19	T10H4.12	y
171737_x_at	4.09	6.17	T12G3.1	y
186383_at	17.95	21.73	T19D12.4	y
176349_s_at	4.59	10.40	T24E12.5	y
190965_at	1.66	6.58	T27C10.4	n
178312_at	3.28	34.66	T27C5.8	y
184207_at	1.89	5.49	Y17G7B.11	y
184208_at	1.82	25.28	Y17G7B.14	y
176347_at	4.38	5.17	Y22D7AL.15	n
173007_s_at	1.49	1.96	Y34D9A.6	y
181665_at	1.33	2.08	Y37D8A.6	y
185425_at	4.06	8.18	Y38E10A.5	y
186316_s_at	1.14	4.67	Y39E4A.2B	y
191219_at	2.25	9.67	Y41C4A.11	y
176044_at	1.37	2.51	Y41D4B.16	y
185145_at	5.80	12.32	Y46D2A.2	y
191333_at	1.73	8.70	Y51A2D.11	y
188587_s_at	2.30	3.81	Y54G11A.6	y

Table 3.4 continued

194098_at	1.09	44.83	ZK1037.5	Y
180920_s_at	2.60	44.20	ZK1037.6	y
182403_at	2.56	5.42	ZK418.7	y
178357_at	2.34	3.38	ZK520.2	y
177700_at	4.60	11.46	ZK896.2	y
177468_at	22.24	59.13	ZK896.4	y
177681_s_at	10.67	25.67	ZK896.5	y
189460_at	1.37	2.52	B0285.9	y
175229_at	1.06	3.59	C08F11.13	y
173224_s_at	1.24	5.47	C17F4.3	y
184533_at	1.01	1.28	C17H12.8	y
183381_at	7.22	24.16	C50F7.5	y
191445_at	1.00	8.38	F01D4.2	y
178843_at	0.93	1.13	F08G5.6	y
177903_s_at	11.40	12.97	F09B9.1	y
180409_at	1.60	4.12	F17C11.5	y
179695_at	0.96	1.81	F35E12.5	y
192636_at	1.58	3.13	F37H8.3	y
183624_at	1.02	3.19	F55G11.5	y
183263_s_at	2.05	4.87	F59B1.8	y
191871_s_at	1.63	4.17	K01D12.11	y
189792_s_at	0.98	1.83	T05E11.5	y
178544_at	0.99	1.71	T06D8.9	y
192974_at	1.04	2.06	W02D3.7	y
176209_at	2.66	6.86	Y58A7A.5	y
176222_at	0.72	2.50	Y82E9BL.10	y
182104_at	0.51	1.10	ZK1025.3	y
184102_s_at	0.90	1.16	ZK1025.8	y

3.14 Materials & Methods

***C. elegans* and their maintenance.** *C. elegans* was maintained using standard techniques on NG medium and the *E. coli* strain OP50 as a food source. The following strains were used in this study: LGI, *glp-4*(bn2); LGII, *rrf-3*(pk1426); LGIV, *kgb-1*(um3); LGIV, *jnk-1*(gk7); LGX, *sek-1*(km4); LGII, *nsy-1*(ky376). All *C. elegans* assays were carried out at 20° C.

Microscopy. Images of *C. elegans* were captured on an Olympus BX-60 microscope using a 10X/0.25 objective and a DVC camera with a 0.5X camera mount.

Bt-toxin and cadmium plate assays. Bt-toxin assays. *E. coli* strains carrying Cry5B and Cry21A are described in (Wei et al., 2003). To induce expression of the toxins, a saturated culture was diluted 1:10 in LB containing 50μg/ml carbenicillin. The diluted culture was grown for 1 hour at 37° C with shaking. IPTG was then added to 50μM and cultures were grown for an additional 3 hours at 30° C. 30ul of bacteria were then spread on *C. elegans* high growth plates (ENG) with 100μM IPTG and 50μg/ml carbenicillin. Where indicated, the toxin expressing *E. coli* was mixed with *E. coli* containing empty vector to make low toxin lawns. The lawns were grown at 25° C and plates were used within one or two days. L4-stage *C. elegans* were picked or pipetted onto plates for toxicity assays.

Cadmium assays. To make plates containing cadmium, the cadmium chloride stock solution was added to the high growth media after autoclaving before the plates were poured. The day before the plates are needed for assays, they were spread with 30μl of an overnight culture of OP50. The lawns were grown at 25° C overnight. Plates were seeded with *C. elegans* in the same way as the Bt-toxin plates.

Growth assays with Cry5B and cadmium. Assays were carried out similarly to those described in (Griffitts et al, 2003) with the following exceptions. The toxin source was purified Cry5B or cadmium chloride. The food source was OP50 at an

optical density of 0.2-0.25 A_{600}. Approximately 30-40 L1 larvae were added to each well. Three trials were performed to calculate an average size and a SEM.

***C. elegans* genetic transformation and intestinal specific rescue.** The *cpr-1* promoter region was fused to the *sek-1* gene by PCR (Hobert, 2002). The *cpr-1* promoter in this construct consists of the 2143bp of sequence immediately upstream of the cpr-1 ATG start codon. The *sek-1* gene was amplified from N2 genomic DNA, starting with the ATG at the 5' end and 1179bp of 3' UTR at the 3' end. The 5' primer for amplification of the *sek-1* piece included an overhang sequence to overlap with the 3' end of *cpr-1* promoter amplicon to enable fusion to the *cpr-1* promoter amplicon by PCR. The P*cpr-1*::*sek-1* PCR product was injected into *sek-1*(km4) mutants with the dominant *rol-6* co-injection marker (pRF4) to obtain stably transmitting lines carrying extrachromosomal arrays. To test if intestinal specific expression of the *sek-1* gene is sufficient to rescue the Cry5B hypersensitivity phenotype of *sek-1* mutants, roller animals were placed on 10% Cry5B *E. coli* plates at the L4 stage with non-transgenic *sek-1*(km4) control animals. Animals were scored after 2 days of toxin feeding.

Microarrays. Sample prepartion and Gene Chip hybridization. *C. elegans* mutant *glp-4*(bn2) was used in place of N2 for studying wild-type responses to Cry5B. For identification of transcriptional targets of the PMK-1 pathway, the *C. elegans* strain *glp-4*(bn2); *sek-1*(km4) was treated side by side with the *glp-4*(bn2) control. For identification of the transcriptional targets of the KGB-1 pathway, the *C. elegans*

strain *kgb-1*(um3); *glp-4*(bn2) was treated side by side with the *glp-4*(bn2) control. Synchronous populations of the appropriate strains were prepared using standard techniques. Animals were grown to L4 stage on high growth plates seeded with OP50. At L4-stage, the worms were washed off these OP50 plates with water, pelleted, washed with 5mL water and pelleted again. For each strain, half of the population was pipetted onto plates seeded with JM103 *E. coli* expressing Cry5B while the other half were plated on JM103 carrying the empty vector. At the end of the three-hour exposure time, the animals were washed off the assay plates with water, pelleted, washed with 5mL water and pellet again. Total RNA was extracted and isolated as described at http://cmgm.stanford.edu/~kimlab/germline and further purified using Qiagen RNeasy columns. 10 µg of RNA were used to generate double stranded cDNA according to Affymetrix protocols (see http://genomics.ucsd.edu/). Biotinylated cRNA was *in vitro* transcribed from the double-stranded cDNA template using the Ambion MessageAmp aRNA kit (manufacturer's protocol). 15 µg of biotinylated cRNA "target" were hybridized to each *C. elegans* genome GeneChip array overnight at 45° C. After several washes, the arrays were doubly stained with streptavidin-phycoerythrin to enhance signal sensitivity (Affymetrix published protocols).

Data analysis. All microarray hybridization data was analyzed using the Corgon program (Sasik et al., 2002) available for download at http://corgon.ucsd.edu/~sasik/ to calculate a normalized signal intensity for each probe set on each gene chip. The statistical package Focus ((Cole et al., 2003); http://microarray.crump.ucla.edu/focus) was used to find genes differentially

expressed between *sek-1*(-) and *sek-1*(+) animals or between *kgb-1*(-) and *kgb-1*(+) animals, relative to appropriate controls, based on the 3 trials. The Focus criteria used were 1) interest score > 7.0, 2) mean expression level in treatment or control > 100, and 3) log-value contrast p-value < 0.01.

Quantitative Real-Time PCR. To confirm transcript levels of *sek-1* and *kgb-1* in the *glp-4*(bn2) strain by real time PCR, cDNA was made from the same total RNA used in the first trial of the Cry5B/empty vector microarray studies (3 hour time-point). To make cDNA, total RNA was treated with RQ1 RNase-free DNase from Promega according to the manufacturer's protocol. The DNase was removed from the RNA using an RNeasy column from Qiagen (manufacturer's protocol). First strand synthesis of cDNA was performed using M-MLV reverse transcriptase from Promega and a poly-dT oligo (manufacturer's protocol). To quantify levels of a particular cDNA species, the Amplifluor Detection System (Serologicals,Inc.) for real-time PCR was used. The PCR reactions included Platinum *Taq* DNA Polymerase, ROX internal control and UDG. Primer concentrations were: 5' primer at 10nM, 3' primer at 100nM, and the Amplifluor Uniprimer at 100nM. Reactions were carried out in the Applied Biosystems ABI Prism 7700 Sequence Detection System with software version 1.6.3. The default PCR program was used for 50 cycles. Transcript levels were normalized to that of an elongation factor gene, *eft-2*, that is not changed by Cry5B treatment as determined by Northern hybridization analysis (not shown). The final results were found using the Relative Standard Curve analysis (Applied Biosystems User Bulletin #2).

RNA interference. RNAi of *pmk-1* was done by feeding using *C. elegans* strain NL2099 carrying mutation *rrf-3*(pk1426) (Simmer et al., 2002). This strain does not show altered sensitivity to Cry5B compared to N2 (data not shown). The feeding protocol was adapted from that described in (Kamath and Ahringer, 2003) with the following modifications. The RNAi plates contained 0.1mM IPTG and 25μg/ml carbenicillin. L4 hermaphrodites were pipetted onto the RNAi feeding plates and allowed to feed for 30-32 hours before replica plating. Adults were allowed to lay eggs on these replica plates for 2-4 hours before being removed. Phenotypes were assessed in these progeny using the plate assays described above. Feeding was done at 20° C. The feeding clone for *pmk-1* was made by amplifying 1086bp of cDNA sequence using PCR with primers containing a XmaI recognition sequence at the 5' end. The PCR amplified insert was then cloned into the L4440 feeding vector at the XmaI site and transformed into the *E. coli* strain HT115.

Aerolysin Experiments. Baby hamster kidney cells were cultured as described in ref. 14, grown to confluence, and incubated or not with 10M SB203580 for 30 min in culture medium in the CO2 incubator. The cells were then treated for either 45 sec or 3 min with proaerolysin at different concentrations, rinsed, further incubated for 6 or 48 h in the incubator, and finally incubated with 2g/ml propidium iodide. Cells were either visualized by fluorescence microscopy or trypsinized, pelleted, and resuspended in PBS 1% FCS for fluorescence-activated cell sorter analysis.

***Staphylococcus aureus* killing assays.** Experiments were performed as described in (Sifri et al., 2003). Data was graphed and analyzed with GraphPad Prism.

Bioassays with Cry5B and salt stress. Assays were set up similar to those described in (Bischof et al., In press) with the following modifications. 10ul of the S-media buffer was substituted with the appropriate stock of NaCl solution or water if the condition called for no excess salt. Asssay plates were incubated at 25 degrees C and scored for dead and alive animals after five days.

Part of this chapter was adapted from segments of the following published paper, of which the author of this dissertation was the primary researcher.

Huffman D.L., Abrami* L., Sasik* R., Corbeil J., van der Goot F.G., and Aroian R.V. (2004). Mitogen-activated protein kinase pathways defend against bacterial pore-forming toxins. *Proceedings of the National Academy of Sciences*. 101(30): 10995-11000.

Sasik and Corbeil performed the statistical analysis of the microarray data. Abrami and van der Goot performed the aerolysin experiements. I would also like to acknowledge the UCSD Genomics Core for Affymetrix chip hybridization and scanning and the real-time PCR experiments.

3.15 References

Albertyn, J., Hohmann, S., Thevelein, J. M., and Prior, B. A. (1994). GPD1, which encodes glycerol-3-phosphate dehydrogenase, is essential for growth under osmotic stress in Saccharomyces cerevisiae, and its expression is regulated by the high-osmolarity glycerol response pathway. Mol Cell Biol *14*, 4135-4144.

Bamberger, D. M., and Boyd, S. E. (2005). Management of Staphylococcus aureus infections. Am Fam Physician *72*, 2474-2481.

Berman, K., McKay, J., Avery, L., and Cobb, M. (2001). Isolation and characterization of pmk-(1-3): three p38 homologs in Caenorhabditis elegans. Mol Cell Biol Res Commun *4*, 337-344.

Bischof, L. J., Huffman, D. L., and Aroian, R. V. (In press). Assays for Toxicity Studies in C. elegans with Bt Crystal Proteins. In C. elegans: Methods and Applications, K. Strange, ed. (Humana Press).

Brewster, J. L., de Valoir, T., Dwyer, N. D., Winter, E., and Gustin, M. C. (1993). An osmosensing signal transduction pathway in yeast. Science *259*, 1760-1763.

Cole, S. W., Galic, Z., and Zack, J. A. (2003). Controlling false-negative errors in microarray differential expression analysis: a PRIM approach. Bioinformatics *19*, 1808-1816.

Constant, S. L., Dong, C., Yang, D. D., Wysk, M., Davis, R. J., and Flavell, R. A. (2000). JNK1 is required for T cell-mediated immunity against Leishmania major infection. J Immunol *165*, 2671-2676.

Dong, C., Yang, D. D., Wysk, M., Whitmarsh, A. J., Davis, R. J., and Flavell, R. A. (1998). Defective T cell differentiation in the absence of Jnk1. Science *282*, 2092-2095.

Griffitts, J. S., Huffman, D. L., Whitacre, J. L., Barrows, B. D., Marroquin, L. D., Muller, R., Brown, J. R., Hennet, T., Esko, J. D., and Aroian, R. V. (2003). Resistance to a bacterial toxin is mediated by removal of a conserved glycosylation pathway required for toxin-host interactions. J Biol Chem *278*, 45594-45602.

Hobert, O. (2002). PCR fusion-based approach to create reporter gene constructs for expression analysis in transgenic C. elegans. Biotechniques *32*, 728-730.

Jonsson, P., Lindberg, M., Haraldsson, I., and Wadstrom, T. (1985). Virulence of Staphylococcus aureus in a mouse mastitis model: studies of alpha hemolysin, coagulase, and protein A as possible virulence determinants with protoplast fusion and gene cloning. Infect Immun *49*, 765-769.

Kamath, R. S., and Ahringer, J. (2003). Genome-wide RNAi screening in Caenorhabditis elegans. Methods *30*, 313-321.

Kamath, R. S., Fraser, A. G., Dong, Y., Poulin, G., Durbin, R., Gotta, M., Kanapin, A., Le Bot, N., Moreno, S., Sohrmann, M.*, et al.* (2003). Systematic functional analysis of the Caenorhabditis elegans genome using RNAi. Nature *421*, 231-237.

Kim, D. H., Feinbaum, R., Alloing, G., Emerson, F. E., Garsin, D. A., Inoue, H., Tanaka-Hino, M., Hisamoto, N., Matsumoto, K., Tan, M. W., and Ausubel, F. M. (2002). A conserved p38 MAP kinase pathway in Caenorhabditis elegans innate immunity. Science *297*, 623-626.

Maeda, T., Takekawa, M., and Saito, H. (1995). Activation of yeast PBS2 MAPKK by MAPKKKs or by binding of an SH3-containing osmosensor. Science *269*, 554-558.

Mizuno, T., Hisamoto, N., Terada, T., Kondo, T., Adachi, M., Nishida, E., Kim, D. H., Ausubel, F. M., and Matsumoto, K. (2004). The Caenorhabditis elegans MAPK phosphatase VHP-1 mediates a novel JNK-like signaling pathway in stress response. Embo J *23*, 2226-2234.

Sasik, R., Calvo, E., and Corbeil, J. (2002). Statistical analysis of high-density oligonucleotide arrays: a multiplicative noise model. Bioinformatics *18*, 1633-1640.

Sifri, C. D., Begun, J., Ausubel, F. M., and Calderwood, S. B. (2003). *Caenorhabditis elegans* as a model host for *Staphylococcus aureus* pathogenesis. Infect Immun *71*, 2208-2217.

Simmer, F., Tijsterman, M., Parrish, S., Koushika, S. P., Nonet, M. L., Fire, A., Ahringer, J., and Plasterk, R. H. (2002). Loss of the putative RNA-directed RNA polymerase RRF-3 makes C. elegans hypersensitive to RNAi. Curr Biol *12*, 1317-1319.

Tanaka-Hino, M., Sagasti, A., Hisamoto, N., Kawasaki, M., Nakano, S., Ninomiya-Tsuji, J., Bargmann, C. I., and Matsumoto, K. (2002). SEK-1 MAPKK mediates Ca2+ signaling to determine neuronal asymmetric development in Caenorhabditis elegans. EMBO Rep *3*, 56-62.

Wei, J. Z., Hale, K., Carta, L., Platzer, E., Wong, C., Fang, S. C., and Aroian, R. V. (2003). *Bacillus thuringiensis* crystal proteins that target nematodes. Proc Natl Acad Sci U S A *100*, 2760-2765.

Zarubin, T., and Han, J. (2005). Activation and signaling of the p38 MAP kinase pathway. Cell Res *15*, 11-18.

Chapter 4

Toxin-Regulated Activation of the PMK-1 MAP Kinase Pathway

4.1 Summary

Cry5B exposure causes *C. elegans* to transcriptionally up-regulate the *ttm* toxin defense genes via the PMK-1 MAP kinase pathway. I was interested in exploring how Cry5B communicates with the PMK-1 pathway. I found that treatment with Cry5B induces activation of the PMK-1 pathway as evidenced by increased levels of phospho-PMK-1 following toxin exposure. While the SEK-1 MAPKK was necessary for this activation of PMK-1, the data indicated that NSY-1 was not absolutely required for toxin-induced activation of the pathway. In an effort to uncover the genes responsible for this NSY-1 independent mechanism of PMK-1 activation, a reverse genetic screen was performed. A gene encoding a putative ceramide glucosyltransferase was identified as an important mediator of Cry5B-regulated activation of PMK-1 and Cry5B defense.

4.2 Introduction

MAP kinase pathways are enzymatic cascades that respond to extracellular cues and transmit that information into changes in cell activity. There are essentially three types of MAP kinases present in mulicellular organisms, the extracellular signal-regulated kinases (ERK), the c-Jun amino-terminal kinases (JNK) and the p38 type kinases. ERK type kinases, in mammals as well as *C. elegans*, have critical roles in development and cell division, but may also have roles in immunity in some instances. JNK and p38 are considered stress activated kinases because they respond to environmental stresses as well as cytokines and bacterial products.

In order to activate a MAP kinase cascade, the upstream kinase, i.e. the MAPKKK, has to first be activated. The mechanisms for MAPKKK activation can be complex, but there are a few well-studied examples that shed light on this critical step. I will briefly cover a few of these examples, focusing on how activation of the MAPKKK is ultimately linked to extracellular signals or conditions.

In mammalian cells, the best-characterized MAPKKK is Raf. Raf is part of the ERK MAP kinase cascades important for cell proliferation. The small GTPase Ras is responsible for recruitment of Raf to the plasma membrane, the initial step in Raf activation. Once at the plasma membrane, further activation steps involve multiple regulatory and scaffolding proteins. Activation of Raf is also influenced by the phosphorylation state of specific Raf residues. As a GTPase, Ras itself is subject to regulation by a guanine nucleotide exchange factor, which, in turn, is regulated by a receptor tyrosine kinase. This receptor tyrosin kinase is regulated by binding of an extracellular ligand and, in this way, is responsive to extracellular signals secreted by nearby cells to induce cell division.

Proper localization is key for other MAPKKKs as well. As haploids, *Saccharomyces cerevisiae* cells exist as one of two different mating types, a or α. Cells of each type secrete a mating pheromone specific for their type. Thus, these mating pheromones are used as a way of bringing together two cells of opposite type in order to mate. Genes required for mating are activated via a MAP kinase cascade where Fus3 is the MAPK, Ste7 is the MAPKK and Ste11 is the MAPKKK. These kinases are held together in the same protein complex by the scaffold protein Ste5. Mating pheromone of the opposite type serves as the extracellular signal that helps activate this cascade. In short, the pheromone binds to a G-protein coupled receptor present at the cell surface (Ste2 or Ste3), which then allows the receptor to bind the Ste5 scaffolding protein and thereby recruiting the entire MAP kinase cascade to the plasma membrane. A protein kinase, Ste20, also present at the plasma membrane, can then phosphorylate the Ste11 MAPKKK, one of the key steps in Ste11 activation.

The ASK1 MAPKKK has been shown to activate both p38 and JNK in mammalian cells. Like other MAPKKKs, ASK1 has multiple means of regulation, but perhaps one of the most elegant is that mediated by its inhibitory binding partner, thioredoxin. In the absence of oxidative stress, thioredoxin is bound to the N-terminus of ASK1, inhibiting its activity. In the presence of reactive oxygen species, however, two of the cysteine residues within the thioredoxin protein form a disulfide bridge, causing it to physically release ASK1 and permit its activity as a kinase. This regulatory mechanism helps explain ASK1 activation under conditions of oxidative stress.

What I hope these examples have illustrated is the extensive diversity in the mechanisms eukaryotes can use to turn an environmental cue into a molecular signal

in order to turn on an intracellular enzymatic kinase cascade. One of the intriguing fundamental questions in biology is how cells, and how organisms, monitor their environments at a molecular level and respond appropriately to that information. As well-conserved as MAP kinase cascades are, understanding how these pathways are specifically activated in response to particular extracellular stimuli can help address this more fundamental issue. With my project on the PMK-1 pathway in *C. elegans*, I was interested in understanding the role of the Cry5B PFT as a signal for host cells and, more specifically, as a signal for the p38 type MAP kinase pathway.

4.3 Cry5B Acts as a Signal to *C. elegans* to Activate the PMK-1 Protective Pathway

The existence of Cry5B defense genes that are activated by toxin exposure via the PMK-1 pathway implied that there must be signaling between the toxin and this host pathway. For the next phase of this project, I was interested in better understanding the mechanism of this communication. In exploring toxin-host communication, the initial question to be addressed was if I could detect increased phosphorylation of PMK-1 when animals are fed Cry5B. If so, this would indicate that the toxin serves as a signal for activation of the MAP kinase cascade. To measure levels of phospho-PMK-1, I made use of a commercial antibody raised against the dual-phosphorylated form of human p38. I found that this antibody cross-reacts specifically with the phosphorylated form of PMK-1 from *C. elegans* (Figure 4.1). Protein extracts from animals exposed to either purified Cry5B protein or buffer only were used in an immunoblot assay with this antibody to determine if animals exposed to Cry5B have a higher level of active PMK-1 compared to buffer treated controls.

An anti-tubulin antibody was used to control for protein loading. The results of these experiments showed that Cry5B exposure does cause an increase in the level of phosphorylated PMK-1 (Figure 4.1). This increase appears to be dose dependent and is consistently observed within 30 minutes of toxin feeding, although increases have been detected in as little as ten minutes (results not shown).

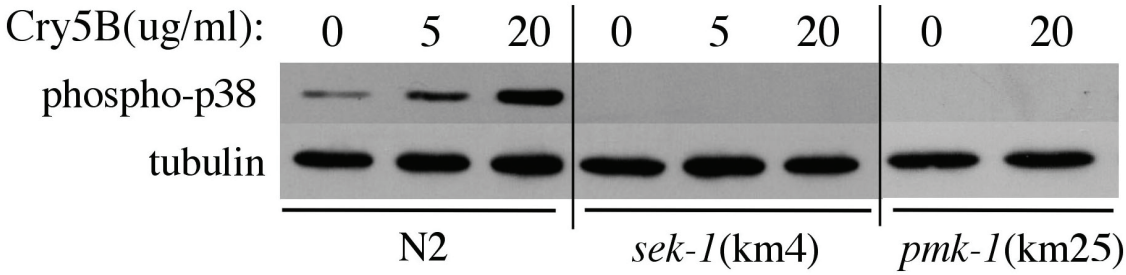

Figure 4.1. Cry5B exposure induces phosphorylation of PMK-1 MAP kinase. Protein extracts from animals treated for 1 hour with 5ug/ml Cry5B, 20ug/ml Cry5B or buffer only (0ug/ml) were probed for phospho-PMK-1 with an anti-phospho-p38 antibody and an anti-tubulin antibody. A *sek-1* or *pmk-1* deletion mutant lacks detectable levels of phospho-PMK-1 in this assay.

I then made use of this immunoblotting procedure to ask what other kinds of stresses are capable of activating the PMK-1 pathway. I found that heat (28°C for 1 hour) caused wild-type *C. elegans* to turn on PMK-1 while 3mM cadmium chloride did not, indicating at least some level of specificity (figure 4.2, A). Worms were also tested in a hyper-osmotic environment by placing them in media supplemented with additional sodium chloride above that which is normally present in the physiological buffer. This form of stress was particularly potent at activating PMK-1 (figure 4.2, A and B). How these different stresses ultimately feed into the same pathway is not clear.

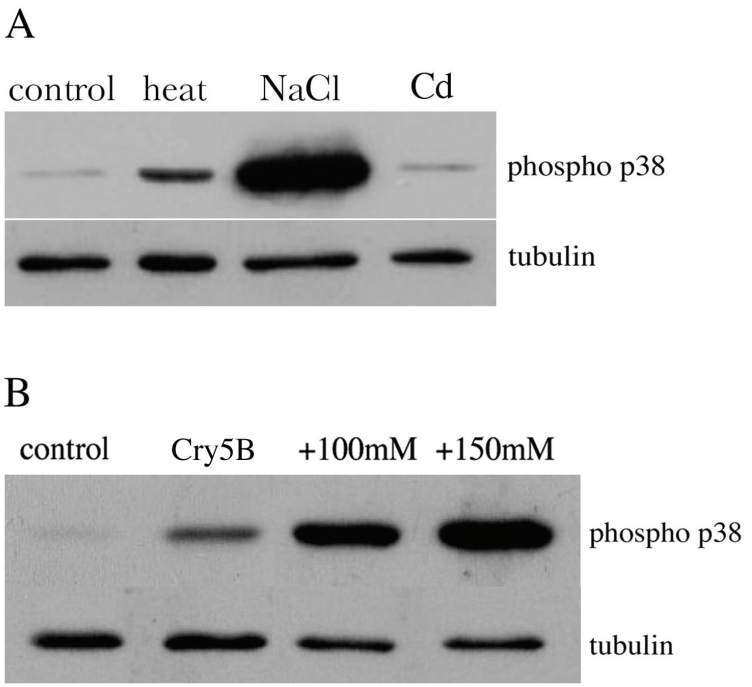

Figure 4.2. The PMK-1 MAP kinase is phosphorylated in response to some stress conditions. A, Protein extracts from N2 L4 larvae exposed for 1 hour to no stress (control), 28 degrees C (heat), 350mM added NaCl (NaCl) or 3mM cadmium chloride (Cd) and probed with the anti-phospho-p38 antibody and an anti-tubulin antibody. B, L4 stage N2 larvae were exposed for 1 hour to media with normal levels of NaCl and no Cry5B (control) or 10ug/ml Cry5B (Cry5B), or media supplemented with additional NaCl above the normal levels (+100mM or +150mM)

Using this same assay, I also examined several mutant *C. elegans* strains for their ability to induce the PMK-1 pathway upon toxin exposure. Interestingly, *kgb-1*(um3) mutant animals appeared to hyper-activate the PMK-1 pathway in response to Cry5B exposure. Perhaps these hypersensitive animals were being hit harder by the toxin than the wild-type strain in this assay and, as a result, they activated the PMK-1 defense pathway even more than wild-type (Figure 4.3, A). This result also argued against a model in which the KGB-1 MAP kinase pathway is responsible for activation of the PMK-1 MAP kinase pathway, at least when Cry5B is the activating stress agent. Also of note, a toxin resistant mutant, *bre-4*(ye13), did not activate PMK-1 in response to Cry5B but does have a normal basal level of active PMK-1

under control conditions (Figure 4.3, B). The *bre-4* mutants are resistant to Cry5B because they lack the intestinal glycosphingolipid that serves as the Cry5B receptor in *C. elegans* (Griffitts et al., 2005; Griffitts et al., 2003). This result indicated that activation of the PMK-1 pathway by Cry5B occurs downstream of toxin-membrane binding. Also, the data with the *kgb-1* and *bre-4* mutants support a positive correlation between sensitivity to Cry5B and activation of PMK-1 in response to Cry5B.

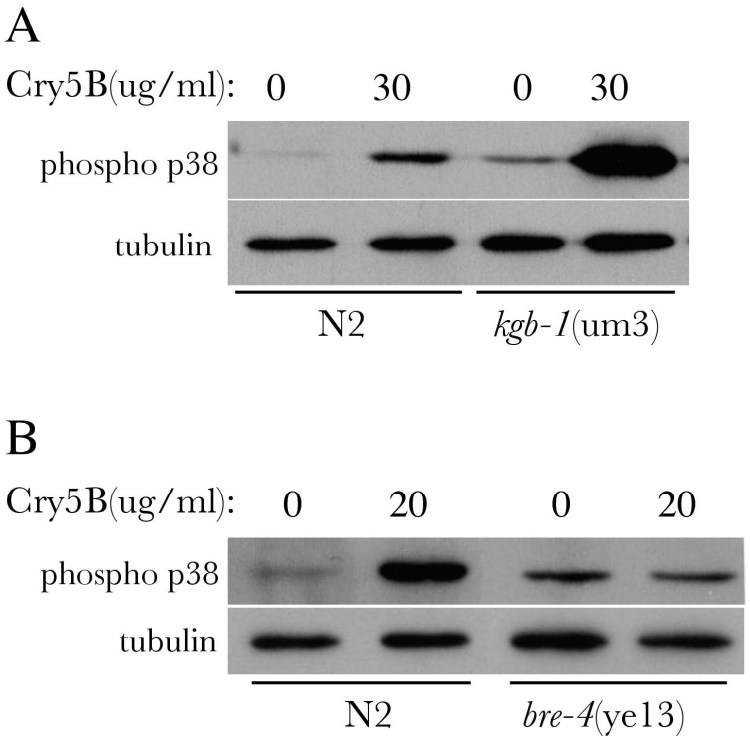

Figure 4.3. The activation of PMK-1 by Cry5B is altered in *kgb-1* and *bre-4* mutants. A, Protein extracts from N2 and *kgb-1*(um3) L4 larvae treated for 40 minutes with 30ug/ml Cry5B or buffer and probed for phospho-p38 and tubulin. B, Protein extracts from N2 and *bre-4*(ye13) L4 larvae treated for 1 hour with 20ug/ml Cry5B or buffer for were probed for phospho-p38 and tubulin.

4.4 The NSY-1 MAPKKK is Not Required for Cry5B-Induced Activation of PMK-1

Of particular interest with respect to PMK-1 activation was my finding with the MAPKKK mutant, *nsy-1*(ok593). Although deletion of the *sek-1* MAPKK gene resulted in a lack of detectable phospho-PMK-1 under both toxin-fed and control conditions, the *nsy-1*(ok593) deletion mutant had a distinctly different phenotype. While wild-type animals had a basal level of phospho-PMK-1 in my assays, *nsy-1*(ok593) animals had no detectable amount of phospho-PMK-1 in the absence of toxin. However, unlike the *sek-1*(km4) mutants, *nsy-1*(ok593) animals still activated PMK-1 in response to Cry5B, although the levels of phospho-PMK-1 in the presence of toxin were lower than in wild-type animals on toxin.

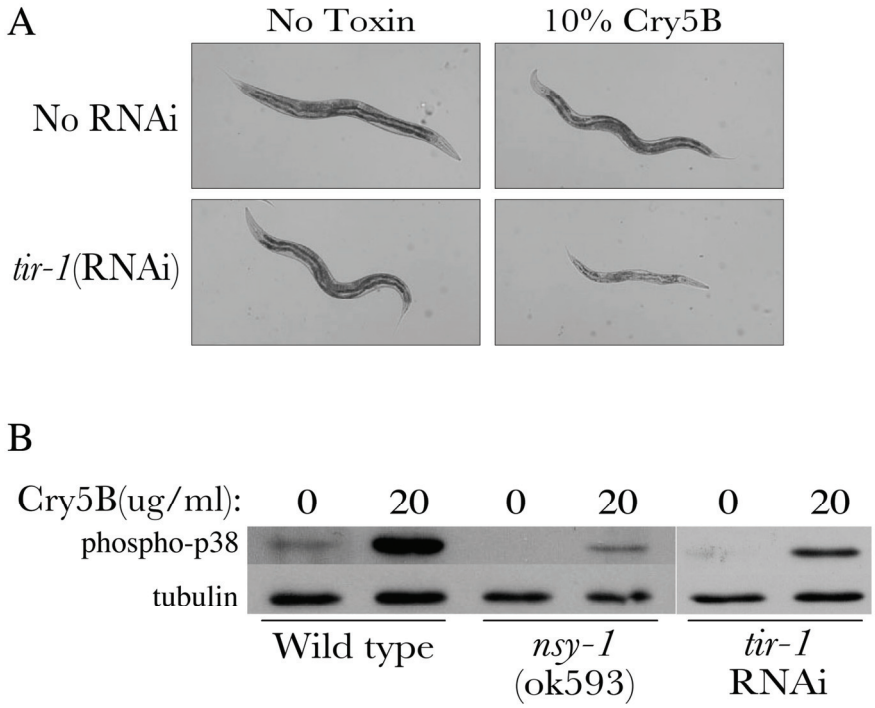

Figure 4.4. *tir-1* is involved in Cry5B defense and loss of *tir-1* or *nsy-1* partially reduces phospho-PMK-1 levels. A, animals fed double-stranded RNA corresponding to *tir-1* appear highly intoxicated compared to control animals on a relatively low dose of Cry5B. B, Protein extracts from the *nsy-1*(ok593) deletion mutant and *tir-1* RNAi animals were probed for phospho-p38 and tubulin.

Similar results were seen with animals knocked down for the gene *tir-1*. The *tir-1* gene encodes a cytosolic protein containing a Toll/interleukin-1 receptor domain and is the ortholog of the human SARM1 protein (sterile alpha and armadillo repeat protein). *tir-1* has been shown to act upstream of *nsy*-1 in innate immunity studies with pathogenic bacteria and, in neuronal cells, it has been further demonstrated that TIR-1 binds to and activates NSY-1 (Chuang and Bargmann, 2005; Couillault et al., 2004). Taken together, my results suggested a model in which the NSY-1/TIR-1 branch of the pathway is responsible for the basal level of active PMK-1 and an alternative pathway that feeds into SEK-1 independent of NSY-1/TIR-1 is capable of activating the pathway in the presence of toxin (Figure 4.5). Recent studies examining the role of the PMK-1 pathway in oxidative stress have also shown that the NSY-1 kinase is not required for PMK-1 activation in response to sodium arsenite exposure and these authors proposed the existence of an alternative MAPKKK that can activate SEK-1 and, subsequently, PMK-1 (Inoue et al., 2005).

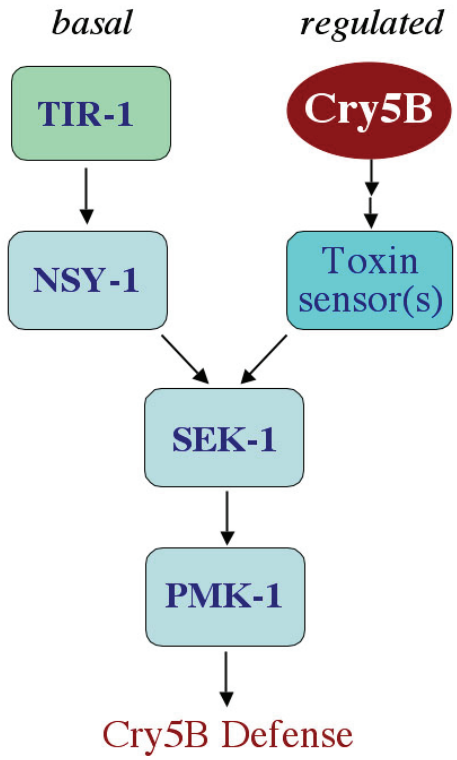

Figure 4.5. A model for PMK-1 activation. In the absence of toxin, some phosphorylated PMK-1 is present in the cell from SEK-1 activation through NSY-1/TIR-1 pathway. Upon Cry5B exposure, the level of active PMK-1 rises as a result of activation through a toxin sensitive pathway.

If the ability to activate PMK-1 in response to Cry5B exposure is an important part of the defense mechanism employed by this host, then we would expect *nsy-1* mutants to be less impaired in toxin defense than a *sek-1* or *pmk-1* mutant because *nsy-1*(ok593) animals still manage to produce some phosphorylated PMK-1 in the presence of Cry5B. In fact, in our Cry5B *E. coli* assays, we frequently observed that *nsy-1* mutants did not look as severely intoxicated as *pmk-1* or *sek-1* mutants, although they were clearly hypersensitive with respect to wild-type. To verify this observation with quantitative data, I examined the *pmk-1*(km25), *sek-1*(km4) and *nsy-1*(ok593) mutants on a range of toxin concentrations to determine the LC_{50} for all three mutants and wild-type. These experiments were performed with the help of postdoctoral

fellow Larry Bischof. The assays were carried out in multi-well plates with liquid media, purified Cry5B protein, an *E. coli* food source and a drug to prevent progeny production. In a single experiment, each condition was set up in triplicate (i.e. three wells with identical Cry5B concentration for each *C. elegans* strain). Three independent experiments were performed. The data were analyzed and plotted on a graph with the software program GraphPad Prism.

The results of this investigation showed that *nsy-1*(ok593) mutants have an LC_{50} of 280ng/ml Cry5B while the *sek-1*(km4) mutants have an LC_{50} of 100ng/ml Cry5B (Figure 4.6). A t-test indicated that these values are significantly different and *nsy-1* mutants are indeed less sensitive than *sek-1* mutants in this assay. However, the results for the *pmk-1*(km25) strain were less certain. In these assays, the dose response curve of the *pmk-1* mutants was much steeper than for the other strains (Figure 4.6). None of the concentrations of Cry5B tested caused an intermediate level of death in the *pmk-1*(km25) animals, suggesting an almost threshold-like effect of Cry5B in this mutant. There are many biological models that could explain why the *pmk-1* mutant behaves differently than a *sek-1* mutant (I cover some of these possibilities in the discussion at the end of the chapter). However, another explanation of this result could involve the curious nature of the *pmk-1*(km25) allele. According to the group that isolated and published on this allele, the km25 deletion removes less than half of the entire kinase domain of the PMK-1 protein, leaving a chance that these mutants retain some PMK-1 activity. In fact, the deletion ok811 is much larger than km25 but is still contained within the *pmk-1* open reading frame and ok811 is lethal to *C. elegans* when homozygous. This information may suggest that a homozygous null mutation in *pmk-1* is lethal and the km25 deletion only partially reduces PMK-1

activity. Alternatively, because *pmk-1* is part of an operon that includes the essential gene *pmk-2*, it is possible that the ok811 deletion disturbs this essential gene product while km25 does not. Note that RNAi of *pmk-1* does not impair worm viability and in our westerns with phospho-PMK-1 antibody, the *pmk-1*(km25) animals looked identical to the *sek-1*(km4) null mutants. Unfortunately, the ambiguity of the km25 allele makes the LC_{50} data for this strain difficult to interpret, but *nsy-1*(ok593) and *sek-1*(km4) alleles are undisputed nulls and the LC_{50} data with these animals supported a positive correlation between ability to activate the MAP kinase pathway and ability to defend against Cry5B.

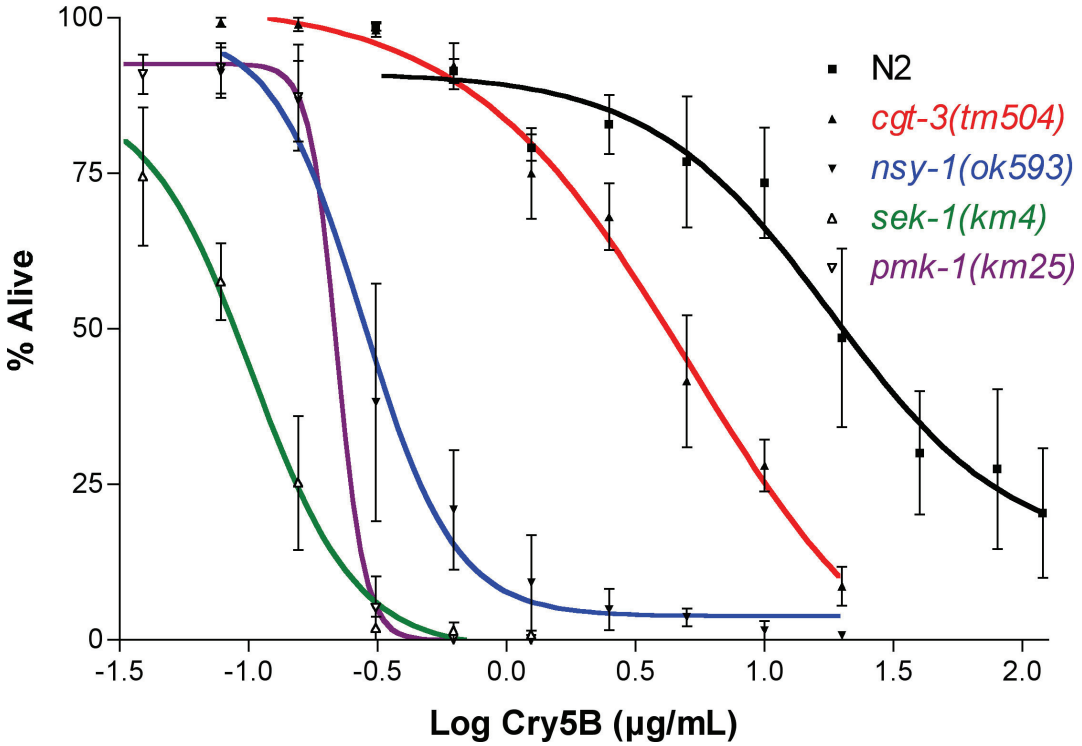

Figure 4.6. Dose response curves for *C. elegans* mutants with increased sensitivity to Cry5B. The *nsy-1*(ok593) mutant is statistically less sensitive than the *sek-1*(km4) mutant. The *cgt-3*(tm504) mutant is statistically more sensitive than N2.

4.5 Genetic Screen for Loss of Cry5B-Induced PMK-1 Activation

Our model for the activation of the PMK-1 pathway by Cry5B requires the existence of host proteins or factors that recognize that Cry5B is present and relay that recognition into activation the SEK-1/PMK-1 pathway. These factors could be recognizing some indirect signal of Cry5B activity, such as a change in cell turgor or ionic imbalance, or they could somehow be responding more directly to the Cry5B toxin once it makes contact with the plasma membrane. Potentially, there could also be other signaling proteins that have yet to be identified as members of this pathway that aid in signal transduction between the toxin-sensor and the SEK-1 kinase. In order to identify genes responsible for toxin recognition and signaling, we developed a reverse genetic screen for genes that influence the activation of PMK-1 by Cry5B. We predicted that any gene critically involved in this process would mutate to a toxin hypersensitive phenotype (a so-called Hpo phenotype for Hypersensitive to Pore-forming toxin). Such a phenotype is simple to score visually, so we designed the first phase of the screen to be a toxin assay to look for animals that appear highly intoxication on a low dose of Cry5B. Because not all toxin defense genes are involved in PMK-1 activation, we needed a secondary screen. The plan for the secondary screen was to take the positive genes from the RNAi (primary) screen and test them further to determine if RNAi of these genes also makes animals unresponsive to Cry5B in the immunoblot assay for PMK-1 activation.

As I had done previously for screening the transcriptional targets of PMK-1, I made use of the Ahringer RNAi feeding library to individually knock-down the genes of the *C. elegans* genome. Roughly 350-550 genes were knocked out each week. The knock-down animals were visually scored to find those that were noticeably more

intoxicated than the negative control animals. With each set, we set up positive controls (*tir-1* and Y71H2B.7) and negative controls (empty RNAi vector). Figure 4.7 shows some representative animals from these controls at the time of scoring.

With the help of a full-time technician, Mindy Hsieh, we completed screening 5669 genes in the primary screen (chromosomes II and IV), 60 of which yielded confirmed Hpo phenotypes. Two of these 60 genes, *nsy-1* and *kgb-1*, were already known to mutate to a Cry5B hypersensitive phenotype, but the remaining 58 represent novel *hpo* genes. Table 4.1 lists the identities of these 58 genes.

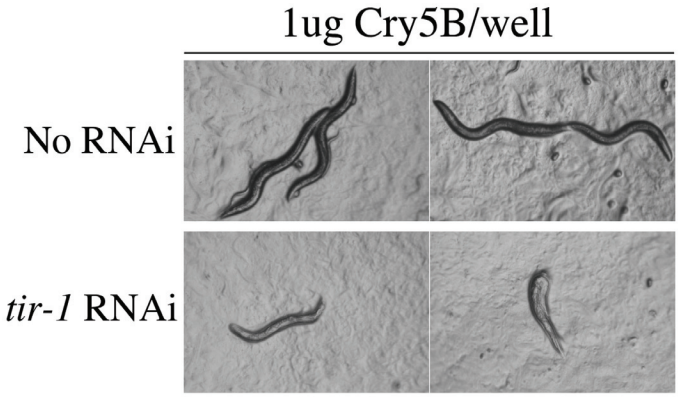

Figure 4.7. Negative control animals (No RNAi) and positive control animals (*tir-1* RNAi) from the primary RNAi screen for the Hpo phenotype.

Table 4.1. The 58 novel *hpo* genes from RNAi screen of chromosomes II and IV

B0491.1	C40A11.5	F16G10.4	*sru-19*	*unc-43*
F52C6.4	K02A2.5	F52C6.5	F20C5.4	Y38f2AR.2
kel-1	T10D4.4	F52C6.7	F28D1.11	Y55F3BR.4
kqt-3	Y57A10C.7	*frm-5*	*let-60*	Y76B12C.7
Y46G5A.18	*pak-8*	M02B7.4	*mca-1*	Y55F3BR.2
Y110A2AL.12	Y48B6A.6	*bath-44*	*ntl-4*	Y41D4B.16
nhx-6	K06A1.6	C29F4.2	*oma-1*	ZC416.4
unc-53	C14A4.3	C33D9.2	*prx-2*	*cap-1*
tag-274	T24H10.37	C42C1.9	T05E11.6	*elo-6*
cgt-3	C44B7.3	C42C1.10	T14G10.7	F42C5.10
tat-4	F42C5.10	C42C1.11	*tag-60*	
F58e1.4	C18E9.9	*ccr-4*	*unc-22*	

Having identified these novel Cry5B defense genes, I checked back on the microarray data to see how many of them showed transcriptional up-regulation or down-regulation by toxin exposure. Of the 58 *hpo* genes, nine were found to be up-regulated by toxin in at least one of the time-points tested on the microarrays and another two were found to be down-regulated. These results are summarized in Table 4.2. I also checked if any of the nine up-regulated genes were dependent on either *sek-1* or *kgb-1* for their induction. That is, I asked if any of the nine genes were on the list of candidate transcriptional targets of these pathways that were identified from the microarray analyses described in Chapter 3. Of these nine genes, none showed statistical dependence on the *sek-1* gene for their induction, but five of them did show dependence on *kgb-1*. The behaviors of these five genes are listed in Table 4.3. Among these five genes is an actin capping protein (D2024.6). The other four do not have any clear homologs outside of the *Caenorhabditis* genus and do not have predicted functions.

Table 4.2. The 9 *hpo* genes identified in the RNAi screen that were also transcriptionally up-regulated by Cry5B. The numbers indicate the fold change of the transcript relative to the control used at that time-point. No changes means the transcript abundance was not statistically different from that in the controls. The bottom row lists the total number of genes up-regulated at each time-point.

	1 hour Cry5B vs. Cry5A	2 hours Cry5B vs. Cry5A	3 hours Cry5B vs. empty vector	4 hours Cry5B vs. Cry5A
F20C5.4	5.3x	4.0x	3.4x	3.4x
ZK809.7	No change	No change	No change	1.4x
Y41D4B.16	No change	No change	2.8x	No change
ZC416.4	No change	No change	4.1x	No change
D2024.6	No change	1.4x	2.0x	1.9x
F42C5.10	No change	No change	3.1x	No change
T24H7.5	1.5x	No change	1.7x	2.0x
C18E9.9	No change	No change	2.2x	2.8x
M01B12.3	No change	No change	No change	1.7x
Total # genes	*263 genes*	*216 genes*	*467 genes*	*345 genes*

Table 4.3. *kgb-1* dependent *hpo* genes. The behavior of the five genes identified in the RNAi screen for Hpo phenotypes that showed kgb-1 dependent up-regulation upon Cry5B exposure in the microarray studies.

transcript	*kgb-1* genotype	fold toxin-induced (Affy)
F20C5.4	+	2.7
F20C5.4	-	1.1
Y41D4B.16	+	1.7
Y41D4B.16	-	0.7
D2024.6	+	1.7
D2024.6	-	1.1
F42C5.10	+	2.7
F42C5.10	-	0.8
C18E9.9	+	2.1
C18E9.9	-	1.6

4.6 A Ceramide Glucosyltransferase Gene is Required for Activation of PMK-1

The 27 positive *hpo* genes from chromosome II were also put through the secondary screen for PMK-1 activation. For some of these genes (*nhx-6*, *tag-274*, *cgt-3* and *unc-53*), a mutant strain was available from the *C. elegans* stock center and so, for these, the genetic mutants were tested in the phospho-PMK-1 immunoblot assay for ability to activate PMK-1 in response to Cry5B exposure. For the remaining genes, the RNAi was repeated, this time using a more efficient, but laborious, protocol that begins the RNAi feeding at the L4 stage and continues until the progeny of these animals have reached L4. These L4 progeny were the ones I assayed for a phenotype in the phospho-PMK-1 immunoblot assay.

The results of the primary and secondary screens revealed one gene, *cgt-3*, that when knocked down by RNAi or mutated genetically results in animals that: 1) have a Hpo phenotype; 2) have normal basal levels of phophorylated PMK-1; and 3) are unable to activate PMK-1 when exposed to Cry5B (Figure 4.8, A and B and Figure 4.6). Interestingly, however, these *cgt-3* mutants do activate the PMK-1 pathway

when exposed to heat or osmotic stress conditions, indicating they are not impaired in their ability to sense and respond to these other stressors (Figure 4.8, C) and suggesting that these different stimuli activate SEK-1/PMK-1 via a somewhat different mechanism than Cry5B. The *cgt-3*(tm504) strain was also tested on cadmium to help us establish if the mutants show general impairment in stress defenses. On two different concentrations of cadmium, the *cgt-3* mutants looked similar to wild-type in general health and appearance (Figure 4.9, A). We were also interested in determining if *cgt-3* might be important for defense against an infectious bacterium. For these experiments, L4 animals (N2 and *cgt-3*[tm504]) were placed on agar plates seeded with a pathogenic strain of *Pseudomonas auriginosa*. Figure 4.9B shows the average and SEM for three *P. auriginosa* plates for each worm strain. These data indicate *cgt-3* may play a minor role, if any, in defense against this bacterium.

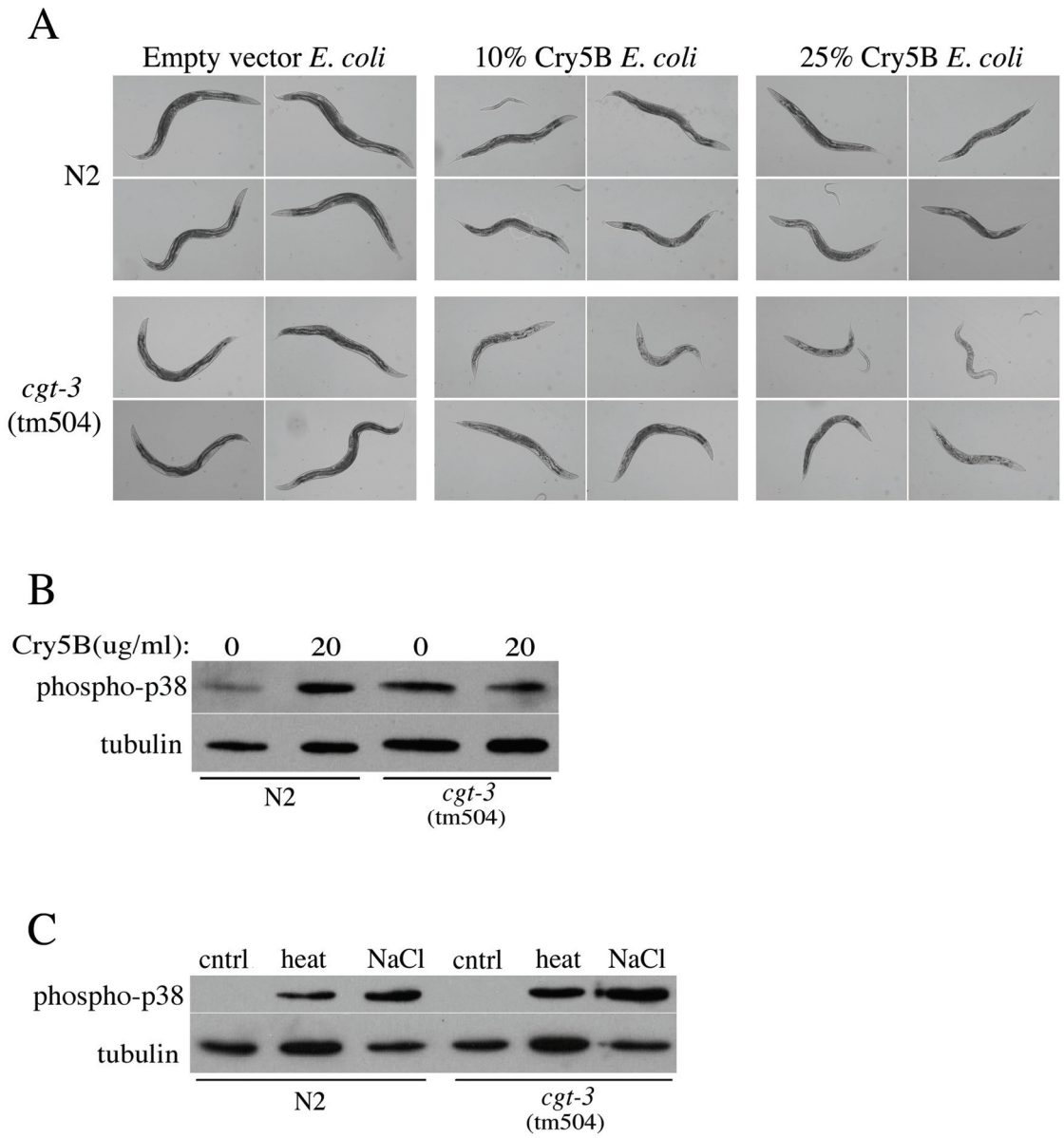

Figure 4.8. The *cgt-3*(tm504) deletion mutant is hypersensitive to Cry5B and fails to activate PMK-1 during toxin exposure. A, N2 and cgt-3(tm4504) animals after two days feeding on empty vector E. coli, 10% Cry5B E. coli or 25% Cry5B E. coli. B, Protein extracts from N2 and cgt-3(tm504) L4 animals were probed with anti-phospho-p38 and anti-tubulin antibodies.

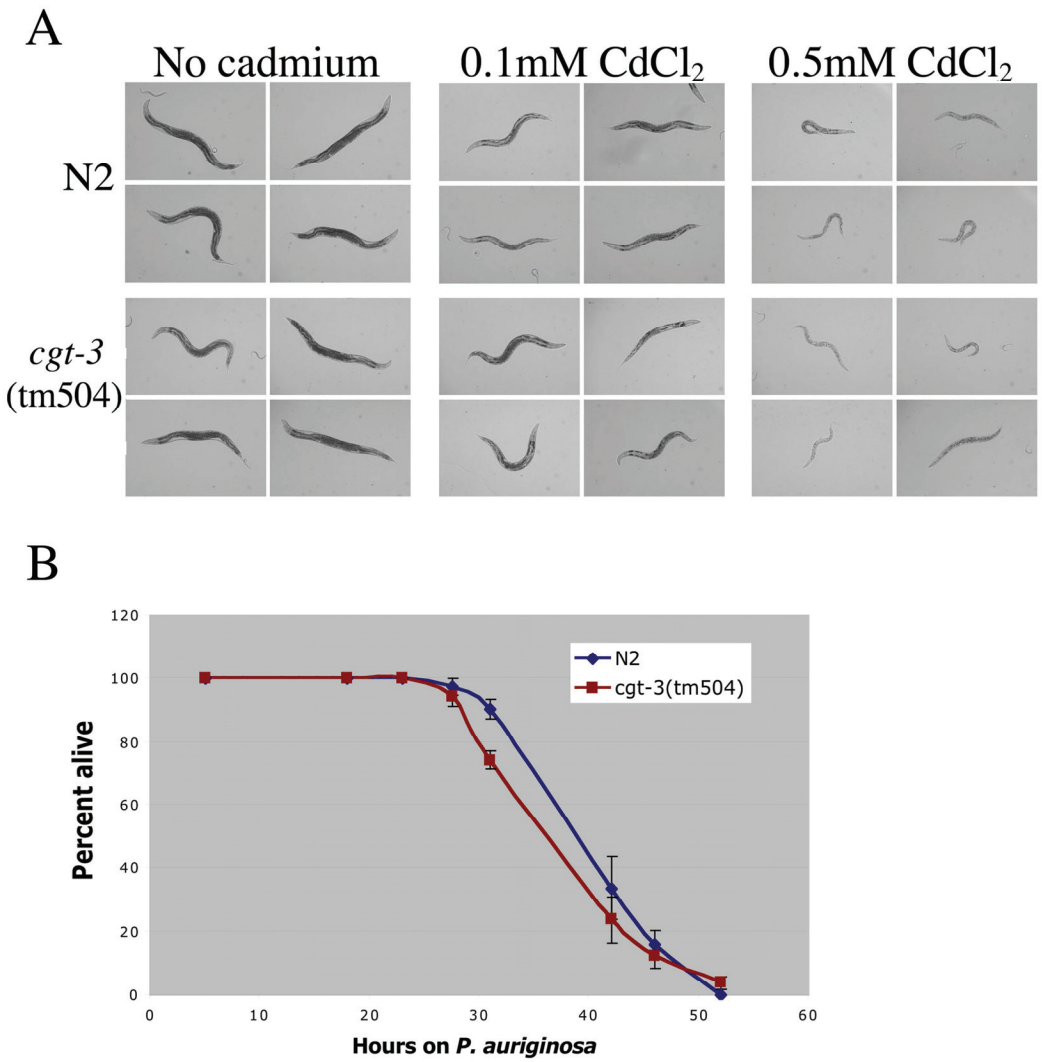

Figure 4.9. *cgt-3*(tm504) mutants on cadmium chloride (A) and *P. auriginosa* (B). A, L4 animals were placed on agar worm growth media supplemented with 0, 0.1 or 0.5mM cadmium chloride and photographed after days. B, L4 animals were placed on lawns of *P. auriginosa* and dead and alive animals worms were counted at the indicated timepoints.

The *cgt-3* gene is one of three genes in the *C. elegans* genome predicted to encode a ceramide glucosyltransferase (see Figure 4.10 for protein alignments). This class of enzymes catalyze the addition of a glucose molecule to the sphingolipid, ceramide. This reaction is the first step in building the carbohydrate structure of glycosphingolipids (GSL). Once this initial glucose is added to the lipid, additional sugars may be added by other various glycosyltransferases to build a more complex

carbohydrate structure. In *C. elegans*, the receptor for the Cry5B toxin is the long oligosaccharide chains found on intestinal GSLs (Griffitts et al., 2005). Cry5B binds the carbohydrate portion of the GSL, which presumably brings the toxin in contact with the intestinal membrane, allowing it to form a pore. Several of the glycosyltransferase genes responsible for building this carbohydrate receptor were identified in the Aroian lab in a genetic screen for mutants that are resistant to Cry5B. These genes were named *bre* for Bacillus toxin resistant. As mentioned earlier (see Figure 4.3, B), a *bre-4* mutant also fails to activate PMK-1 in response to Cry5B, indicating the signal for PMK-1 activation is dependent on receptor binding. Given this background, my finding that a ceramide glucosyltransferase gene can mutate to a toxin hypersensitive phenotype raised many questions.

Figure 4.10. ClustalW alignment of the *C. elegans* CGT-3 amino acid sequence (Ce CGT-3) with the sequence of the UDP-glucose ceramide glucosyltransferase protein (Hs CGT) from humans.

In biosynthesis of the GSL Cry5B receptor, the BRE-3 enzyme adds the second sugar, a mannose, to the carbohydrate chain. To test the genetic relationship between the *bre* genes and *cgt-3*, I constructed a *cgt-3*(tm504); *bre-3*(ye28) double mutant *C. elegans* strain. The double mutant strain was then tested on high and low doses of Cry5B to determine if it has a hypersensitive phenotype, like a *cgt-3* mutant,

or a resistant phenotype, like the *bre-3*(ye28) strain. The double mutant was in fact resistant to Cry5B, indicating that *bre-3* is epistatic to *cgt-3*. This result placed *cgt-3* genetically downstream of toxin/GSL binding and discounted the possibility that CGT-3 is the only ceramide glucosyltransferase that can add the first glucose to the GSL toxin receptor.

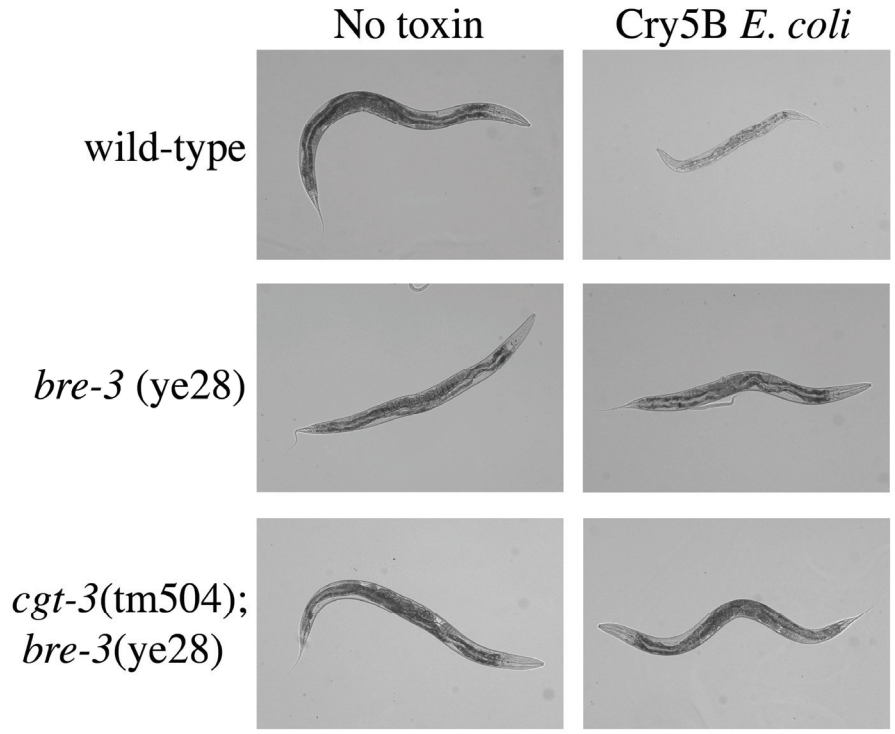

Figure 4.11. The *cgt-3*(tm504); *bre*-3(ye28) double mutant is resistant to Cry5B.

4.7 Testing for Changes in the Total PMK-1 Protein Levels

In my immunoblot assays for activation of PMK-1, I used a commercial antibody to measure the relative amounts of phosphorylated PMK-1 in *C. elegans* protein extracts and an anti-tubulin antibody to control for differences in protein loading. Presumably, an increase in the amount of phospho-PMK-1 indicated that the

pathway was activated and the PMK-1 protein already present in the cell had been phosphorylated by SEK-1. Alternatively, increases in phospho-PMK-1 seen after toxin treatment could have been the result of increased levels of total PMK-1 protein due to increased *pmk-1* transcription or decreased protein degradation. Because the increase in phospho-PMK-1 levels happened so quickly (consistently within 30 minutes), I believe that increased phosphorylation was responsible. To help us confirm that the increase in phospho-PMK-1 levels observed in wild-type animals exposed to Cry5B was not due to increases in the total amount of PMK-1 protein, I attempted to produce and purify a polyclonal antibody that recognizes both phosphorylated and unphosphorylated PMK-1.

To produce a suitable antigen for antibody production, I made a GST fusion construct with a fragment of the PMK-1 coding region corresponding to amino acids 232-365 cloned downstream of the GST open reading frame. This segment of the PMK-1 protein was chosen because it is less identical to the p38 protein from mammals in this region, hopefully making the antigen more immunogenic. The construct was expressed in *E. coli* and the GST fused to a piece of the PMK-1 protein was purified with glutathione agarose. The fusion protein was sent to Cocalico Biologicals for injection into rabbits. From the sera obtained from the company, I purified a fraction that has activity against PMK-1 in a western blot with *C. elegans* extracts (Figure 4.12). The antibody preparation recognized a protein in wild-type extracts that is the size of PMK-1 (Figure 4.12, A) and this protein was also present in extracts from *sek-1* mutants (Figure 4.12, C). However, this same protein was not detected with this antibody in extracts from *pmk-1* mutants (Figure 4.12, B). Other proteins were also recognized using this antibody indicating that it is not specific only

for PMK-1 protein. Even so, this antibody could be used to determine if total PMK-1 levels change in toxin exposed animals. Such an experiment is underway currently.

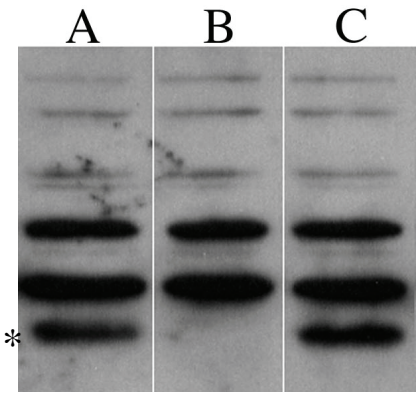

Figure 4.12. A western blot using anti-PMK-1. *C. elegans* protein extracts from N2 (lane A), *pmk-1*(km25) mutants (lane B) and *sek-1*(km4) mutants (lane C). The (*) indicates the band corresponding to the PMK-1 protein.

4.8 Discussion

When the pore-forming toxin Cry5B is fed to *C. elegans*, the animals quickly activate the PMK-1 MAP kinase pathway. This observation is consistent with what has been reported for other PFTs including the α-hemolysin of *Staphylococcus aureus*, streptolysin O from *Streptococcus pyogenes*, anthrolysin O from *Bacillus anthracis* and *Streptococcus pneumoniae* pneumolysin, all of which activate p38 in mammalian cells at sub-lytic concentrations (Ratner et al., 2006; Stringaris et al., 2002). Many of these toxins are unrelated in sequence and structure, suggesting that it is this pore-forming activity that they all share that is responsible for inducing p38 activation.

The MAPKK SEK-1 appeared to be absolutely required for phosphorylation of PMK-1, as a *sek-1* deletion mutant lacked any detectable level of phospho-PMK-1. To date, the only MAPKKK that has been shown to phosphorylate and activate SEK-1 is NSY-1. NSY-1 is the *C. elegans* ortholog of the mammalian protein ASK-1, a

MAPKKK that has been placed upstream of both p38 and JNK type MAP kinases. Given my finding that a *nsy-1* deletion mutant can produce phospho-PMK-1 when the pathway is stimulated with Cry5B, there must exist a mechanism for SEK-1/PMK-1 activation that is independent of NSY-1. Furthermore, this NSY-1 independent mechanism for pathway activation must be regulated by Cry5B because loss of *nsy-1* does not abrogate Cry5B-induced phosphorylation of PMK-1. However, loss of *nsy-1* does cause deficiencies in basal PMK-1 activity. Therefore, NSY-1 could be responsible for the basal level of phosph-PMK-1 that is present under non-stressful conditions (Figure 4.5). In the literature, there are numerous examples of MAPKKs being activated by more than one upstream kinase, so our model describing two independent means of activating SEK-1 is not inconsistent with what is known about MAP kinase signaling.

In an effort to test for a correlation between phospho-PMK-1 levels and Cry5B defense, I quantified more precisely the Cry5B sensitivity levels of the three kinase mutants, *pmk-1*(km25), *sek-1*(km4) and *nsy-1*(ok593). The prediction for these experiments was that loss of *nsy-1* would have a less severe effect than loss of *sek-1* or *pmk-1* because *nsy-1*(ok593) mutants have some amount of phospho-PMK-1 in the presence of Cry5B while the other two mutants have none (or none that I can detect). With regard to *sek-1* and *nsy-1*, this prediction held true. For *pmk-1*(km25) however, the results were surprising. At a toxin dose of 156ng/ml, the *pmk-1* mutants were nearly all alive in all three trials of the experiment. At the next highest dose in the assay, 312ng/ml, these mutants were nearly all dead. Assuming the km25 allele is truly a null, this rapid drop in viability could have an important biological explanation behind it. For instance, perhaps in the absence of PMK-1, the SEK-1 MAPKK is able

to phosphorylate and activate some other MAP kinase. This alternative MAPK may be able to function in the place of PMK-1 as long as the toxin concentration is not too high. Once the concentration gets above a certain threshold however, this theoretical MAPK would no longer be a sufficient back-up for PMK-1 and the animals would start behaving like a *sek-1* mutant. Another possibility is that, even in wild-type animals, SEK-1 is part of two MAP kinase pathways that both mediate defense to Cry5B. This model would explain why the *sek-1* and *pmk-1* mutants behave differently in the dose response study, but does not address why *pmk-1*(km25) mutants have such a steep killing curve.

The alternative upstream activators of the SEK-1/PMK-1 pathway have to include molecules that perceive the presence of Cry5B and relay that information to the MAP kinase cascade. Our 2-step screening procedure was our approach for identifying the genes involved in this regulated branch of the MAP kinase pathway. However, in addition to finding a gene that acts upstream of PMK-1, we also identified 58 genes involved in Cry5B defense that we were previously unaware of. Using the online *C. elegans* database (wormbase), I examined the homologies and predicted functions of our 58 novel *hpo* genes identified in the primary RNAi screen and a few interesting trends were observed. For example, in addition to *cgt-3*, four more putative glycosylation enzymes (M02B7.4, F25D1.11, B0491.1 and C14A4.3) were also identified in this screen. Additionally, two more of the 58 genes encode enzymes believed to be involved in glycosylphosphatidylinositol (GPI) anchor biosynthesis (T05E11.6 and T14G10.7). Perhaps there exists a critical defense protein at the surface of the plasma membrane that is anchored there by a GPI linkage and disruption of this linkage impairs this defense. Another two of the genes are

homologs of diacylglycerol (DAG) kinase (*tag-274* and K06A1.6). Because these enzymes downregulate DAG signaling, the finding that two putative DAG kinases are involved in Cry5B defense could suggest the existence of a DAG signaling pathway in *C. elegans* that promotes or enables intoxication. I believe, for years to come, the data obtained from this primary RNAi screen will be useful to those researchers in the field trying to understand toxin defense mechanisms.

The secondary screen for animals that fail to activate PMK-1 when fed Cry5B led us to the ceramide glycosyltransferase homolog *cgt-3*. The *cgt-3*(tm504) deletion mutant, provided to us by the Lesa lab, was hypersensitive to Cry5B in intoxication assays with Cry5B *E. coli*, but was insensitive to Cry5B in our immunoblot assay for PMK-1 activation. Together, these phenotypes fit what we expected if the mutation took out the Cry5B-regulated upstream branch of the MAP kinase pathway. The predicted function of this gene in glycosphingolipid (GSL) biosynthesis presents an interesting conundrum. Other genes involved in adding sugars to GSLs (specifically, the *bre* genes) mutate to a Cry5B resistant phenotype. Why does *cgt-3* mutate to the opposite phenotype? Even more intriguing, *cgt-3* and *bre-4* are both required for the toxin to activate PMK-1, so, in this regard, the two genes mutate to identical phenotypes. When both *cgt-3* and *bre-3* are mutated, the animals are strongly Cry5B resistant, just like a *bre-3* single mutant. This result would indicate that *cgt-3* acts downstream of *bre-3* in Cry5B intoxication. It remains possible, however, that CGT-3 can work with, and just upstream of, the BRE enzymes in the synthesis of the GSL receptor, but some other CGT fills this role when the *cgt-3* gene is mutated. I will now discuss some potential models for the mechanism of *cgt-3* mediated defense and PMK-1 activation and how these models could be tested in the future.

Model 1: The toxin-sensor GSL

This model involves two GSL species in the animal. One is the Cry5B receptor that binds toxin and allows it to form a pore. The BRE enzymes work with any of the three CGT enzymes (they would act redundantly in this model) to build the carbohydrate structure on this GSL receptor. The other GSL species in this model would be one that senses changes in plasma membrane integrity and activates SEK-1/PMK-1 when there has been a disturbance from, for example, a pore-forming toxin. Figure 4.13 illustrates this model. One prediction of this model is that CGT-3 is responsible for activating the PMK-1 pathway in response to any pore-forming agent.

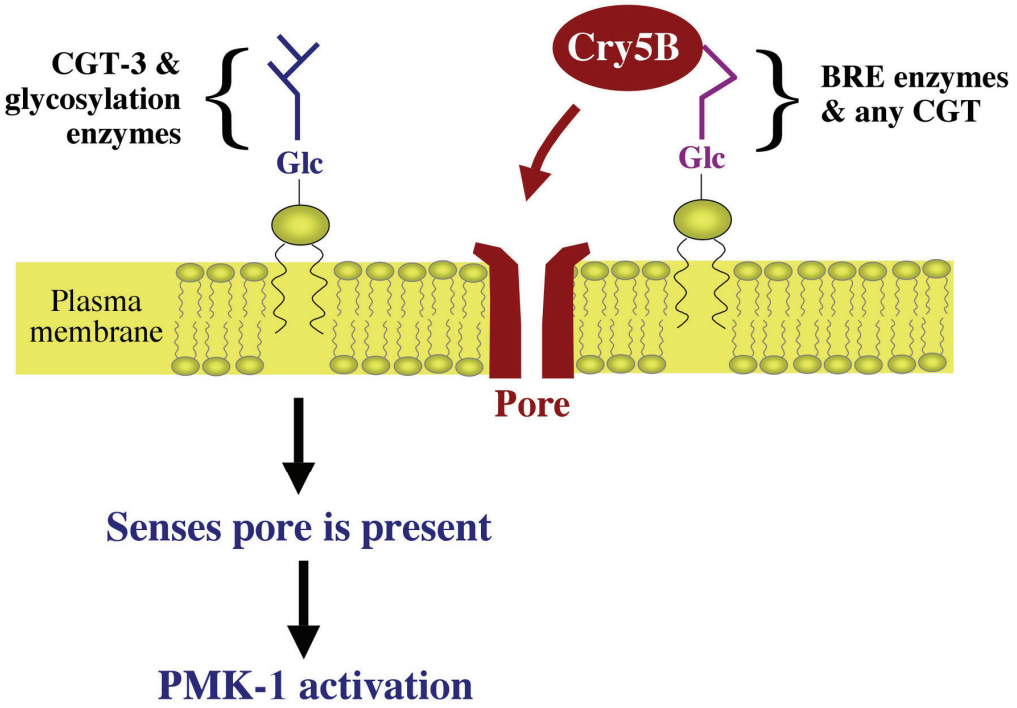

Figure 4.13. Model 1. The toxin-sensor GSL

Model 2: Two toxin-binding GSLs

This model takes into consideration the fact that, in the immunoblot assay for PMK-1 activation by Cry5B, the only *bre* mutant that I have tested is *bre-4*(ye28). In this model, one or more of the BRE enzymes are involved in the synthesis of two different GSL species. Both GSL molecules are capable of binding Cry5B, perhaps because the carbohydrate structures share some physical properties. One GSL, however, acts as the toxin receptor, enabling Cry5B to form a pore once it has bound. The sugars on this GSL would be added by the BRE enzymes and any of the three CGT enzymes. The other GSL in this model would serve as the MAP kinase activator, triggering phosphorylation of SEK-1/PMK-1 when the toxin binds. The synthesis of this GSL would specifically require CGT-3 and BRE-4. The other *bre* genes may or may not also contribute to this GSL. Testing the other bre mutants in the immunoblot assay for PMK-1 activation would be a good way to start testing this model. We would also predict from this model that any PFT that does not bind GSLs would not activate PMK-1 in a CGT-3 or BRE-4 dependent manner. This model is illustrated in Figure 4.14.

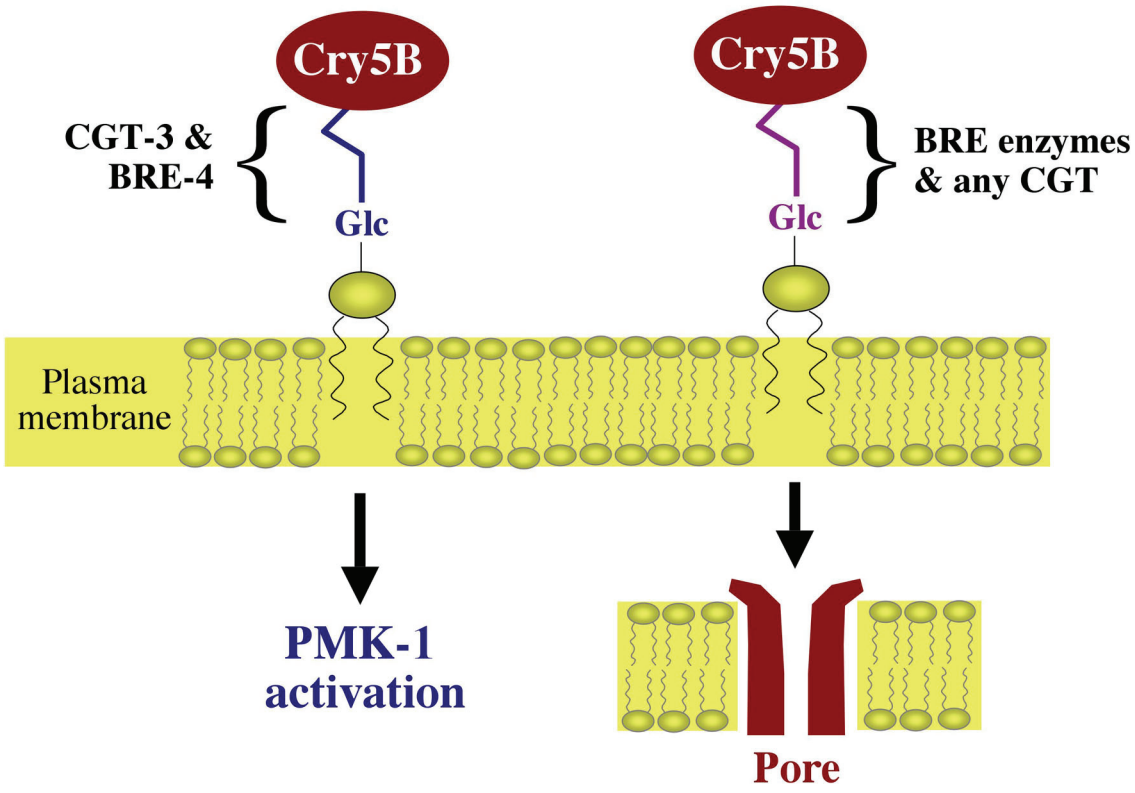

Figure 4.14. Model 2. Two toxin-binding GSLs

Model 3: Lipid rafts mediate PMK-1 signaling

In the literature, there is ample evidence that, for several signal transduction pathways, efficient signaling requires lipid microdomains in the plasma membranes. These so-called lipid rafts are enriched for ceramide and GSLs (for review see (Bollinger et al., 2005)). In this third model for CGT-3 defense, activation of the PMK-1 pathway is dependent on the presence of these rafts, perhaps because the rafts promote clustering of some critical membrane receptor that responds to a pore-induced signal (see Figure 4.15 for illustration). In this model, CGT-3 is required for proper assembly or architecture of these lipid rafts and, in a *cgt-3* mutant, signaling to PMK-1

is disturbed as a result of these deficiencies. One could biochemically test if *cgt-3* mutants have lipid rafts defects as a test of this model.

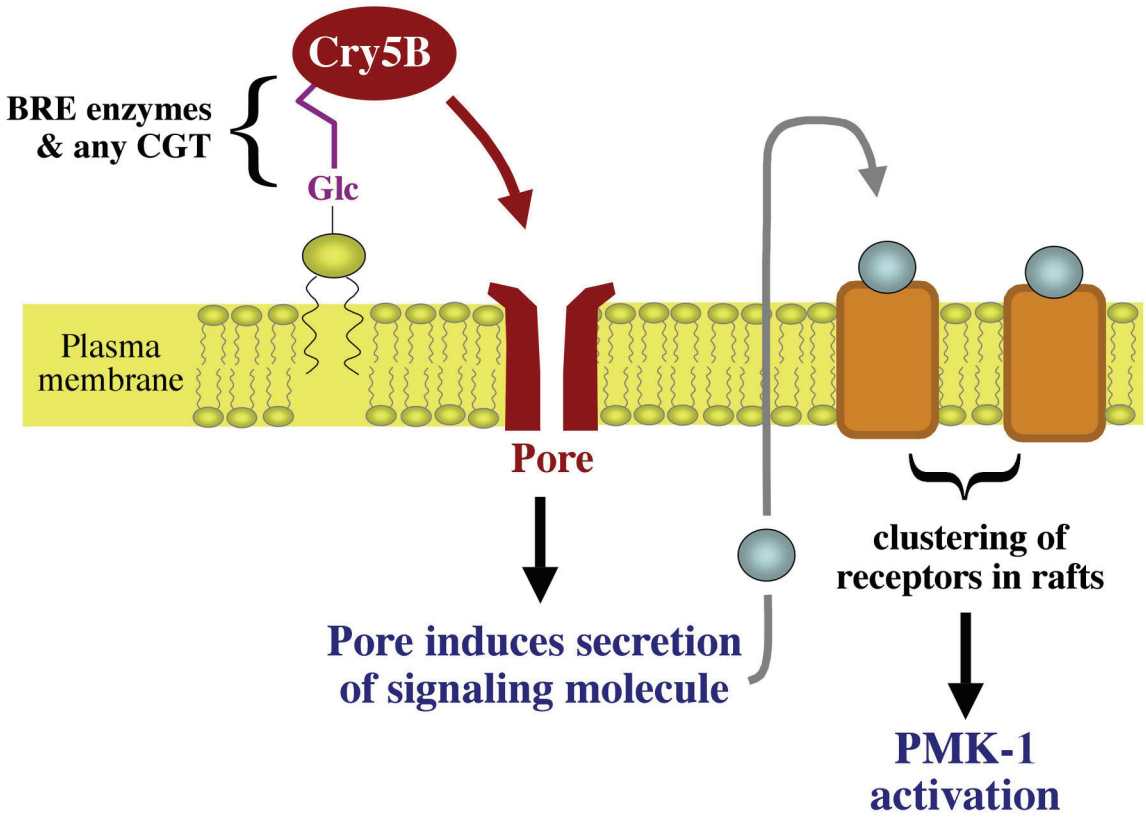

Figure 4.15. Model 3. Lipid rafts mediate PMK-1 signaling

In addition to the models presented here, many others are feasible. Further screening of the remaining *C. elegans* chromosomes could be the single most important approach for further elucidating the players in toxin-regulated activation of PMK-1 and making sense of the role of *cgt-3* in this process.

No discussion on signal transduction pathway activation in response to a bacterial product would be complete without mentioning toll-like receptors (TLRs). In mammals, TLRs are pathogen recognition receptors (PRRs) that mediate innate

immunity through their binding of pathogen associated molecular patterns (PAMPs). For instance, TLR4 binds to LPS, TLR3 binds double-stranded RNA and TLR9 binds CpG-DNA. LPS, double-stranded RNA and CpG-DNA are all examples of PAMPs. A total of 13 TLRs have been identified in mice, 10 in human. As mentioned earlier, *C. elegans*, has a protein called TIR-1, a cytosolic protein with a Toll interaction domain that acts upstream of the PMK-1 pathway. Apart from *tir-1*, *C. elegans* has a single Toll homolog, *tol-1*, that appears to function neuronally in pathogen avoidance behavior, but apparently does not contribute to defense against killing by pathogenic bacteria or defense to Cry5B (Pujol et al., 2001 and unpublished observations). Therefore, it seems for worms, it is still unclear if this organism relies on PRRs to recognize bacterial pathogens and products.

Finally, I would like to discuss the evidence that Cry5B induced activation of PMK-1 is an important part of the worm defense against this toxin. Clearly, the pathway itself is important, but how critical is it that the animals be able to quickly increase their pool of phospho-PMK-1 in their cells in order to fight off an intoxication process that takes several days. Finding a mutant [*cgt-3*(tm504)] that is both Cry5B hypersensitive and fails to activate PMK-1 in response to Cry5B suggests that it is at least somewhat important. However, the *cgt-3* mutants are not dramatically hypersensitive compared to any one of the three kinase mutants. Furthermore, they are not even as sensitive as the animals missing the *nsy-1* gene and *nsy-1* mutants do respond to toxin with PMK-1 activation. Importantly, however, *nsy-1* mutants have reduced levels of phosph-PMK-1 in the presence Cry5B relative to wild-type. It may be worth investigating in the future if *nsy-1* mutants are hypersensitive because they lack a basal level of PMK-1 activity or if hypersensitivity

is more a result of the attenuated levels of phospho-PMK-1 that they make after Cry5B has been encountered. Additionally, isolating mutations that affect the timeliness of Cry5B induced PMK-1 activation could prove informative as well. To date, I have not tested any of the genes from the primary RNAi Hpo screen for defects in timing of the Cry5B response.

4.9 Materials and Methods

***C. elegans* and their maintenance.** *C. elegans* was maintained using standard techniques on NG medium and the *Escherichia coli* strain OP50 as a food source. The following strains were used in this study: LGII, *rrf-3*(pk1426); LGX, *sek-1*(km4); LGII, *nsy-1*(ok593) and *cgt-3*(tm504); LGIV, *pmk-1*(km25). All *C. elegans* assays were carried out at 20°C unless otherwise noted.

Microscopy. Images of *C. elegans* were captured on an Olympus BX-60 microscope using a 10X/0.25 objective and a DVC camera with a 0.5X camera mount, except in figure 4.7 where the animals where photographed with a Nikon CoolPix995 digital camera mounted to a dissecting microscope.

Bt-toxin and cadmium plate assays for testing of the *cgt-3* mutant strain.

Bt-toxin assays. The *E. coli* strain carrying Cry5B is described in (Wei et al., 2003). To induce expression of the toxin, a saturated culture was diluted 1:10 in LB containing 50μg/ml carbenicillin. The diluted culture was grown for 1 hour at 37°C with shaking. IPTG was then added to 50μM and cultures were grown for an

additional 3 hours at 30° C. 30µl of bacteria were then spread on *C. elegans* high growth plates (ENG) with 100µM IPTG and 50µg/ml carbenicillin. Where indicated, the toxin-expressing *E. coli* was mixed with *E. coli* containing empty vector to make low toxin lawns. The lawns were grown at 25°C and plates were used within one or two days. L4-stage *C. elegans* were picked or pipetted onto plates for toxicity assays.

Cadmium assays. To make plates containing cadmium, the cadmium chloride stock solution was added to the high growth media after autoclaving before the plates were poured. The day before the plates are needed for assays, they were spread with 30µl of an overnight culture of OP50. The lawns were grown at 25°C overnight. Plates were seeded with *C. elegans* in the same way as the Bt-toxin plates.

RNA interference of *tir-1* in Figure 4.4A. RNAi of *tir-1* was done by feeding using *C. elegans* strain NL2099 carrying mutation *rrf-3*(pk1426) (Simmer et al., 2002). This strain does not show altered sensitivity to Cry5B compared to N2 (data not shown). The feeding protocol was adapted from that described in (Kamath and Ahringer, 2003) with the following modifications. The RNAi plates contained 0.1mM IPTG and 25µg/ml carbenicillin. L4 hermaphrodites were pipetted onto the RNAi feeding plates and allowed to feed for 30-32 hours before replica plating. Adults were allowed to lay eggs on these replica plates for 2-4 hours before being removed. Phenotypes were assessed in these progeny using the plate assays described above. Feeding was carried out at 20°C. The feeding clone for *tir-1* was obtained from the Ahringer RNAi library.

Immublotting for phospho-PMK-1. Preparation of *C. elegans* protein extracts. L4 stage animals were washed off OP50 *E. coli* plates with M9 worm buffer and collected in 15mL tubes. The larvae were concentrated by centrifugation and pipetted into 0.6mL tubes along with OP50 and purified Cry5B protein in citrate buffer (or citrate buffer alone, as control). For the assays with NaCl or cadmium, the indicated levels of these reagents were added to the tubes in place of the Cry5B. The tubes were placed at 20° C for the indicated length of time. For the animals treated with heat stress, the tubes were placed at either 28°C or 30°C, as indicated in the text. Afterwards, 6x SDS-PAGE loading buffer containing the phosphatase inhibitors sodium orthovanadate and sodium fluoride was added directly to the 0.6mL tubes and the tubes were placed in a boiling water bath for 4 minutes to make protein extracts.

Western blotting. The protein extracts were electrophoresed by SDS-PAGE and transferred to a PVDF membrane. The membrane was probed for phospho-PMK-1 with the anti-active p38 antibody from Cell Signaling Technology according to manufacturer protocol. Following ECL detection, the membrane was stripped in stripping buffer (62.5mM Tris pH 6.8, 1% SDS, 0.7% beta-mercaptoethanol) for 1 hour at 65°C, washed, blocked and probed for tubulin with the DM1α antibody from Sigma. ECL reagent was again used for detection of tubulin.

RNAi screening for Hpo phenotype. Bacteria from the Ahringer library (384-well plates) were replica plated to 96-well plates containing LB agar with 50μg/ml carbenicillin and 12μg/ml tetracycline. From these replica plates, liquid cultures of the RNAi bacteria were grown to saturation in LB with 50μg/ml

carbenicillin, also in 96-well plates. 24-well plates filled with NG agar media containing IPTG were seeded with the saturated bacterial cultures so that each well contained a different RNAi clone. These 24-well plates were always set up in duplicate and the *E. coli* lawns were allowed to grow overnight at room temperature. The following day, L1-stage *rrf-3*(pk1426) larvae were pipetted onto each well of the 24-well agar plates with approximately 15 worms per well. 48 hours later, when the larvae reached the late L4-stage, 1µg of purified Cry5B protein was pipetted directly on top of each well of the worm plates. Two days after adding toxin, the plates were visually scored to find those wells in which the animals are noticeably more intoxicated than the negative control animals. With each set, we set up positive controls (*tir-1* and Y71H2B.7) and negative controls (empty RNAi vector). The Cry5B protein was purified as described in (Griffitts et al., 2001).

LC_{50} assays. The protocol for these assays is described in (Bischof et al., In press). Three separate trials were performed for each strain. In each trial, conditions were set-up in triplicate wells.

Data analysis. For each individual trial, the percentage of animals alive in each of the three triplicate wells was calculated and these percentages were averaged to obtain the mean level of survival at each toxin concentration for each worm strain. Then, the three averages from the three different trials were entered into the GraphPad Prism software program to obtain an LC_{50} value for each strain and generate the graph depicted in Figure 4.6. This same program was used to perform a t-test to verify

statistical differences between the *sek-1*(km4) strain and the *nsy-1*(ok593) strain (P= 0.0236)and between N2 and *cgt-3*(tm504) strain (P= 0.0377).

***Pseudomonas auriginosa* killing assay.** The *P. auriginosa* strain PA14 was used for these experiments. Overnight cultures of PA14 were grown to saturation in LB broth. 20µl of saturated culture were spread onto NG agar plates and plates were incubated at 37°C for 24 hours. After 24 hours, the plates were allowed to sit at room temperature for 4 to 6 hours before being seeded with >30 L4 *C. elegans* larvae. Animals were considered dead when they did not respond to touch.

PMK-1 antibody purification. Expression and purification of GST::PMK-1 fusion. A piece of the *pmk-1* cDNA that encodes amino acids 232-365 was cloned into the pGEX-6P-1 vector (Amersham) at BamHI/SalI restriction sites. The construct was transformed in *E. coli* strain BL21 for protein expression. Two 10mL cultures of transformed *E. coli* were grown overnight in LB with 50µg/ml carbenicillin. The next day, each 10mL culture was added to a flask containing 1L LB+carbenicllin. These cultures were grown for 3 hours at 37°C with shaking. After this three hour incubation, IPTG was added to the cultures to 1mM. The cultures were grown another five hours. Cells were then harvested and frozen in –80°C freezer for at least one day. To purify the GST::PMK-1 fusion protein, cells were thawed in lysis buffer (50mM NaH_2PO_4; 300mM NaCl; 10mM imidazole; pH 8) containing the protease inhibitors PMSF and Benzamidine HCl (50mL lysis buffer per 500mL *E. coli* culture). Lysozyme powder was added to 1mg/ml and the cells were incubated on ice

for 15 minutes. The cells were then sonicated on ice (Fisher 550 Sonic Dismembrator) for 8 10-second pulses. The lysates were centrifuged at 11,000 x g for 30 minutes to pellet the insoluble matter. The supernatent from this spin was mixed with glutathione agarose (Sigma) equilibrated in lysis buffer (1.5mL agarose per 50mL lysate) and let incubate on 4°C shaker for three hours. The agarose was then washed with 4 volumes of wash buffer (1X PBS; 250mM NaCl; 0.1% tween-20; 1mM DTT; 2mM Benzamidine HCl) and poured into a disposable column. The GST::PMK-1 fusion protein was eluted with 8 1mL fractions of elution buffer (50mM Tris; 10mM glutathione; 75mM KCl). 8mg of this purfied fusion protein was sent to Cocalico Biologicals for injection into two rabbits.

Purification of anti-PMK-1 antibodies. 100µl of a 1mg/ml stock of purified GST::PMK-1 protein was spotted onto a piece of nitrocellulose membrane and allowed to dry. The nitrocellulose was then blocked overnight at 4°C in PBS with 5% milk. The next day, the membrane was transferred to a solution of 5mL PBST with 5% milk and 200µl of each of the two serum samples sent to us by Cocalico Biologicals. The membrane was allowed to incubate with the sera overnight at 4°C. The next day, the membrane was washed three times in PBS (20 minutes per wash). A small disposable column (Bio-Rad #732-6008) was filled with P6 resin swelled in 1M HEPES pH 8. The column was equilibrated in blocking buffer. After membrane was washed in PBS, it was cut into small pieces and the pieces were divided between two 2mL centrifuge tubes, each containing 1.5mL of elution buffer (0.1M glycine pH 2.3, 0.4M NaCl, 100ug/ml BSA, 0.05% Tween 20). Let membrane pieces incubate in the elution buffer about five minutes. Pipetted the elution buffer out of the tubes and

onto the column, collecting the 3mL of flow-through. For western blots, this flow-through was used as the primary anti-PMK-1 antibody at a dilution of 1:10.

4.10 References

Bischof, L. J., Huffman, D. L., and Aroian, R. V. (In press). Assays for Toxicity Studies in C. elegans with Bt Crystal Proteins. In C. elegans: Methods and Applications, K. Strange, ed. (Humana Press).

Bollinger, C. R., Teichgraber, V., and Gulbins, E. (2005). Ceramide-enriched membrane domains. Biochim Biophys Acta *1746*, 284-294.

Chuang, C. F., and Bargmann, C. I. (2005). A Toll-interleukin 1 repeat protein at the synapse specifies asymmetric odorant receptor expression via ASK1 MAPKKK signaling. Genes Dev *19*, 270-281.

Couillault, C., Pujol, N., Reboul, J., Sabatier, L., Guichou, J. F., Kohara, Y., and Ewbank, J. J. (2004). TLR-independent control of innate immunity in Caenorhabditis elegans by the TIR domain adaptor protein TIR-1, an ortholog of human SARM. Nat Immunol *5*, 488-494.

Griffitts, J. S., Haslam, S. M., Yang, T., Garczynski, S. F., Mulloy, B., Morris, H., Cremer, P. S., Dell, A., Adang, M. J., and Aroian, R. V. (2005). Glycolipids as receptors for Bacillus thuringiensis crystal toxin. Science *307*, 922-925.

Griffitts, J. S., Huffman, D. L., Whitacre, J. L., Barrows, B. D., Marroquin, L. D., Muller, R., Brown, J. R., Hennet, T., Esko, J. D., and Aroian, R. V. (2003). Resistance to a bacterial toxin is mediated by removal of a conserved glycosylation pathway required for toxin-host interactions. J Biol Chem *278*, 45594-45602.

Griffitts, J. S., Whitacre, J. L., Stevens, D. E., and Aroian, R. V. (2001). Bt toxin resistance from loss of a putative carbohydrate-modifying enzyme. Science *293*, 860-864.

Inoue, H., Hisamoto, N., An, J. H., Oliveira, R. P., Nishida, E., Blackwell, T. K., and Matsumoto, K. (2005). The C. elegans p38 MAPK pathway regulates nuclear localization of the transcription factor SKN-1 in oxidative stress response. Genes Dev *19*, 2278-2283.

Kamath, R. S., and Ahringer, J. (2003). Genome-wide RNAi screening in Caenorhabditis elegans. Methods *30*, 313-321.

Pujol, N., Link, E. M., Liu, L. X., Kurz, C. L., Alloing, G., Tan, M. W., Ray, K. P., Solari, R., Johnson, C. D., and Ewbank, J. J. (2001). A reverse genetic analysis of components of the Toll signaling pathway in Caenorhabditis elegans. Curr Biol *11*, 809-821.

Ratner, A. J., Hippe, K. R., Aguilar, J. L., Bender, M. H., Nelson, A. L., and Weiser, J. N. (2006). Epithelial cells are sensitive detectors of bacterial pore-forming toxins. J Biol Chem *281*, 12994-12998.

Simmer, F., Tijsterman, M., Parrish, S., Koushika, S. P., Nonet, M. L., Fire, A., Ahringer, J., and Plasterk, R. H. (2002). Loss of the putative RNA-directed RNA polymerase RRF-3 makes C. elegans hypersensitive to RNAi. Curr Biol *12*, 1317-1319.

Stringaris, A. K., Geisenhainer, J., Bergmann, F., Balshusemann, C., Lee, U., Zysk, G., Mitchell, T. J., Keller, B. U., Kuhnt, U., Gerber, J.*, et al.* (2002). Neurotoxicity of pneumolysin, a major pneumococcal virulence factor, involves calcium influx and depends on activation of p38 mitogen-activated protein kinase. Neurobiol Dis *11*, 355-368.

Wei, J. Z., Hale, K., Carta, L., Platzer, E., Wong, C., Fang, S. C., and Aroian, R. V. (2003). *Bacillus thuringiensis* crystal proteins that target nematodes. Proc Natl Acad Sci U S A *100*, 2760-2765.

Chapter 5

Conclusions, Implications and Future Directions

5.1 Summary

This work began with the global characterization of the *C. elegans* genomic response to the pore-forming toxin Cry5B. From a list of over 1000 toxin-regulated genes, the focus quickly narrowed to a single genetic pathway, the p38 MAP kinase cascade. This protective pathway is activated by Cry5B to orchestrate a defense that includes transcription of genes that fight intoxication (Figure 5.1). With this last chapter, I will discuss some implications and relevance for this work in the areas of immune signaling, *C. elegans* toxin defenses, and *Bacillus* virulence.

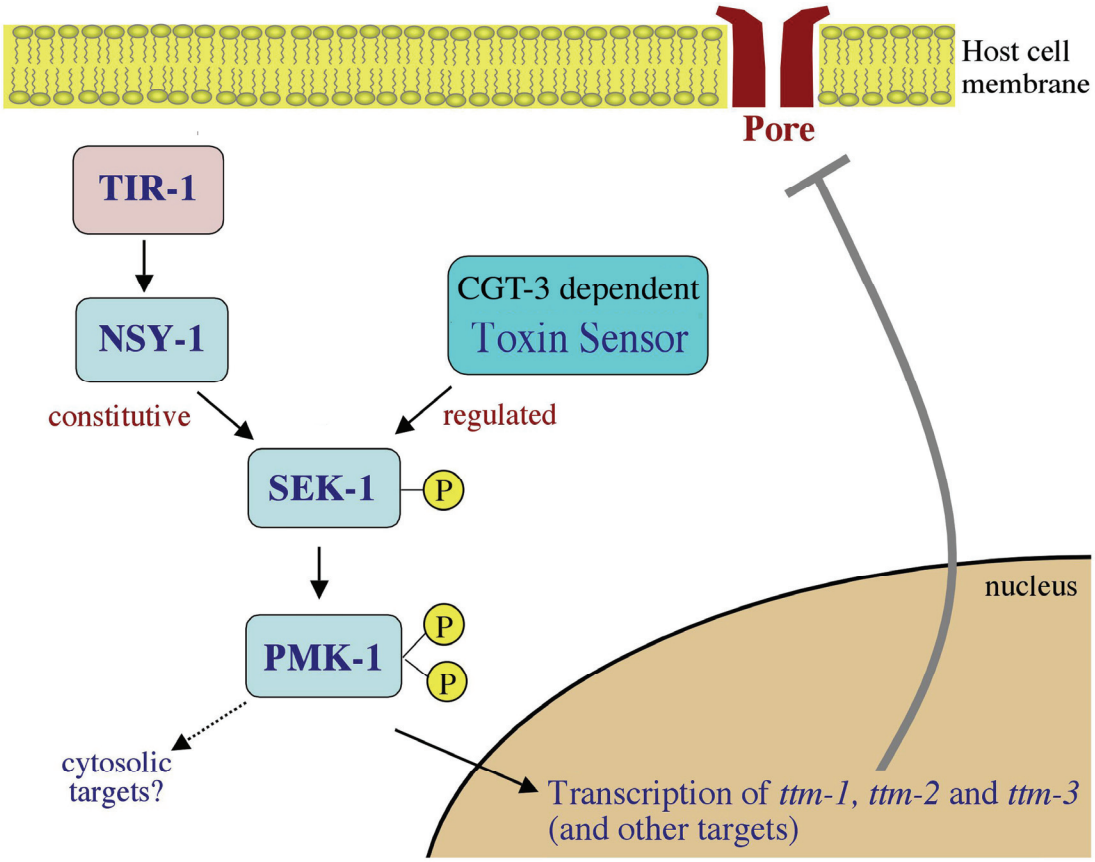

Figure 5.1. A model summarizing my work in the Aroian lab.

5.2 Pore-Forming Toxins in Immunity

The results presented in this dissertation would indicate that pore-forming toxins can serve as cellular signals for immune pathways and can also be the targets of that signaling. Does Cry5B activate the PMK-1 pathway via a similar mechanism as *Staphylococcus aureus* α-hemolysin and other structurally unrelated PFTs that activate p38 in mammalian cells? That several different PFTs induce p38 phosphorylation suggests that the mechanism is dependent on pore-formation, as opposed to some other feature or activity of the protein. It would also be unlikely,

since these different toxins use different host receptors, that the toxin/receptor binding step alone is sufficient to activate p38

To date, it is not clear how the pore generates a signal for p38 activation, but new evidence points to a role for an osmotic imbalance as a trigger for signaling. In a recent publication, Ratner et. al. examined mammalian epithelial cells exposed to *Staphylococcus aureus* α-toxin, *Streptococcus pyogenes* streptolysin O and *Bacillus anthracis* anthrolysin O and *Streptococcus pneumonia* pneumolysin (Ratner et al., 2006). All these toxins caused activation of p38 at sublytic concentrations and, interestingly, this activation was inhibited when high molecular weight osmolytes were added to the media. The authors went on to suggest that the activation of p38 is the result of an osmotic imbalance that signals the cell to mount an immune response. Much of our data in *C. elegans* seems consistent with such a model. For instance, we found one of the key transcriptional targets of PMK-1 was an enzyme predicted to be involved in pumping cations out of the cell. We also found that excessive levels of sodium chloride in the media caused dramatic activation of the pathway and that salt stress enhanced the potency of the Cry5B toxin. However, the *cgt-3* mutant was still able to activate PMK-1 in response to high salt, even though it could not do so in response to the Cry5B PFT, indicating that high salt and a PFT use different means for activating MAP kinase. Could it be that Cry5B activates PMK-1 differently from how a PFT from a human pathogen activates p38? It may be critical to characterize the importance of *cgt-3* in response and defense to other PFTs that do not rely on the same glycosphingolipid receptor as Cry5B, for example, Cry21A.

Not only does Cry5B serve as a signal for the PMK-1 innate immunity pathway, but it is also a target of that pathway in that part of the pathway's function is to ameliorate the toxin's effects. There are many examples of bacterial toxins serving as signals for the host immune system, but few examples exist of bacterial toxins being specifically targeted by an organism's immune arsenal. In general, pore-forming toxins might make better candidates for targets of the innate immune system than other kinds of bacterial toxins. Membranes are dynamic structures in continual movement and cells need ways of tolerating small disruptions to their membranes that occur from normal mechanical stress. So, the evolution of PFT defenses may really have been a new use for genes already existing in the organsism's genome that deal with this kind of constant stretching and movement of membranes.

5.3 Cry5B Defense in *C. elegans*

The RNAi screen for a Hpo phenotype (hypersensitivity to pore-forming toxin Cry5B) unearthed 58 genes with roles in Cry5B defense that we previously did not know about. Screening the remaining four chromosomes (which is currently in progress in the lab) will certainly reveal many more. Some of these genes can be grouped together based on predicted function or conserved protein domains. Ultimately, however, to truly start making sense of the plethora of data that this screen has and will continue to generate, the genes need to be grouped into genetic pathways. We now know some of the Cry5B defense pathways in the worm including the *pmk-1* pathway, the *kgb-1* pathway and the ER stress pathway (unpublished). Some of the new *hpo* genes will likely be part of one of these pathways while many others may be

part of previously undiscovered defense pathways. At this time, we have assays for determining if a particular gene is upstream of PMK-1 (with the phospho-p38 immunoblot) or upstream of the ER stress pathway (using an assay that measure splicing of the xbp-1 mRNA). I think we could also determine if a particular *hpo* gene is downstream of one of these known Cry5B defense pathways by knocking down the *hpo* gene with RNAi in a *sek-1*, *kgb-1* or ER stress mutant (null) background. If RNAi of the *hpo* makes these mutants even more sensitive to Cry5B, then the genes are likely part of two separate genetic pathways.

What will also be interesting is determining which genes are involved in general stress defense, which genes seem to be specific for pore-forming toxins or membrane damaging agents and which genes, if any, seem specific for Bt Cry toxins. Our lab has long supported the model that soil nematodes and Bt co-evolved as a host-pathogen pair (or bacterial feeder-bacterial food source pair, depending on the perspective). If so, then *C. elegans* may have defense genes that evolved to specifically combat Bt Cry toxins. An interesting comparison for this idea is the mammalian Toll receptors, where each receptor binds a particular pathogen-associated molecular pattern (PAMP) or set of PAMPs. These Toll ligands tend to be bacterial features that are common to many different bacterial species (cell wall components, for example), but if Bt is a significant pathogen for soil-dwelling bacterial-feeding nematodes, then Cry toxins may be such a PAMP for this host.

5.4 Cry Toxins as Bt Virulence Factors

Our lab has seen that when *C. elegans* and Bt (or *B. cereus* or *B. anthracis*) are placed together in liquid culture, Bt can infect *C. elegans* in a Cry toxin dependent manner. The infection phenotype is quite striking, eventually resulting in nothing but a nematode cuticle filled completely with *Bacillus* spores and vegetative rods (unpublished data). Does defending against Cry5B help *C. elegans* attenuate *Bacillus* virulence? Could humans possibly fight infection from bacteria like *S. pyogenes* and *S. aeureus* by up-regulating their defenses to PFTs?

For *C. elegans*, I think it is worth exploring what it is about Cry5B intoxication that enables *Bacillus* to devour *C. elegans* so completely. Is the toxin needed for the bacteria to make it through the pharyngeal grinder so it can enter the intestinal lumen still in-tact? If so, then the toxin plays a role in allowing the bacteria access to the infection site. An alternative hypothesis is that Cry5B compromises *C. elegans* health to such a degree that the animals cannot stave off infection. In this scenario, the toxin functions to make the host more susceptible to the bacterium, a kind of immuno-compromised worm. Or, simply, maybe the cell membranes of toxin-fed animals tend to leak intracellular nutrients into the intestinal lumen, creating a more favorable growth environment for the bacteria there.

Although I have been focused on the toxin, my work on Cry5B defense genes could be useful for understanding interactions between the *C. elegans* host and *Bacillus* pathogen. Specifically, it could provide a means for probing the relationship between the host's ability to fight off Cry5B intoxication and ability of the *Bacillus* pathogen to infect *C. elegans*. For instance, how do Cry5B hypersensitive mutants

behave in a Bt infection assay? Is less toxin needed to observe maximal infection rates? Also, one could ask if increased toxin sensitivity changes certain features of the infection process, like the time it takes for bacterial accumulation to first begin or the rate at which the infection spreads. Addressing these questions could be a step toward understanding the role of PFT defense in the process of infection.

5.5 Cell Mediated Immunity

Although we often think of the immune system as a highly advanced arrangement of specialized cell types and proteins, the most ancient kind of immunity may have evolved at the level of the cell. That is, the cell under attack (by a bacterial toxin, in this case) responded to that attack in an effort to protect the cell itself. In our work with *C. elegans* and Cry5B, the data suggest this kind of model. The tissue targeted by the Cry5B toxin is the intestine and it is in these intestinal cells that the PMK-1 protective pathway mediates toxin defense. Fighting off intoxication in the whole organism, therefore, means fighting off the toxin one cell at time.

5.6 References

Ratner, A. J., Hippe, K. R., Aguilar, J. L., Bender, M. H., Nelson, A. L., and Weiser, J. N. (2006). Epithelial cells are sensitive detectors of bacterial pore-forming toxins. J Biol Chem *281*, 12994-12998.